VULNERABILITY AND RESILIENCE OF PEOPLE AND PLACES TO HURRICANE DAMAGE IN THE U.S. GULF AND ATLANTIC COASTS FROM 1950 TO 2018

by

Gainbi Park

A Dissertation Submitted in
Partial Fulfillment of the
Requirements for the Degree of

Doctor of Philosophy
in Geography

at
The University of Wisconsin-Milwaukee
August 2021

ABSTRACT

VULNERABILITY AND RESILIENCE OF PEOPLE AND PLACES TO HURRICANE DAMAGE IN THE U.S. GULF AND ATLANTIC COASTS FROM 1950 TO 2018
by

Gainbi Park

The University of Wisconsin-Milwaukee, 2021
Under the Supervision of Professor Zengwang Xu

Extreme weather events are expected to increase as a consequence of climate change, increasing the intensity and frequency of natural hazards. Their catastrophic impact is attributable to both the geophysical characteristics of a hazardous event itself and the socio-demographic characteristics of people who are at a greater risk of harm in the aftermath of natural hazards. Previous studies have largely used a place-based approach, measuring the relative level of social vulnerability between places using a social vulnerability index (SoVI), a prevalent spatially explicit method in geographic scholarship. As a composite index, SoVI, has been criticized by scholars due to its over-generalization; it cannot indicate the contribution of specific local social indicators to vulnerability, obscuring demographic heterogeneity and making it difficult to understand who is vulnerable. In contrast to the spatiality of vulnerability, the temporal dynamics of social vulnerability have been relatively understudied. This dissertation seeks to address these drawbacks of the SoVI approach and to assess hazard-specific vulnerability by incorporating geophysical characteristics of natural hazards and differential vulnerabilities of affected populations.

There are four primary objectives of this study: (1) To investigate major patterns in the spatial and temporal dynamics of social vulnerability of U.S. counties from 1970 to 2010 using quantile standardization, sequence alignment analysis, and cluster analysis; (2) To identify the

contributions of the components of SoVI and the local primary factors that contribute to social vulnerability using geographically-weighted principal component analysis (GWPCA) and explore how those factors have evolved over time using Greater Houston as a case study; (3) To estimate the spatial extent and intensity of storm surge inundation and wind damage caused by hurricanes along the Gulf and Atlantic Coasts in the United States from 1950 to 2018 using geospatial analysis; and (4) To understand differential vulnerabilities of distinctive demographics within hurricane at-risk areas using a spatial and temporal analysis.

The results show that the U.S. counties have four major temporal trajectories, revealing areas of persistently low and high vulnerabilities and areas with dynamically changing vulnerabilities. The application of GWPCA reveals the most influential local social factors that constitute the SoVI index. Moreover, the spatial and temporal trends of the local factors can indicate what socioeconomic conditions are prevailing and consistently affect the vulnerability of a particular region. In terms of the vulnerability of people to hurricane hazards, this study also identifies generalized patterns of demographic changes that are within hurricane-risk zones and which population groups are increasingly or decreasingly exposed.

The results in this study have significant implications for policymakers and national disaster management in surveilling vulnerable areas and establishing potential hazard mitigation plans. The findings reported here shed new light on social vulnerability assessment urging decision-makers to provide more resources to the hardest-hit groups living in the most exposed counties. This study is the first comprehensive investigation of hurricane-specific vulnerability encompassing the Atlantic and Gulf Coasts and at a national scale. The analytical framework suggested in this study can enrich the approach to vulnerability assessment of natural hazards by converging geographic and demographic perspectives.

TABLE OF CONTENTS

LIST OF FIGURES

LIST OF TABLES

Chapter 1. Introduction

1.1. Introduction

In recent decades, the human population has seen unprecedented growth and redistribution. Its demographic composition has also undergone major changes along with alteration of social and natural environments. Anthropogenic activities from unbridled consumption of fossil fuels, indiscriminate land development, and deforestation have been exacerbating climate change and global warming. The incidents of extreme weather events are projected to increase worldwide as a consequence of continued global climate change, increasing the intensity and frequency of natural hazards (National Academies of Sciences, 2016). Such human-induced environmental stresses amplify risk and vulnerability, which necessitates a comprehensive understanding of the extent to which human society is susceptible to natural hazards such as wildfires, drought, heavy rainfall, floods, and hurricanes. In response to a high risk of natural hazards, understanding the extent to which the United States is vulnerable to natural hazards over space and time is imperative to prepare for and mitigate potential impacts of natural disasters (Cutter & Finch, 2008; Park & Xu, 2020; Van Aalst, 2006).

Natural hazards are directly impacted by the geophysical characteristics of the areas in proximity to destructive events, as well as the social characteristics of people situating themselves in vulnerable conditions (Cutter, 1996; Tobin & Montz, 1997; Wisner, Blaikie, Blaikie, Cannon, & Davis, 2004). Socially vulnerable populations are less likely to have resources, information, and coping capacity thereby having greater risk and disproportionate impacts in the aftermath of natural disasters. The most damaging hurricane events in U.S. history, such as Hurricane Katrina (2005), Superstorm Sandy (2012), Hurricane Harvey (2017), Hurricane Irma and Maria (2017), substantiate that natural disasters cannot be simply considered

"natural" and rather are socially constructed (Cannon, 1994; Hewitt, 1995; Logan, 2009; N. Smith, 2006). The socio-demographic factors are directly related to who is more vulnerable and who will be more seriously affected.

Considering the interaction between the physical mechanisms of a hazardous event and the social dimensions that contribute to natural hazards vulnerability, social scientists have incorporated this relationship into vulnerability research by defining it as the "social causation of vulnerability" or "social vulnerability" (Birkmann, 2006; Cutter, 1996; Pelling, 2003; Wisner et al., 2004). In particular, a place-based approach has been the main approach used in natural hazards vulnerability research over the past few decades, emphasizing identification of the spatial distribution of social vulnerability based upon the conceptual framework – "Hazards of Place (HOP)" model (Cutter, 1996; Cutter, Mitchell, & Scott, 2000; Moser, 2010). In an attempt to implement the concept of the HOP model, Cutter, Boruff, and Shirley (2003) developed a social vulnerability index (SoVI) that measures the relative degree of social vulnerability among different places. Most studies on geographic vulnerability research have relied heavily on the SoVI to answer questions about what locations are more vulnerable to natural hazards at various geographic scales (Cutter, 2009; Cutter et al., 2003).

For decades, the SoVI approach has driven empirical case studies to measure the spatial variation of social vulnerability to all types of natural hazards or specific hazard events (C. G. Burton, 2010; Myers, Slack, & Singelmann, 2008; Rygel, O'Sullivan, & Yarnal, 2006; C. Wang & Yarnal, 2012; Yoon, 2012). Although widely accepted, the SoVI method suffers from several limitations – the ecological fallacy, the validity of SoVI in predicting the actual disaster outcome, and uncertainty/sensitivity issues in constructing the composite indicator (Barnett, Lambert, & Fry, 2008; Fekete, 2009; Jones & Andrey, 2007; Rufat, Eric, Emrich, & Antolini, 2019;

Spielman et al., 2020; Tate, 2012; Tellman, Schank, Schwarz, Howe, & de Sherbinin, 2020; Wood, Burton, & Cutter, 2010). Moreover, research on the subject of social vulnerability has been mostly limited to "vulnerable spatialities," paying particular attention to the cross-sectional variation of social vulnerability and ignoring temporal dynamics (Cutter, 1996; Findlay, 2005; Park & Xu, 2020). Another limitation of the SoVI approach is the "obscurity" of the aggregated values of the indicator so it cannot single out the primary factors contributing to vulnerability (Wood et al., 2010). Future vulnerability research should incorporate the dynamic aspects of social vulnerability by considering its temporal shifts and local variation.

Beyond the generalized profile of social vulnerability, hazard-specific vulnerability presents its own unique challenges. For example, hurricanes and cyclones impact different populations with varying degrees of social vulnerability, primarily in coastal communities. The increasing presence of at-risk human populations along the Gulf and Atlantic Coasts is substantially increasing the potential hazards. The continued concentration of people and property in coastal areas creates a perpetual risk of exposure to biophysical hazards. The U.S. population has experienced significant growth, diversification, and spatial reallocation in the past few decades (Donner & Rodríguez, 2008; Magnus, 2008; Thomas, Phillips, Lovekamp, & Fothergill, 2013). These changing geo-demographics (i.e., demographic profile of groups of people by where they live) have altered the social vulnerability of places across the United States. In facing the challenge of climate change and increasing risk from natural hazards, it is essential to understand how populations have been historically affected and what population groups have demonstrated the most vulnerability. An inter-categorical intersectional approach has been widely adopted in quantitative research (e.g., health, ageing, or life-course studies) to reveal consequences of inequality stratified by cross-coded categories (e.g., young Black women

or men) representing the intersection of different population subgroups. The term "intersectional approach" in this dissertation indicates cross-coded categorization based upon multiple demographic attributes, taking into account the data available on race/ethnicity, gender, and age groups in demographic datasets (Bauer & Scheim, 2019; Holman & Walker, 2020). The use of the intersectional approach varies across the social science disciplines. Age is not as straightforward as gender, race, class, etc. as an axis of inequality of the intersectional approach, but it is relevant in examining population vulnerability in an aging society. Using the demographic intersections of race, gender, and age, this dissertation attempts to comprehend how this intersectionality can be applied to population vulnerability to hurricane hazards along the Gulf and Atlantic Coasts (Kadetz & Mock, 2018; Kuran et al., 2020; Ryder, 2017). Due to practical constraints and data availability, the inter-categorical intersectional approach adopted in this study is limited to 'thin description' rather than 'thick description', only providing superficial and fragmentary information, and cannot provide in-depth historical, cultural, and structural contexts (Geertz, 1973) in explaining the experiences of marginalized groups in disaster vulnerability. A full discussion of intersectional social vulnerability to disasters lies beyond the scope of this study and needs qualitative data collection and analysis.

1.2. Research Objectives

The overall goals of this dissertation are to provide complementary methods to address the shortcomings of the social vulnerability index (SoVI) approach and to assess hazard-specific vulnerability. The primary aims of this study are to address the following research gaps:

1. Social vulnerability is a temporally dynamic process. Despite the importance of understanding spatial and historical transitions of social vulnerability, most studies have not treated the temporal progressions of vulnerability in a systematic and quantitative

manner. Considering it as a spatio-temporal process evolving over time and across space, part of this dissertation investigates the major patterns in the spatial and temporal dynamics of social vulnerability of U.S. counties from 1970 to 2010 (Chapter 3.1).

2. Methodologically, the SoVI is an aggregated composite index based upon a linear combination of a few selected social-demographic variables created from a statistical reduction technique such as principal component analysis. This highly aggregated indicator cannot determine the degree to which specific local social factors contribute to vulnerability. This study explores the differential contributions of the integral components of SoVI using a local spatial statistical model and further examines how the local primary determinants have evolved over time (Chapter 3.2).
3. Drawing upon the hazards of place (HOP) model, this study aims to understand the geography of hurricane-specific coastal vulnerability in the U.S. using geophysical modeling of hurricane-related damage to answer the following research questions (Chapter 4): (1) what is the spatial extent and intensity of storm surge inundation and wind damage caused by hurricanes along the Gulf and Atlantic Coasts in the United States from 1950 to 2018? and (2) what regions have been hardest hit by hurricanes in US coastal counties over the past decades since 1950?
4. The SoVI approach tends to obscure demographic heterogeneity so that it is difficult to fully understand *who* is more vulnerable. A number of studies have analyzed unitary demographic variables (e.g., age, gender, race/ethnicity) as separate elements, overlooking how people's identities at the intersections of multiple systems of inequality shape disaster vulnerability. Thus, this study aims to unravel the overall population distribution and composition within the hurricane at-risk areas to understand *differential*

demographic vulnerability through the application of an inter-categorical (i.e., cross-coded variables) intersectional approach. This can be an additional approach to complement the indicator-based vulnerability assessment, providing a nuanced picture of the vulnerable segments of population groups. Specifically, this study will answer the following research questions (Chapter 5): (1) what population groups have been increasingly or decreasingly exposed to hurricane-related damage over time within the hurricane-prone regions? and (2) how are socially vulnerable people spatially distributed within at-risk areas and how has that distribution evolved over time?

1.3. Dissertation Structure

The overall structure of this dissertation is organized into six themed chapters. Chapter 2 begins by laying out the theoretical backgrounds of this research and reviews literature on vulnerability science, theoretical frameworks of social vulnerability, and the SoVI approach and its limitations. This chapter also presents the demographic trends of coastal populations and their diversification in the hurricane coasts in the United States to corroborate why vulnerability research needs to incorporate demographic differential vulnerability, specifically focusing on populations exposed to hurricane risk.

Chapter 3 consists of two subsections addressing social vulnerability to natural hazards at local and at national scales. The first part deals with the spatial and temporal dynamics of social vulnerability at county level in the contiguous United States from 1970 to 2010 to provide general spatial and longitudinal patterns. The second part presents the application of a local spatial statistical method – geographically weighted principal component analysis (GWPCA) –

to help identify a complementary approach to the social vulnerability index by examining local determinants. The Houston-The Woodlands-Sugar Land metropolitan area was selected as a case study.

Chapter 4 estimates the wind and storm surge damage of all hurricanes that made landfall along the Gulf and Atlantic Coasts from 1950 to 2018. Both the spatial extent and intensity of these storms will be estimated to determine physical vulnerability to hurricane-related damage using the historical hurricane tract database and geospatial analyses. Based upon the spatial extent of hurricane at-risk areas, Chapter 5 further investigates the overall demographic changes over time from 1970 to 2018 by employing intercensal county data and the decennial census. Chapter 6 summarizes the major findings of this dissertation and suggests possible future work.

Chapter 2. Literature Review

2.1. Introduction

Vulnerability science has been extensively applied to a wide variety of academic fields such as ecology, public health, sustainable science, environmental justice, and disaster risk management. The question is what exposes people and places to greater harm from environmental hazards (Füssel, 2007)? Within risk, hazard, and disaster scholarship, vulnerability science has long encompassed three different but intersecting domains: physical/natural systems (i.e., exposure to risk), human systems including social systems and built environment, and local spatial characteristics of places (Cutter, 2003, 2009). Indeed, vulnerability is multi-dimensional, and it is thus imperative to comprehend how these systems interact with each other. The resultant complex human-environment interactions affect the vulnerability of people and places to many hazards.

The remaining part of this chapter proceeds as follows: It first gives a brief overview of a paradigm shift from hazard-oriented to integrative perspectives on vulnerability. Second, it discusses how vulnerability to multiple hazards has been studied within geographic scholarship and its endeavors to address these research gaps. Third, it further examines how the intersection of multiple social-demographic categories (i.e., race/ethnicity, gender, age, social class) contributes to differential social vulnerability.

2.2. Paradigm Shifts of Social Vulnerability

Vulnerability refers to a series of pre-existing conditions of people and locales that may adversely affect their capacity to withstand, cope with, and recover from potential harm and disastrous outcomes (Adger, 2006; Cutter, 1996). It was not until the 1970s and 1980s that

natural hazards research moved away from a hazard-oriented or engineering paradigm in which the geophysical agent (i.e., exposure to risk) was considered the primary source of vulnerability and societal conditions were only secondary factors (Berkes, 2007; Birkmann, 2006; Hewitt, 1995). This traditional managerial view of the hazard paradigm has been challenged by scholars critiquing the overemphasis on the "naturalness" of natural disasters (O'Keefe, Westgate, & Wisner, 1976). Starting in the early 1980s, scholars began reappraising their technological and engineering perspectives on natural disasters and for the first time considering the interaction between society and nature. Viewed in this light, natural disasters are hardly natural; rather they should be considered "unnatural" and "social catalysts" (Cannon, 1994; Hewitt, 1995; Kates, 1971; Kates & White, 1986). For example, growing pressure of human development and overbuilding along the coast increase the potential for more destructive hurricanes, increasing the risk of causalities and property damage. In addition, inconsistent residential building codes or regulations can make coastal communities more vulnerable to hurricane damage (Chmutina & Von Meding, 2019).

Adding the perspective of political ecology introduced a new "hazards in context" framework, emphasizing social causation of vulnerability whereby social and political dimensions of a given society are incorporated to understand the differential impacts of natural hazards (Cutter, 2001; Pulwarty & Riebsame, 1997). This new social vulnerability paradigm is rooted in a broader societal context. In other words, how environment-society systems engender different impacts of natural hazards and what makes certain groups of people and places more vulnerable are the major concern of vulnerability analysis (Cutter, 1996, 2001; Tobin & Montz, 1997; Wisner et al., 2004). As Smith (2006:1) maintained: "There is no such thing as a natural disaster. In every phase and aspect of a disaster– causes, vulnerability, preparedness, results and

response, and reconstruction – the contours of disaster and the difference between who lives and who dies is to a greater or lesser extent a social calculus." As such, natural hazards are a confluence of biophysical vulnerability and social vulnerability. Despite having the same degree of risk and exposure, socially vulnerable populations are disproportionately affected by disaster-related outcomes compared to less socially vulnerable populations due to the lack of resources and coping capacity. Wealthier people are more likely to own homes with flood insurance and other protective measures to protect property damage from hurricanes and floods. In addition, affluent people tend to have greater accessibility to evacuation shelters and financial reserves than their counterparts to recover from the catastrophic impacts of natural disasters. On the other hand, vulnerable populations are more likely to reside in flood-prone areas with cheaper real estate and that often do not have flood insurance due to their economic status. Social vulnerability can be determined by the socio-economic and demographic characteristics of people and places that are associated with unfavorable and susceptible conditions in the wake of natural hazards. This in turn influences the extent to which vulnerability impacts different populations (Cannon, 1994; Cutter, 1996; Park & Xu, 2020; Wisner et al., 2004).

2.3. Theoretical Frameworks of Vulnerability

The vulnerability of individuals and locales is subject to both physical and social vulnerability. In the conventional hazards paradigm of risk and disaster research, the great concern was to reduce biophysical vulnerability (i.e., exposure, intensity, frequency of natural hazards) by identifying human occupancy within the at-risk zones (Cutter, 2001; Keith Smith, 2013). Measuring social vulnerability is not as straightforward as quantifying the physical vulnerability due to its complex and multi-dimensional properties arising from environment-society interactions. Social constructions of vulnerability have been conceptualized and refined

by scholars in vulnerability research. The theoretical frameworks are all anchored with a human ecological framework, each with a different focus (C. G. Burton, Rufat, & Tate, 2018). Since these theoretical models have become the cornerstone of vulnerability science at present, it is imperative to systematically review what efforts have been made to measure vulnerability. This section briefly elucidates the trajectories and the characteristics of major vulnerability frameworks to date.

2.3.1. Pressure and Release Model

In the pressure and release (PAR) model, natural disasters are seen as the embodiment of two different realms in which the underlying processes shaping vulnerability and the hazardous events converge. Both socio-economic processes and physical exposure put pressure on a particular location, increasing vulnerability of place (i.e., pressure). As place vulnerability accumulates, it reaches a tipping point where the conditions in an area become unsafe and have a greater potential for disastrous outcomes (i.e., release). This model conceptualizes how disasters arise when natural hazards affect vulnerable populations, focusing on the "progression of vulnerability". The transformation of vulnerability is addressed in three steps: root causes, dynamic pressures, and unsafe conditions (Birkmann, 2006; Wisner et al., 2004).

Root causes are indirect factors that give rise to vulnerability on a global scale such as social-demographic and political processes that can affect unequal access and distribution of resources among different social groups in a given society. They are pervasive and exert their influence on a global scale such as inadequate governance, a weak economic system, and limited influence in decision making. Dynamic pressures encompass both macro- and micro-level social processes that transfer the root causes into unsafe conditions such as rapid population change, urbanization, and environmental degradation. Combined with the occurrence of natural

hazards, each step in the progression of vulnerability gradually builds up and transforms the root causes into unsafe conditions, increasing pressure on the entire social system. Unsafe conditions are when human vulnerability is substantiated in space and time coupled with a hazard. These conditions can include populations or communities residing in hazard-prone areas which lack disaster relief and mitigation strategies.

Overall, the PAR model is significant in vulnerability research in that it seeks to explain the socially constructed vulnerability to natural hazards in macro-level social contexts, taking into account the nexus of underlying drivers and dynamic processes, and how these social factors and unsafe conditions interact with natural hazards in a sequential fashion. Nonetheless, this model has been criticized for being too extensive and ambiguous to distinguish the causal relationships between root causes, dynamic pressures, and unsafe conditions in a quantitative way (Birkmann, 2006). Therefore, this conceptual model leaves the question to researchers on how this framework can be applied to practical empirical studies.

2.3.2. Hazards of Place (HOP) Model

Vulnerability is manifested in space and place at various levels of geography in the shape of human settlement in hazard-prone areas. The hazards of place (HOP) model posits vulnerability as a latent and multi-dimensional feature of society within the geographic domain. The HOP model is a place-based approach that integrates both biophysical risk exposures and underlying social conditions (Cutter, 1996, 2003). Spatial locality is the focal point of this conceptual framework, and it also includes the time dimension given the temporal dynamics of vulnerability (Figure 1).

In this model, vulnerability is represented by an assemblage of risk (likelihood of meteorological or geophysical events) and mitigation measures (social interventions to lessen the

impacts of disasters such as planning), which subsequently generate the initial place-specific hazard potential. The hazard potential can be transformed into biophysical vulnerability and social vulnerability when it infiltrates the layer of geographical contexts (i.e., location-specific conditions such as proximity to hazardous areas) and the layer of social fabrics (i.e., social-demographic characteristics of people and places), respectively. For example, if a hurricane has high wind speeds it demonstrates high biophysical vulnerability. However, if it has low wind speeds then the area it affects will be only exposed to low biophysical vulnerability. In terms of social vulnerability, the concept is the same as if a hurricane hits a wealthy community, the overall social vulnerability from that hazard potential would be reduced. In contrast, if the same hurricane affected a community with multiple socially vulnerable conditions, then the hazard potential would be transformed into high social vulnerability. The overall place vulnerability is a consequence of the interaction between biophysical vulnerability and social vulnerability, and this in turn influences future risk management and mitigation strategies.

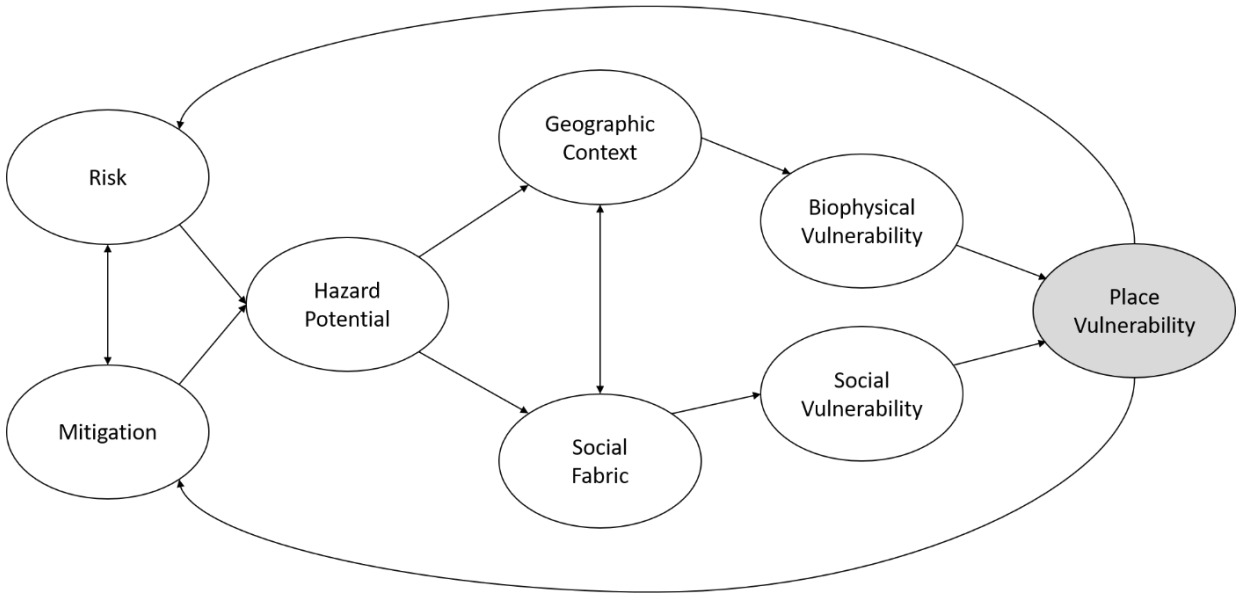

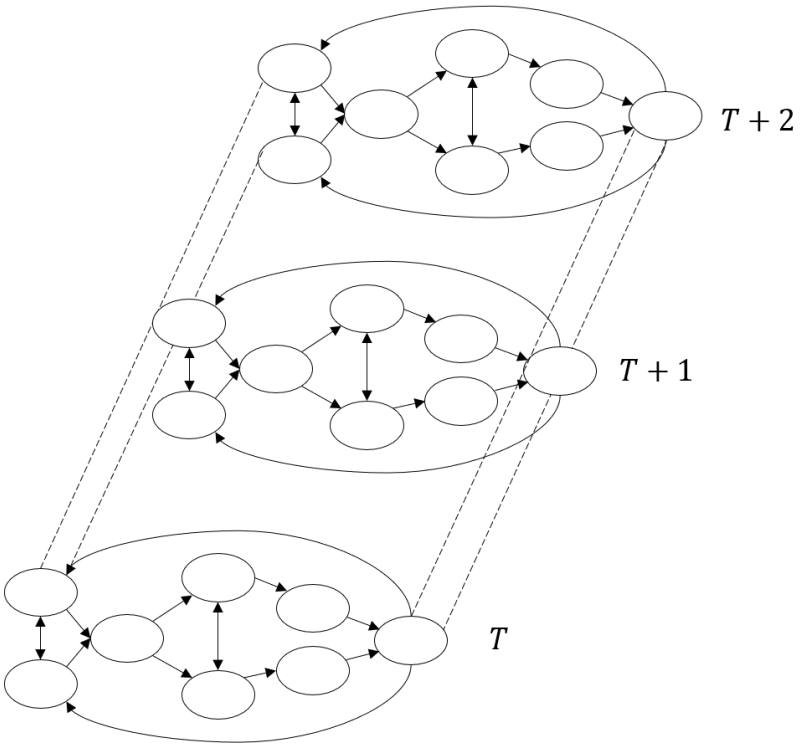

Figure 1. Hazards of Place (HOP) model of vulnerability (adapted from Cutter, 1996)

Unlike the intricate PAR model, the HOP model is relatively intuitive. It looks at the relationships between biophysical vulnerability and social vulnerability to a single or multi-hazard through the lens of local spatial contexts. It puts more emphasis on the role of locale or place, enabling social scientists to capture the socio-spatial variability of vulnerable places and people (Cutter, 2003). This place-specific conceptual model has laid the foundation for assessing vulnerability in a quantifiable way using the social vulnerability index (SoVI) approach (Cutter et al., 2003). Consequently, the HOP model has been widely employed in extensive empirical studies during the past decades (C. G. Burton et al., 2018).

2.3.3. Vulnerability Framework in Sustainability Science

Turner et al. (2003) contend that the PAR model subordinates the role of biophysical subsystems to socio-economic and political factors. As an alternative, the vulnerability framework of sustainability science addresses the interaction between the biophysical

environment and human society. This model attempts to explain how vulnerability (exposure and sensitivity) can be amplified or mitigated through different ways of responding (resilience and adaptation) in a feedback loop across scales (C. G. Burton et al., 2018). The environmental and societal factors are all non-directional and scale-dependent, which means the factors contributing to vulnerability have a nonlinear bidirectional causality with each other at various spatial scales. For instance, during the 2005 hurricane Katrina event, New Orleans was disproportionately affected by both location-driven factors and factors that were working from outside the city. Specifically, New Orleans was built in low-lying flood plains, contributing to its high biophysical vulnerability. This was compounded by income inequality and the placement of low-income communities in the most vulnerable areas of the city. Outside of the city itself, the governmental response to the crisis led to greater havoc in the city both during and after the initial disaster event occurred. The complexity of the situation makes it impossible to decipher between which factors are causative and which are consequential. Instead, they all operate in a feedback loop, leading to amplified local vulnerability. Although this framework acknowledges the multi-scale properties of vulnerability assessment, it is fundamentally in accord with the HOP model in that it emphasizes the importance of the place-based approach to understanding how vulnerability varies from location to location. The place-based analysis is indispensable to elicit a set of generalized characteristics of place vulnerability in the linked human-environment system.

In summary, vulnerability science has shifted its focus from biophysical hazards to social vulnerability in the context of human-environment interaction. Such conceptualization of vulnerability is directly related to how we can measure its sensitivity to a single or multi-hazard. The HOP model (Cutter, 1996) is the most commonly adopted in empirical vulnerability studies through the lens of geography, space, and place to reveal the spatial variation of vulnerability

(Cutter, 2009). Despite this holistic perspective, however, critical issues and challenges still remain in vulnerability assessment (C. G. Burton et al., 2018). This dissertation research is also predicated on the HOP model, but it aims to bridge the model's gaps and shortcomings, which will be discussed in the following section.

2.4. The Social Vulnerability Index

Social vulnerability could impinge on people's ability to prepare for, deal with, and recuperate from the impacts of a natural hazard event. Most research on vulnerability assessment is based upon composite indicators that measure the absolute level of susceptibility and resilience. The HOP model is at the core of the spatial representation of social vulnerability to natural hazards at the local level (C. G. Burton et al., 2018; Cutter, 2003; Rufat, 2013). Cutter et al. (2003) first introduced the social vulnerability index (SoVI) in an attempt to translate the multi-dimensional "social space of vulnerability" into a spatially informed quantifiable measurement.

The SoVI quantifies and identifies the degree to which social vulnerability is spatially differentiated with a single composite index. Focusing on particular places and localities, it captures the cross-sectional and spatial variation of social vulnerability based on the underlying socio-economic and demographic characteristics of populations (Park & Xu, 2020). It allows us to better understand where our society is vulnerable to the loss potential of natural hazards due to social conditions, and thus it is crucial in helping establish more effective mitigation strategies (Cutter, 2009; Cutter et al., 2003; Cutter & Finch, 2008; David King & MacGregor, 2000; Morrow, 1999).

2.4.1. Design of the Social Vulnerability Index

An extensive body of literature has investigated how to disentangle the complexity of social vulnerability into a single-value indicator using proxy variables that are often place-based aggregate data. Previous studies are largely based upon a deductive, hierarchical, or inductive approach to creating indicators in which the major difference is the structural design of index construction (Tate, 2012). The first approach tries to deduce what social variables can represent the social vulnerability of a given society and what proxy variables can be included in building a composite indicator. Since it is based on a priori theory or general principles from the literature, the resultant index is composed of a small set of social variables, typically fewer than ten. This approach was adopted in the early empirical studies on social vulnerability indices (Cutter et al., 2000; Wu, Yarnal, & Fisher, 2002). The hierarchical method is a hybrid approach integrating participatory processes and local knowledge from stakeholders in determining the relevant social variables and the relative importance of those proxy variables. Generally, the composite index derived from this approach consists of ten to twenty variables wherein the social variables are grouped into several sub-categories (levels) according to the same latent characteristics of vulnerability (C. G. Burton et al., 2018; Tate, 2012). The Center for Disease Control (CDC)'s social vulnerability index (SVI) is a typical example of the hierarchical model (Chakraborty, Tobin, & Montz, 2005; Flanagan, Gregory, Hallisey, Heitgerd, & Lewis, 2011).

Last but not least, the inductive approach is data-driven, and the SoVI is widely known as an example of this approach (Cutter et al., 2003). In order to develop a systematic social vulnerability index, it synthesizes a large number of social variables (more than twenty indicators) that influence unequal exposure and differential effects of natural hazards (Tate, 2012; Yoon, 2012). A number of vulnerability studies have used the SoVI to reveal the regional

discrepancies and spatial distribution of social vulnerability of all-natural hazards (Cutter & Finch, 2008; Park & Xu, 2020; Yoon, 2012) or specific hazard events such as floods (C. Burton & Cutter, 2008; Fekete, 2012; Rufat, Tate, Burton, & Maroof, 2015), tsunami (Wood et al., 2010), sea-level rise (Wu et al., 2002), and hurricane-related damage (C. G. Burton, 2010; Myers et al., 2008; Rygel et al., 2006; C. Wang & Yarnal, 2012).

2.4.2. The Process of Aggregating Social Vulnerability Variables

Once a set of indicators are selected according to the structural design, several more steps are required to compute the composite scores: (1) data standardization (i.e., normalization), (2) data reduction, (3) weighting, and (4) aggregation (Jones & Andrey, 2007; Schmidtlein, Deutsch, Piegorsch, & Cutter, 2008; Tate, 2012; Yoon, 2012). First, all the original variables measured at different scales must be transformed into a common scale by data standardization such as *z* scores (typically used in inductive approach) or linear scaling (e.g., min-max rescaling transformation, maximum value/ratio of value transformation) to make them comparable. In the case of the deductive approach, all the normalized values are aggregated to create final composite scores of social vulnerability for each spatial unit (Tate, 2012; Yoon, 2012). Meanwhile, the inductive approach employs a large set of variables and thereby requires statistical techniques such as principal component analysis (PCA) to identify a smaller number of uncorrelated latent factors, representing a significantly large portion of the variability in the original variables. It is common to use a rotation method to extract a few major independent components, such as the varimax rotation—one of the orthogonal rotations either maximizing or minimizing the loadings (i.e., the correlation between original variables and the components)—for easy interpretation (Rencher & Christensen, 2012; Rogerson, 2014; Schmidtlein et al., 2008).

During the last stage of the index creation, the sign (positive or negative) of the component loadings is adjusted to reflect their known contribution to social vulnerability before aggregation. In other words, the directionality of component loadings is modified to assure whether those components increase or decrease the level of social vulnerability, applying equal weights. Each component may have different weighting considering its relative importance, but the choice of weighting scheme is still inconclusive owing to a lack of scientific and theoretical evidence (Barnett et al., 2008; Tate, 2012). The extracted component scores (or factor scores) are then linearly combined to produce the final composite scores for each geographic unit. Following this procedure, the SoVI is constructed with several dominant factors that are statistically reduced from extensive sets of socio-economic and demographic variables. The specific procedure for creating the SoVI is well-documented (Cutter et al., 2003; Jones & Andrey, 2007; Schmidtlein et al., 2008; Yoon, 2012).

2.4.3. Caveats of Social Vulnerability Index Approach

The SoVI-based approach has been widely popularized over the past two decades due to its applicability in capturing the multidimensionality of social vulnerability to natural hazards. Yet, there exist some critical challenges in its reliability and robustness. The end product of SoVI is subject to change depending on spatial scales (i.e., the level of aggregation), selection of proxy variables, and methodological choices (e.g., weighting schemes, aggregation methods), all of which inevitably entail the researchers' subjectivity and preferences (Barnett et al., 2008; Flanagan et al., 2011; Jones & Andrey, 2007; Spielman et al., 2020). The resultant index is bound to incorporate issues of sensitivity, instability, and uncertainty. There is still no consensus on choosing the best approach and the social variables that truly reflect the multidimensional and latent nature of vulnerability, and different sets of social variables will affect the results of PCA

and SoVI (Tarling, 2017). Several studies have assessed the indices' performance and validity by conducting sensitivity and uncertainty analysis (Schmidtlein et al., 2008; Tate, 2012, 2013).

Some recent studies have raised questions about the predictability of SoVI indicators and have underscored the validation of social vulnerability indices in practical contexts. The empirical ancillary data (e.g., actual property damage or fatality data) have been tested to assess the "explanatory power" of composite indices. Can the exploratory SoVI indices explain the actual outcome of natural hazards in real-world situations (Bakkensen, Fox-Lent, Read, & Linkov, 2017; C. G. Burton et al., 2018; Fekete, 2009; Rufat et al., 2019; Tellman et al., 2020)? Indeed, these methodological challenges and validation issues are primarily concerned with the way in which the social vulnerability indices are formulated. The following caveats and limitations provide the grounds for the improvement of the SoVI-based approach in Chapter 3.

2.4.4. Caveat 1. Social Vulnerability as Spatial and Temporal Dynamics

The aggregated indicator, SoVI, reveals the spatial variation of social vulnerability using categories in which the absolute magnitude is classified ranging from low to high. Much of the current literature on social vulnerability has focused on "vulnerable spatialities," paying special attention to the cross-sectional variation of social vulnerability (Findlay, 2005). In vulnerability science, the place-based approach solely focuses on "spatiality" and "mapping of vulnerability" predominates over the time-based approach (Barnett et al., 2008; Cutter, 2003). Traditional vulnerability studies have been mostly restricted to limited comparison of spatial patterns as a static phenomenon at a particular point in time.

However, as noted by Barnett, Lambert, and Fry (2008, p.15), "vulnerability is the product of phenomena occurring at a range of interlinked spatiotemporal scales." Social vulnerability is not only spatially-variant but also temporally variant because the underlying

social drivers of vulnerability change over time (Birkmann, 2006; Cutter, 1996). Indeed, social vulnerability is temporally dynamic rather than being stationary (Bolin & Kurtz, 2018). Nonetheless, the spatial and temporal dynamics of social vulnerability have not been characterized in a systematic and quantitative way. This is primarily due to the latent nature of social vulnerability, which makes it not directly measurable. Different sets of social variables are used to create SoVIs at different time points, which are often constructed by different numbers of variables and components. This makes the SoVI at different time points not directly comparable (Park & Xu, 2020).

2.4.5. Caveat 2. Social Vulnerability Index Conceals the Heterogeneous Local Contributors

The composite index SoVI has been very useful to quantify the relative magnitude of the overall social vulnerability, providing a practical approach to address the social-spatiality of social vulnerability (Cutter & Finch, 2008; Hogan & Marandola Jr, 2005). But previous studies using the SoVI approach have been limited to the spatial distribution and/or temporal evolution of overall vulnerability (Cutter & Finch, 2008; Park & Xu, 2020) and have not dealt with specific social conditions that contribute to social vulnerability. The index is subject to the common caveats of the aggregate social indicators, especially the unrealistic assumption of spatial heterogeneity of the statistical methods the indicators rely on (Barnett et al., 2008; Frazier, Thompson, & Dezzani, 2014; Hinkel, 2011).

The aggregate composite index SoVI is composed of accumulated layers of multiple social-demographic variables (Fekete, 2012), so it does not account for the specific local social indicators that serve as the proxy of the primary determinants significantly affecting local social vulnerability. The values of the SoVI simply indicate an average level of vulnerability of the areal units, causing “compensability” in which the local primary determinant of social

vulnerability is sacrificed, and it cannot inform what specific social conditions determine the high or low social vulnerability at the locale (Fekete, 2012; Jones & Andrey, 2007; Rufat et al., 2015; Tate, 2013). Understanding the local primary determinants is of great need in policymaking and disaster mitigation, as they identify the specific contexts creating high social vulnerability. Most social vulnerability studies have only focused on the measures and patterns of the overall social vulnerability, and the underlying processes that drive high social vulnerability and its change over time have been largely ignored.

The issues of SoVI are largely rooted in its methodology in which multiple social variables are linearly combined into a few principal components while preserving the greatest variability in the original social variables, and the principal components are then grossly aggregated into the SoVI, a simple global indicator that only shows high or low magnitude (Hinkel, 2011). The statistical reduction techniques such as classic Principal Component Analysis (PCA) or factor analysis are non-spatial statistical methods that assume that the social variables contribute to the principal components homogeneously across space (or across the universe of the dataset). As a result, the SoVI inevitably conceals the local heterogeneity and the differential influences of the social variables to social vulnerability at different spatial locations (Demšar, Harris, Brunsdon, Fotheringham, & McLoone, 2013; Fotheringham & Brunsdon, 1999; Robinson, Lindley, & Bouzarovski, 2019).

2.5. Hurricane Hazards and Coastal Population Trends in the United States

Hurricanes are extreme meteorological events that are likely to be affected by climate change, of which global warming and sea level rise are two foreseeable changes that could impact the consequences of hurricane disasters. The frequency and/or intensity of hurricanes are projected to increase in the coming decades, producing high-speed winds and heavy precipitation

(Arkema et al., 2013; Changnon, Pielke Jr, Changnon, Sylves, & Pulwarty, 2000; Emanuel, 2011; National Academies of Sciences, 2016; Rahmstorf, 2017; Shepherd & Knutson, 2007). Hurricanes have historically proven to be some of the most devastating and costliest natural disasters in the Gulf of Mexico and Atlantic coasts regions of the United States, causing the highest number of fatalities (6,593) and the most damage ($945.9 billion total with the highest average event cost ($21.5 billion per event) between 1980 and 2020 (Diaz & Pulwarty, 2012; NOAA Office for Coastal Management). The primary causes of the massive damage and loss of life are storm-surge flooding and high-speed winds. In particular, drownings from storm surges have been blamed for most hurricane-related casualties and injuries (Dolan & Davis, 1994; Glahn, Taylor, Kurkowski, & Shaffer, 2009; Lin, Emanuel, Smith, & Vanmarcke, 2010)

Increasingly destructive hurricane activities pose a threat to coastal communities along the U.S. Gulf of Mexico and Atlantic coasts. The fast-growing coastal population and demographic shifts along the coastal regions are playing a major role in substantially aggravating the consequences of hurricanes (Changnon et al., 2000; Cutter, Johnson, Finch, & Berry, 2007; Donner & Rodríguez, 2008; Lam, Arenas, Li, & Liu, 2009). Approximately 123.3 million people, which amounts to 39 percent of the total U.S. population, resided in hurricane-prone coastal areas in 2010, increasing to 127 million people in 2016. The population was expected to grow to 134 million (i.e., an 8% increase) from 2010 to 2020 in coastal zones. Coastal populations are projected to increase up to 144 million people (i.e., 20% increase) by 2025 within 100 km of the coastal areas in the United States, thereby continuously increasing coastal population' vulnerability to natural hazards (Crossett, Ache, Pacheco, & Haber, 2013; Culliton et al., 1990; Maul & Duedall, 2019; NOAA Office for Coastal Management).

Rapid coastal population growth puts more people in harm's way, and rising property values by accelerating urbanization and intensive development have put more environment-related stresses along coastal areas (Lam et al., 2009). The burgeoning coastal settlement and coastal-dependent economic activities (e.g., shipping, tourism, fisheries, and petroleum industry) are attracting more people to move to the hurricane coasts. Specifically, the Gulf of Mexico regions have seen an 8.5% increase in population employed in construction industries and a 10.8% increase of employment in maintenance occupations, which is higher than the national rate (D. Cohen, 2019). Overdevelopment due to the high demand for second homes and coastal real estate has increased the risk and exposure of people and infrastructure to hurricane-related damage more than ever before (Changnon et al., 2000; Cutter et al., 2007; Pielke, 1997; Pompe & Haluska, 2011; Keith Smith, 2013).

Coastal communities have experienced tremendous diversification in their demographic characteristics. Over the last several decades, we have seen a rapid increase in aging populations in coastal regions as a huge influx of retirees and second-home owners continue to grow in the hurricane-prone coastal counties. The downward trend of the middle-class in the coastal megalopolises continues, widening the economic polarization between the wealthy and the low-income bracket. However, the declining middle-class population is offset by an inflow of immigrants who are racial minority groups (especially, Hispanic/ Latino) employed in tourism-related service sectors in coastal counties (Crossett et al., 2013; Cutter & Emrich, 2006; Cutter et al., 2007). Coastal counties have become more racially and ethnically diverse than non-coastal counties, which may influence the extent of disaster impacts and social vulnerability across a different set of geodemographics, and thereby complicate the analysis of its vulnerability and resilience to hurricane damage (D. Cohen, 2019; Cutter et al., 2007; Mileti, Darlington,

Passerini, Forrest, & Myers, 1995). In this respect, this dissertation will discuss the overall changing demographics of hurricane at-risk areas in light of demographic differential vulnerability.

2.6. Demographic Differential Vulnerability from an Intersectional Perspective

Recently, a growing interest in intersectional perspective in health outcome and environmental inequalities has led to an analytical framework for social-environmental justice (Alvarez & Evans, 2021; Bauer & Scheim, 2019; Green, Evans, & Subramanian, 2017; Ryder, 2017). Intersectionality theory originated in Black feminist scholarship to explain mutually interconnected systems of social oppression that shape inequalities based on multiple axes of social characteristics such as race/ethnicity, gender, age, class, nationality, immigration status, and other social identity categories. The intersectional approach posits that socio-environmental systems of oppression are inextricably interwoven with an intersection of multiple social identities (Hopkins, 2019; Penner & Saperstein, 2013; Viruell-Fuentes, Miranda, & Abdulrahim, 2012).

Although there is a growing body of literature on intersectionality in population health research, far too little attention has been paid to an intersectional approach in the context of vulnerability research. Social vulnerability to natural hazards has an intrinsic and inseparable relationship with social stratification, which emphasizes the role of intersectionality. Hence, adopting an intersectional perspective allows us to understand how different socio-demographic intersections can collectively shape social vulnerability and how the intersectional factors make certain population groups more susceptible to environmental risk and hazardous events (Bauer & Scheim, 2019; Ryder, 2017). Despite the importance of inter-categorical intersectionality, most vulnerability studies have tended to employ single unitary categorical variables (race or class)

rather than using cross-classified categories (e.g., elderly White males/females) representing intersecting social-demographic identities between demographic groups.

Intersectionality is currently well-documented as a critical conceptual framework in the domain of health research and social sciences. However, intersectional methodological approaches have not yet been fully specified in the research literature ranging from survey analysis, in-depth interviews, biographical analysis, and statistical multi-level analysis (Bauer & Scheim, 2019; Green et al., 2017; Hopkins, 2019). There is no standardized approach to investigate how socio-demographic identities produce spatial and societal inequalities and oppression. One criticism of intersectionality is that, as the number of social dimensions increases, the more difficult it is to interpret the meaning of social stratification, posing methodological challenges for large-scale quantitative analyses (Alvarez & Evans, 2021; Bauer & Scheim, 2019; Evans, 2019; Green et al., 2017; Lutz, 2015; Penner & Saperstein, 2013).

In Chapter 6, this study attempts to understand how different intersectional demographic group memberships can contribute to vulnerability to environmental risks and harms, focusing on hurricane-related damage. Considering diversification of coastal populations, vulnerability to hurricane hazards should analyze racial inequalities in the coastal regions in tandem. Instead of using a single axis of category independently, this study adopts a descriptive inter-categorical intersectional approach based on multiple axes of social dimensions simultaneously—race/ethnicity, gender, and age—to explore the intersection of racial disparities and vulnerability to hurricane hazards in the US Gulf and Atlantic coasts. However, the descriptive intersectional approach employed in this study cannot elucidate the causal processes that contribute to social inequalities (Bauer & Scheim, 2019; Evans, 2019).

Chapter 3. Social Vulnerability Studies at Local and National Scales

3.1. Introduction

Social vulnerability has been widely adopted in identifying vulnerable people and places for disaster preparedness and mitigation. The multi-dimensional properties of social vulnerability cannot be directly measured or observed, and therefore necessitates development of social vulnerability indices (SoVIs) to simplify the latent and complex social conditions that situate certain population groups or places in vulnerable conditions using an aggregate composite indicator (Beccari, 2016; Cutter et al., 2003; Flanagan et al., 2011; Flanagan, Hallisey, Adams, & Lavery, 2018; Yoon, 2012).

As discussed in the previous chapter, social vulnerability has not been fully understood as a spatially explicit and temporally dynamic process changing over time and across space in the literature. Most studies based on the SoVI approach have exclusively focused on the spatial manifestation of vulnerability, neglecting the temporal evolution of vulnerability. But the temporal progression of vulnerability is also a critical element and thus should be incorporated into the analysis of vulnerability in tandem with the spatiality of social vulnerability. The vulnerable status is not firmly fixed or stable, and the vulnerable phase is temporally shifting over time (Cutter, 1996).

Use of the SoVI has been greatly favored in various social science disciplines, in particular geography, environmental studies, disaster research, and epidemiology/public health. It has been criticized for not explicitly explaining what specific local social indicators can serve as proxies for “local primary determinant of social vulnerability (i.e., local indicator variable).”

This is attributed to the way in which the SoVI is designed, relying on principal component analysis (C. G. Burton et al., 2018; Tate, 2012; Yoon, 2012).

While the HOP model emphasizes the importance of the temporal aspects of social vulnerability and local geographic contexts, there has been few empirical investigations into temporal progression and the local determinants of social vulnerability. Chapter 3 mainly addresses two caveats of the social vulnerability index (SoVI) through an empirical analysis of the United States at both local and national scales. Chapter 3.1. presents the spatial and temporal dynamics of social vulnerability at county level in the United States from 1970 to 2010, and addresses the following research questions: “How has social vulnerability changed in the U.S. during the past five decades from 1970 to 2010?” and “What were the prominent trajectories of social vulnerability change across U.S. counties over the last five decades?” Chapter 3.2. further explores the differential contributions of the constituent components of SoVI and investigates how the local indicator variables have evolved over time and across the Greater Houston metropolitan area as a case study using the geographically weighted principal components analysis. Specific research questions are as follows: “How has social vulnerability changed in the Greater Houston from 1970 to 2010?” and “How have the local primary determinants of social vulnerability evolved over time across the study area?” The remainder of this chapter will present the findings of the research.

3.2. Spatial and Temporal Dynamics of Social Vulnerability in the United States from 1970 to 2010: A County Trajectory Analysis[1]

3.2.1. Objectives

The objective of this subsection is to systematically investigate the temporal dynamics of social vulnerability as a critical component in understanding disaster vulnerability. This study aims to provide an overview of the spatial and temporal dynamics of social vulnerability in the United States using U.S. county-level socio-economic and demographic data from 1970 to 2010. There are three primary aims of this study: (1) to examine the prominent trajectories of social vulnerability change in U.S. counties over time; (2) to determine the extent to which the county level social vulnerability is stationary or mutable over time; and (3) to identify locations where social vulnerability has deteriorated over time.

3.2.2. Data

The county-level social, economic, and demographic variables for each decade from 1970 to 2010 were obtained from the U.S. Census Bureau and Social Explorer, which provides tabulated data of the U.S. decennial censuses since 1790. The variables of each decennial census prior to 2010 have been interpolated to the 2010 census county boundaries. The number of variables available to this study varies depending on the census year: 26 (1970), 27 (1980), 30 (1990, 2000), and 31 (2010). The specific variables are shown in Table 1. In addition to the different number of variables available in different censuses, some of the variables might have slightly different definitions depending on the census year. Overall, these variables include a wide range of socio-economic, demographic, and built environment characteristics, which

[1] Portions of this chapter have been published in the *International Journal of Applied Geospatial Research*, co-authored with Dr. Zengwang Xu

represent the county-level vulnerability measured at different social dimensions—e.g., age, gender, race and ethnicity, educational attainment, household structure, income level, language proficiency, housing tenure status, occupation, and other built environment factors, etc.

Some spatial data processing was implemented to ensure the contiguity and comparability of the county-level data. The decennial censuses provide separate statistics for a number of independent cities from the counties in which they are geographically embedded. According to the legal/statistical area description (LSAD) of the U.S. Census Bureau, Virginia has 39 independent cities among 134 counties/county equivalents; both Maryland and Nevada have one independent city. These independent cities and their social variables were merged with nearby counties to form contiguous geography. In total, 41 cities were merged into nearby counties, thereby resulting in 3,067 counties in the conterminous United States, which were the geographical base in this study.

Table 1. Variables used to calculate the social vulnerability index for each decade from 1970 to 2010 (the symbol ✓ represents that the variable is used to calculate the SoVI for the decade)

Variable Description	1970	1980	1990	2000	2010
Percent of females	✓	✓	✓	✓	✓
Percent of population under 5 years old	✓	✓	✓	✓	✓
Percent of population over 65 years old	✓	✓	✓	✓	✓
Median age	-	-	-	-	✓
Percent of other races (1970)	✓	-	-	-	-
Percent African American	✓	✓	✓	✓	✓
Percent Native American	-	✓	✓	✓	✓
Percent Asian	-	✓	✓	✓	✓
Percent Hispanic	-	-	✓	✓	✓
Percent of persons in group quarters (mental hospital, home for the aged and dependent, other institution)	✓	✓	✓	✓	✓
Percent of population 5 years and older in linguistically isolated households	-	✓	✓	✓	✓
Percent of population less than high school graduate	✓	✓	✓	✓	✓
Average income for population 14 years and older (1970), Per capita income (in dollars) (1980-2010)	✓	✓	✓	✓	✓
Percent of families below poverty line	✓	✓	✓	✓	✓
Percent of female-headed households with own children under 18 years old at present	✓	✓	✓	✓	✓
Percent females participating in civilian labor force	✓	✓	✓	✓	✓
Percent of civilian labor force unemployed	✓	✓	✓	✓	✓
Percent employed in primary extractive industries	✓	✓	✓	✓	✓
Percent employed in transportation and material-moving occupation	✓	✓	✓	✓	✓
Percent employed in service occupation	✓	✓	✓	✓	✓
Percent of families/households earning $50,000 and over	✓	✓	✓	✓	✓
Percent of rental occupied housing units	✓	✓	✓	✓	✓
Percent of housing units that are mobile homes	✓	✓	✓	✓	✓
Percent of housing units that were built 1939 or earlier	✓	✓	✓	✓	✓
Percent housing units with 5 or more (1980), 10 or more units in structure (1970, 1990-2010).	✓	✓	✓	✓	✓
Average value of owner-occupied housing unit	✓	✓	✓	✓	✓
Average rent (in dollars) for renter-occupied housing units	✓	✓	✓	✓	✓
Percent households with no television set (1970), no telephone service available (1980-2010)	✓	✓	✓	✓	✓
Percent of household with no automobiles or vehicles	✓	✓	✓	✓	✓
Percent of foreign-born population	✓	✓	✓	✓	✓
Percent of households with social security income	✓	✓	✓	✓	✓
Percent urban population	-	✓	✓	✓	✓

3.2.3. Methodology

To begin with, this study constructed the county-level social vulnerability index (SoVI) for each decennial year from 1970 to 2010 by adopting the procedure proposed by Cutter et al. (2003). For each decennial year, principal components analysis (PCA) was performed to derive a new set of independent principal components that together represent the majority of variation in the original variables. The first step to construct the SoVI is to convert all original variables to z-scores so that they can be compared to one another. The next step is to apply a linear transformation (i.e., rotation) method to create the uncorrelated components that represent a large portion of the variance in the original variables (Rogerson, 2014). The varimax rotation employed in this study is one of the orthogonal rotations, which either maximize or minimize the loadings (i.e., correlation between original variables and the components) for easy interpretation of the components (Rencher & Christensen, 2012). A few major components are selected to represent the majority of variation in the original variables, and then these components are linearly combined to create the SoVI for each county.

One of the major challenges of the SoVI is that different years should not be directly compared due to the multi-dimensional attributes of social vulnerability, data availability, and the different variables selected at different times (C. G. Burton, 2010; Fekete, 2009; Jones & Andrey, 2007; David King, 2001; Yoon, 2012). In this study, the SoVI can be used to assess the relative level and the spatial variation of social vulnerability in the United States for each decade from 1970 to 2010. However, they should not be directly compared across different decades, as the values of SoVI at different decades are essentially not comparable to each other.

To compare over different years, the SoVIs of counties in each decade from 1970 to 2010 were converted into a series of ordinal vulnerability states in accordance with the five 20-

quantiles of the SoVI (i.e., 0-20% as low, 21-40% as medium-low, 41-60% as medium, 61-80% as medium-high, and 81-100% as high). The social vulnerability of each county in each decade was represented as one of the ordinal categories corresponding to the 20-quantiles. Each county has a sequence of social vulnerability categories from 1970 to 2010, which represent the county's changing social vulnerability states over different years. The sequence of social vulnerability states can be represented in the state-sequence (STS) format (Gabadinho, Ritschard, Studer, & Müller, 2009). For example, the SoVI of Maricopa County in Arizona has a "low" social vulnerability state in 1970 and 1980, "medium-high" in 1990, "medium" in 2000, and "high" in 2010, the state-sequence format of the changing social vulnerability of Maricopa County is (low, low, medium-high, medium, high) from 1970 to 2010.

Counties having a sequence of SoVI states can then be classified according to the similarity (or dissimilarity) of their changing social vulnerability states over time by using sequence alignment analysis (Delmelle, 2016). The sequence alignment (or optimal matching) analysis was initially developed in the field of molecular biology to determine the extent to which two DNA configurations are similar (Kruskal, 1983). It was not until the late 1980s that social scientists adopted the sequence alignment analysis in exploratory spatial data analysis (ESDA) (Hollister, 2009; Stehle & Peuquet, 2015). Since then, sequence alignment analysis has been widely used to assess the similarity among categorical sequences (strings) and to extract the prominent pattern among a collection of sequences (Shoval & Isaacson, 2007). Many researchers have utilized this method to investigate the development process of welfare programs (Abbott & DeViney, 1992), career trajectory and life courses (Abbott, 1991; Abbott & Tsay, 2000; Brzinsky-Fay & Kohler, 2010), and transportation research (Joh, Arentze, Hofman, & Timmermans, 2002; Kwan, Xiao, & Ding, 2014; J. H. Lee, Davis, Yoon, & Goulias, 2017). A

recent study quantified U.S. neighborhoods as a series of categorical typologies based on longitudinal socio-economic, demographic, and housing characteristics to examine how the spatial patterns of urbanization process and neighborhood poverty have evolved over time in the United States (Delmelle, 2016; K. O. Lee, Smith, & Galster, 2017). This study adopts a similar procedure to that used by Delmelle (2016) to explore the spatial and temporal dynamics of social vulnerability at the county level in the United States from 1970 to 2010.

The key to the sequence alignment method is to calculate the similarity (or dissimilarity or distance) between sequences of states. Each sequence consists of a set of elements observed at multiple points in time, and each element in a sequence represents a categorical state or event (Hollister, 2009). There are three methods to assess the similarity of sequences: Longest Common Prefix (LCP), Longest Common Subsequences (LCS), and Optimal Matching distances (OMA). All the approaches use different ways to define the dissimilarity (or distance or cost) between the sequences of states. The OMA, which is the most commonly used approach, measures the distance (or dissimilarity) between sequences by using the substitution cost (Delmelle, 2016; Gabadinho et al., 2009; Hollister, 2009; Lesnard, 2006; Studer & Ritschard, 2016). To select the most appropriate method, researchers should try out different methods rather than relying exclusively on one method (Brzinsky-Fay & Kohler, 2010; Studer & Ritschard, 2016).

The LCS and OMA produced the same distance matrix in this analysis since LCS can generate the same sequence as OMA does when LCS finds an optimal match between sequences (Lember, Matzinger, & Vollmer, 2014). The OMA was adopted in this study to determine the similarity of the sequences of social vulnerability states of counties. It determines the degree of dissimilarity by computing the minimum number of editing operations (i.e., insertion, deletion,

and substitution) to make the two sequences identical, and this is also known as substitution cost (Abbott & Tsay, 2000; Brzinsky-Fay & Kohler, 2010; Joh et al., 2002; Studer & Ritschard, 2016). The Needleman-Wunsch algorithm, which is implemented in the TraMine package in R, is widely used to find the least substitution cost to match a source sequence to a target sequence through the insertion/deletion substitution operations (Needleman & Wunsch, 1970). The more operations involved in transforming two sequences into the identical conformation, the greater the substitution cost. The resulting cost is derived in a symmetrical $n \times n$ matrix, W:

$$W = \begin{bmatrix} w_{11} & \cdots & w_{1n} \\ \vdots & w_{ij} & \vdots \\ w_{n1} & \cdots & w_{nn} \end{bmatrix}$$

where n represents the number of unique states in the sequences (Gabadinho et al., 2009; Needleman & Wunsch, 1970; Studer & Ritschard, 2016), w_{ij} represents the substitution cost between two sequences (for example, s_i and s_j), and W is the symmetrical substitution-cost matrix (w_{ij}=w_{ji}).

Typically, substitution cost has been measured in different ways based on a priori knowledge, e.g., the attributes of the states, quantitative indices, or transition rate (Hollister, 2009; Studer & Ritschard, 2016). To avoid subjectivity, transition rate is often used to determine the similarity among all possible combinations of states. More precisely, for $i \neq j$, the substitution cost derived from transition rate can be calculated as follows: $2 - p(i|j) - p(j|i)$, where $p(i|j)$ is the transition rate or probability that state i at time t has changed into a different state j at time $t + 1$. In this study, we employed the transition rate approach to obtain the substitution cost between sequences of social vulnerability states of counties. The less frequent

transition rate between the states, the higher the substitution cost (Delmelle, 2016; Hollister, 2009; Studer & Ritschard, 2016).

Table 2 illustrates the substitution costs calculated based on the transition rates. In this study, there are not many counties that change their social vulnerability states directly from low to high, so the cell of low (row) to high (column) in the substitution cost matrix has the maximum value. Meanwhile, the transition from medium-low to medium or medium-high to high is more frequent, and the corresponding cells have relatively low values.

Table 2. Substitution cost matrix between different states of social vulnerability

	Low	Medium-Low	Medium	Medium-High	High
Low	0	1.51	1.80	1.90	1.96
Medium Low	1.51	0	1.50	1.76	1.92
Medium	1.80	1.50	0	1.52	1.84
Medium High	1.90	1.76	1.52	0	1.57
High	1.96	1.92	1.84	1.57	0

The sequence alignment analysis offers a quantitative means to study many changing social phenomena (Brzinsky-Fay & Kohler, 2010). It allows us to study the temporal dynamics of social vulnerability in a rigorous manner in this study. As social vulnerability is considered a place-based characteristic that varies over time, this method enables us to examine more accurately the different place-based trajectories of changing social vulnerability and where they occur in the United States. The overall methodology is described in Figure 2. All analyses were carried out using SPSS 25.0 and the TraMineR package in the statistical software R (Gabadinho, Studer, Mueller, Bergin, & Ritschard, 2016).

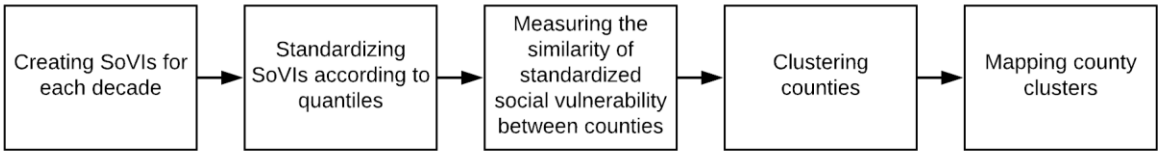

Figure 2. Overall methodology to study social vulnerability dynamics

3.2.4. Spatial Patterns of Social Vulnerability in the United States

This study employed the PCA method to derive a SoVI to assess the relative magnitude of social vulnerability of counties based on the hazards of place (HOP) model proposed by Cutter et al. (2003). The inductive approach was chosen for county-level data of every decade from 1970 to 2010. The Kaiser-Meyer-Olkin (KMO) test was performed to determine if the number of variables is adequate for PCA analysis. The variables are usually considered being suitable for the PCA method if the KMO index is greater than 0.5 (Williams, Onsman, & Brown, 2010). The KMO indices of the variables at each decade from 1970 to 2010 were at least 0.78. For every decade, the PCA analyses produced seven to eight principal components that explained 72 to 78 percent of the total variability in the original variables.

Table 3 summarizes the principal components derived from the original county-level variables for each decade from 1970 to 2010. The components are named based on the original variables that have significant contribution to the components (i.e., those variables with high loading, which represents the correlation between the variable and component). Although the names assigned to the dominant components are based on the high-loading variables, other variables also contribute to the components, just not as much (Rygel et al., 2006). As can be seen in Table 3, although the 7-8 principal components are characterized by a few socio-economic and demographic characteristics, each component contains different variability of the original

variables during different decades. The main county-level variables for the major components are socioeconomic status and wealth. Other variables significantly contributing to social vulnerability include age (i.e., percent of elderly and children), race (i.e., percent of African American, Asian, Hispanic, and Native American), gender (i.e., percent of female population), and built environment (i.e., housing type and housing tenure status etc.). This is consistent with what has been found by Cutter and Finch (2008).

Mapping SoVI can reveal the spatial variation of social vulnerability. As shown in Figure 3, distinctive spatial patterns exist in the social vulnerability in the United States. During the study period (1970 – 2010), the most socially vulnerable counties are located along the U.S. - Mexico border (Arizona, New Mexico, and Texas), in the Pacific Southwest region (California and Nevada), and the Gulf Coast region; and the least vulnerable counties are located in Northeast and East North Central in the Midwest. High and medium-high socially vulnerable counties are also found in Appalachia (especially, in Kentucky and West Virginia in the central Appalachian region) from 1970 to 2000, but the social vulnerability of these counties decreased in 2010. There is a concentration of high social vulnerability in the West North Central region (North Dakota, South Dakota, and Nebraska) since 2000. The entire southern tip of Florida has become highly vulnerable since 2000. The Midwest and inland areas in the South-Atlantic (Tennessee, North Carolina, and South Carolina) - Mid-Atlantic regions progressively turn into low vulnerability after 1970. These spatial patterns are consistent with what has been found by Cutter and Finch (2008) and Yoon (2012).

Table 3. The principal components used to construct the SoVI of U.S. counties from 1970 to 2010

Year	1970	1980	1990	2000	2010
Percentage of total variance explained	71.5	76.6	78.1	77.9	75.1
Number of components	7	8	7	7	8
Major components (% variance explained)	1. Socioeconomic status (23.3) 2. Age (17.7) 3. Housing type & Immigration (8.7) 4. Primary sector employment (6.9) 5. Population in group quarters & Female (5.7) 6. Service sector employment (5.1) 7. Unemployment (4.0)	1. Wealth (26.2) 2. Socioeconomic status & Race (Black) (14.1) 3. Age (10.3) 4. Built environment & Transportation workers (7.3) 5. Language barrier & Ethnicity (Hispanic) (6.2) 6. Population in group quarters & Service sector employment (4.6) 7. Unemployment (4.2) 8. Race (Native American) (3.6)	1. Wealth (28.5) 2. Socioeconomic status & Race (Black) (17.5) 3. Language barrier & Ethnicity (Hispanic) (9.3) 4. Age (7.6) 5. Built environment & Transportation workers (6.4) 6. Race (Native American) (5.1) 7. Population in group quarters & Female (3.8)	1. Wealth (27.7) 2. Household composition & Poverty (19.0) 3. Language barrier & Ethnicity (Hispanic) (8.6) 4. Age (7.0) 5. Built environment (6.0) 6. Population in group quarters & Female (5.6) 7. Race (Native American) & Service sector employment (3.9)	1. Wealth (24.1) 2. Socioeconomic status (18.6) 3. Age (8.3) 4. Language barrier & Immigration (6.3) 5. Vehicle availability & Tenure (5.6) 6. Population in group quarters & Female (5.1) 7. Race (Native American) (3.8) 8. Service sector employment (3.2)

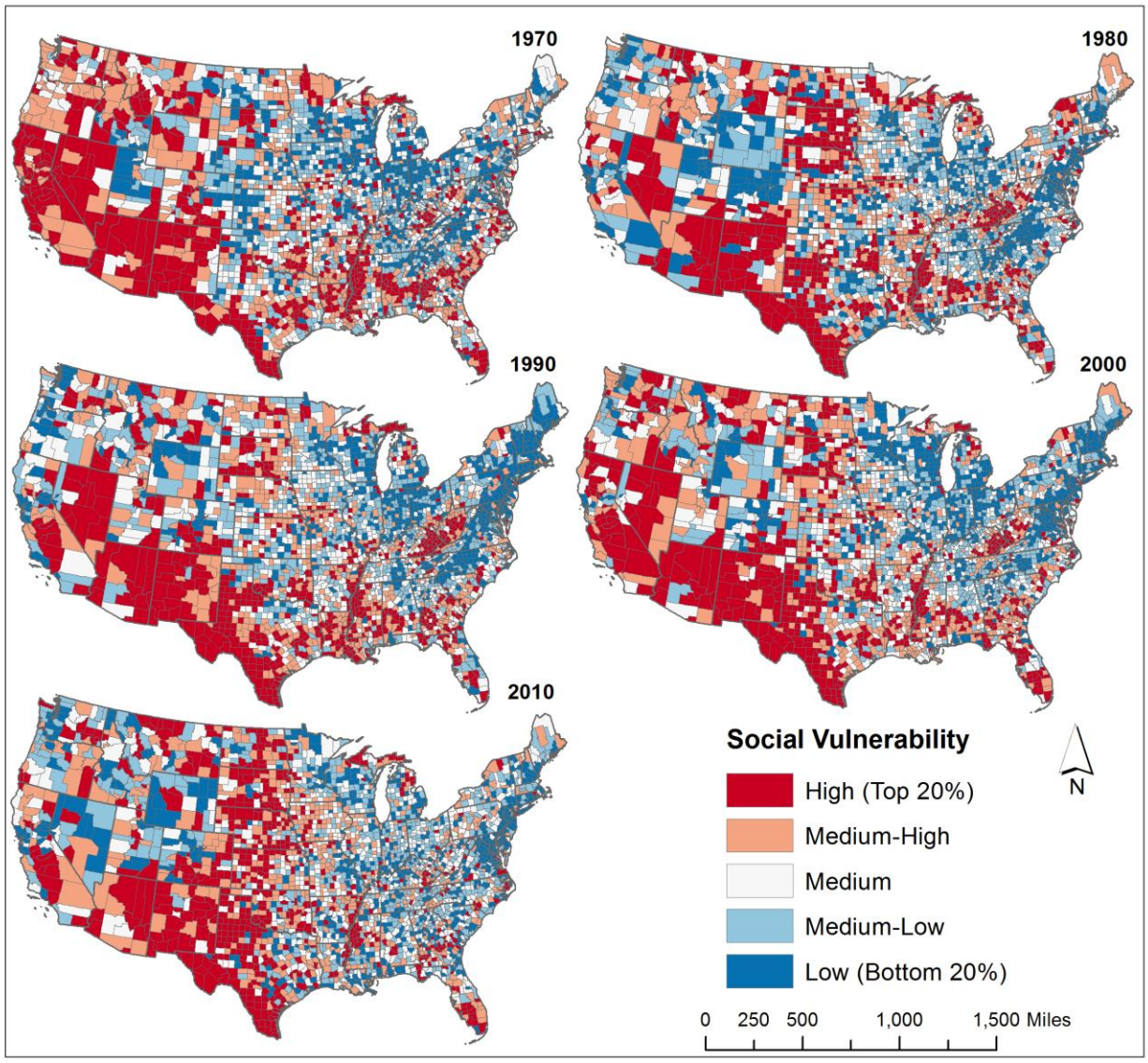

Figure 3. Spatial patterns of decadal social vulnerability indices (1970-2010)

3.2.5. Social Vulnerability Trajectories of U.S. Counties

This study further examines the temporal dynamics of social vulnerability of U.S. counties from 1970 to 2010 in a quantitative way. The changing vulnerability of each county from 1970 to 2010 is represented as a sequence of vulnerability states. The sequence represents the profile of the county's changing social vulnerability over time. Sequence alignment analysis in conjunction with hierarchical clustering analysis (Ward's method) is used to find similar or

distinct profiles of changing social vulnerability of counties (Gabadinho, Ritschard, Mueller, & Studer, 2011; T. King, 2013). Four clusters are found in U.S. counties, and each has a unique profile of social vulnerability change over time. Figure 4 plots the changing frequency of counties in different vulnerability states in each cluster. Figure 5 presents the counties in each cluster.

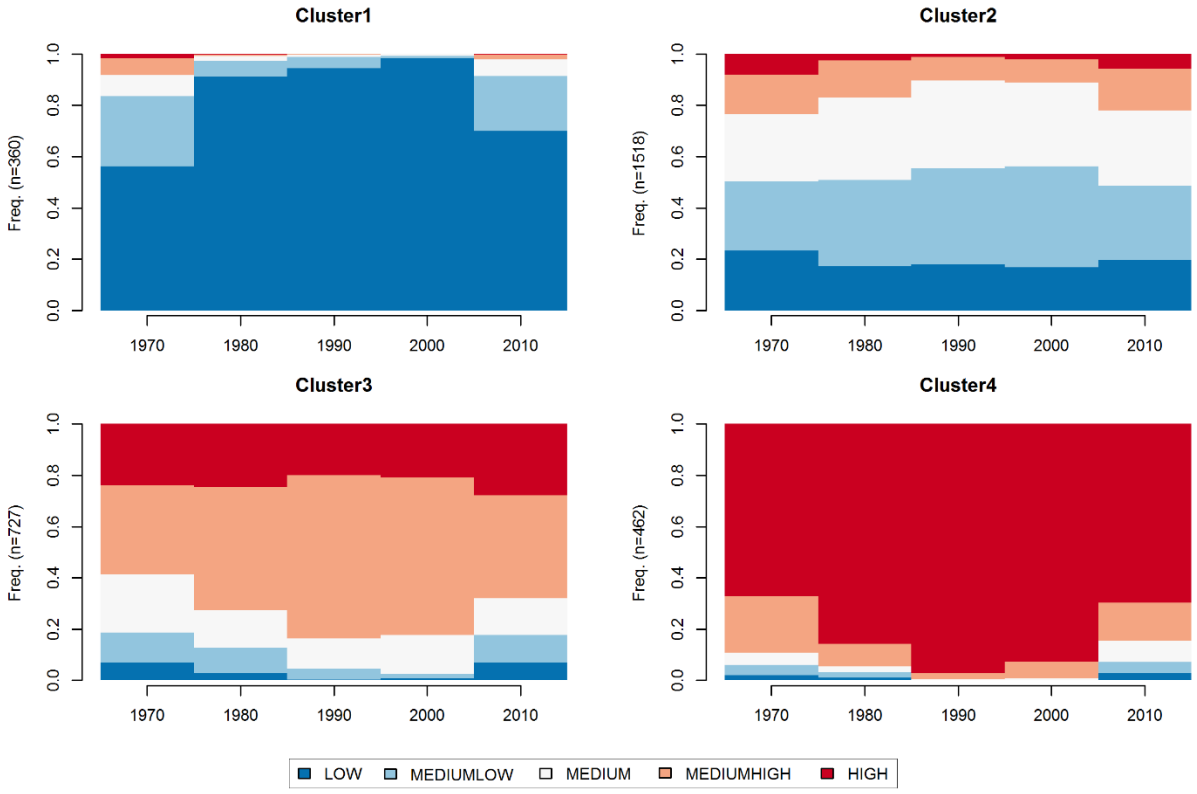

Figure 4. Frequency of counties in different vulnerability states in each decade in each cluster

Figure 4 shows the frequency of counties of different social vulnerability states in each cluster of counties, and how the portions of counties in each vulnerability state changed over time. For instance, the majority of counties in cluster 1 have persistent low vulnerability over time whereas in cluster 4 most counties have high vulnerability. Clusters 2 and 3 have varying degrees of vulnerability. The plot of cluster 2 shows that over time only a small portion of

counties have high social vulnerability, and the rest of counties spread in other social vulnerability states. The plot of cluster 3 shows that over time only small portions of counties have low, low-medium, or medium social vulnerability, and large portions of counties have high or medium-high social vulnerability. The four clusters of counties are mapped to show where these four different temporal dynamics of social vulnerability occur in the United States (Figure 5). The mean trajectories of social vulnerability of each cluster are plotted in Figure 6. Each cluster has demonstrated distinctive characteristics.

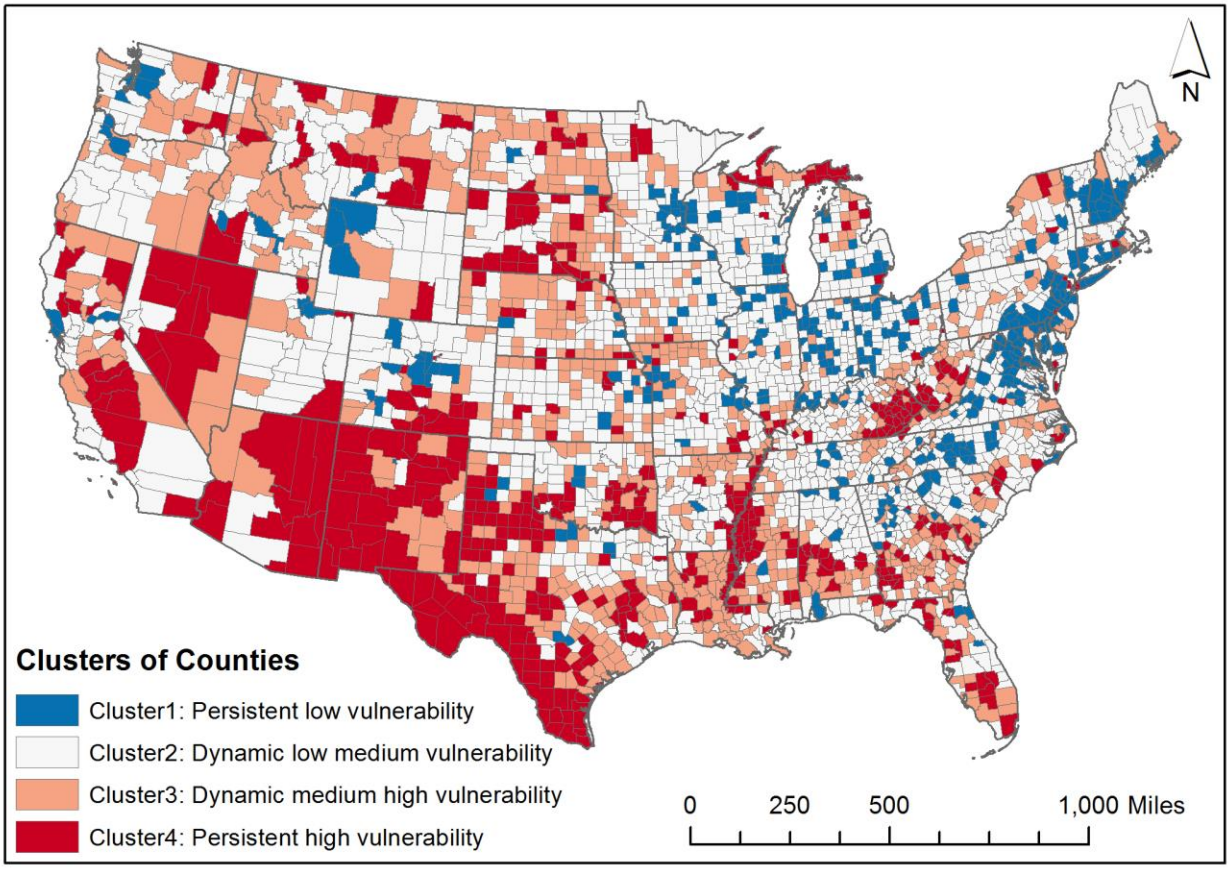

Figure 5. Spatial distribution of the counties in different clusters from 1970 to 2010

Cluster 1 – Persistent low vulnerability: Counties in cluster 1 are characterized by their persistent low social vulnerability over time with 360 (out of 3,067) counties falling into this category. More than 80% of counties have low or medium-low social vulnerability in each

decade from 1970 to 2010. These counties are mainly concentrated in the Northeast: New England, south of the Middle Atlantic, and northern part of the South Atlantic region, and some others spread out across the East North Central region in the Midwest.

Cluster 2 – Dynamic low-medium vulnerability: The majority of counties in cluster 2 are characterized by low, medium-low, or medium level of social vulnerability with 1518 (out of 3,067) counties falling into this cluster. Only a small portion of counties have high social vulnerability. The proportions of counties in the other social vulnerability states are relatively large and stable over time (Figure 4). In each decade, around 80% of counties in this cluster have lower than medium social vulnerability. The counties in this cluster are mainly located in the hinterland of the northern coastal plain and in the eastern Great Plains. Several clusters can be identified in the Rocky Mountain region (Wyoming, Utah, Colorado), the northwest region (Oregon), the northeast/mid-Atlantic region (Maine, New York, Pennsylvania), and the upper south-central region (Arkansas, Mississippi, Tennessee).

Cluster 3 – Dynamic medium-high vulnerability: Counties in cluster 3 are characterized by medium-high social vulnerability with 727 (out of 3,067) counties falling into this cluster. In each decade, more than half of the counties in this cluster have medium-high or high social vulnerability. About 20% of the counties have high social vulnerability in each decade from 1970 to 2010. In 1970, the counties having medium-high social vulnerability were 30 to 40%, but the proportion of counties continued to increase up to approximately 60% in 2000 (Figure 4). In 2010, the mean social vulnerability of cluster 3 dropped slightly (Figure 6). About a 10% increase in the number of counties with medium, medium-low, and low vulnerability states appears to contribute to lowering the mean level of social vulnerability comparing with 2000 (Figure 4 and Figure 6). Counties in this cluster disperse across the United States; small clusters

appear in southern Texas and Louisiana near the Mississippi River and in the northern Great Plains. In most cases, they surround or are immediately adjacent to counties of high social vulnerability and serve as the buffer between clusters 2 and 4.

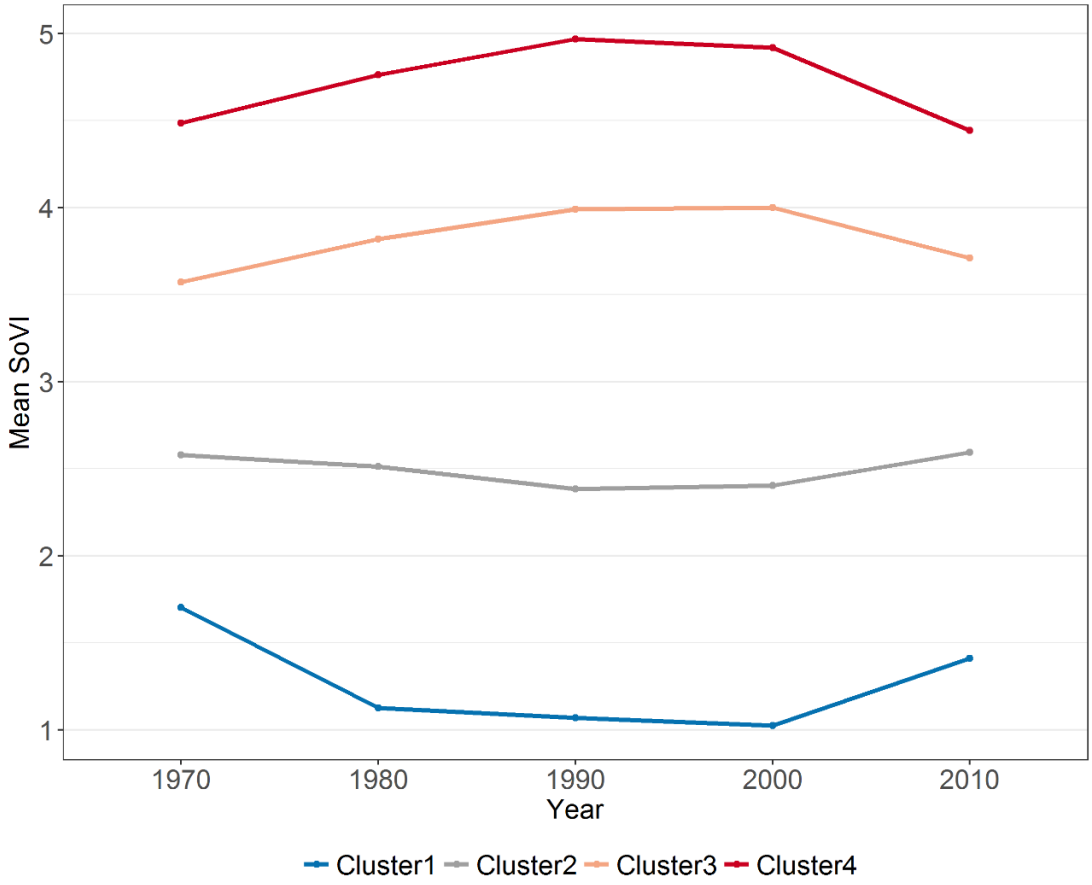

Figure 6. The trajectories of mean social vulnerability of each cluster

Cluster 4 – Persistent high vulnerability: Counties in this category have the opposite vulnerability state to counties in cluster 1, and more than 80% of the counties (100% in 1990 and 2000) have been dominated by high or medium-high social vulnerability in every decade since 1970 with 462 (out of 3,067) counties falling into this cluster. Figures 4 and 6 illustrate that cluster 4 has an upward trajectory in social vulnerability since 1970, reaching an all-time high in 1990 and 2000. In 2010, the vulnerability declined as a result of the increase in counties with

low, medium-low, and medium social vulnerability (Figure 4). These most socially vulnerable counties are located in the Pacific Southwestern and the U.S.-Mexico border regions. They are also concentrated in the Appalachian region and along the lower Mississippi River. Small clusters spread in the lower coastal plain. Since these areas have persistent high social vulnerability over time, particular attention should be paid to mitigation efforts here. Hazards occurring in these areas could result in aggravated consequences due to their vulnerable social condition.

We further explored the social variables that contribute to the differential social vulnerability of the clusters of counties. We calculated the medians of all the social variables at different times for counties in each cluster. Ten variables that have the largest contrast in their medians between cluster 1 and cluster 4 are listed in Table 4. Counties in cluster 4 (in comparison with cluster 1) have higher median values in percent of African-Americans, percent of population with less-than-high-school education, percent of families below the poverty line, percent of female-headed households with own children younger than 18 years old present, percent employed in primary extractive industries, percent of households with no telephone service, percent of households with no automobile/vehicles available, and percent of housing units that are mobile homes (except 1970). In addition, counties in cluster 4 have relatively lower medians in per capita income and percent of female persons participating in the civilian labor force. The higher/lower values of these variables reflect the disadvantaged (or favorable) social conditions in racial composition, poverty and income levels, education, and resource availability that all together result in the persistent high social vulnerability of counties in cluster 4 (or low social vulnerability in cluster 1). The medians of the variables of cluster 2 and cluster 3 are in accordance with their respective levels of social vulnerability between cluster 1 and cluster 4.

Table 4. Median values of ten variables with highest contrast in cluster 1 and cluster 4 (1970 – 2010)

Variables	Clusters	1970	1980	1990	2000	2010
Percent of the population that are African American	Cluster1	0.77	0.93	1.12	1.50	2.05
	Cluster2	1.25	1.21	1.28	1.50	1.66
	Cluster3	1.05	0.95	1.49	1.78	2.06
	Cluster4	3.05	2.69	2.82	3.26	3.48
Percent of population with education less than high school graduate	Cluster1	28.31	16.74	21.99	14.57	10.52
	Cluster2	34.12	22.06	27.42	19.77	14.44
	Cluster3	37.37	25.77	31.03	23.71	17.72
	Cluster4	41.99	29.91	38.76	30.85	23.38
Per capita income	Cluster1	3248.1	6962.0	13656.0	21435.0	27148.0
	Cluster2	2784.3	6100.5	11017.0	17414.5	22342.0
	Cluster3	2571.7	5589.0	9832.0	15715.0	20516.0
	Cluster4	2390.2	4965.5	8914.5	13965.0	17691.0
Percent of families below poverty level	Cluster1	8.65	6.50	5.83	4.80	6.11
	Cluster2	13.40	10.02	10.65	8.61	9.85
	Cluster3	18.03	13.29	14.56	11.89	12.24
	Cluster4	24.36	18.35	20.92	17.28	16.05
Percent of female-headed households with own children < 18 years old present	Cluster1	3.75	10.86	5.29	5.99	6.38
	Cluster2	4.15	11.86	5.84	6.54	7.01
	Cluster3	4.31	12.45	6.08	6.63	7.37
	Cluster4	5.59	14.44	7.91	8.69	9.27
Percent of female persons participating in civilian labor force	Cluster1	38.61	47.35	56.68	58.68	57.93
	Cluster2	35.40	42.42	49.58	53.13	53.21
	Cluster3	32.60	38.95	45.22	48.85	49.84
	Cluster4	30.89	36.70	41.79	44.59	46.01
Percent of employed in primary extractive industries	Cluster1	6.32	4.19	3.51	1.65	1.40
	Cluster2	10.22	8.03	6.17	4.08	3.77
	Cluster3	15.82	12.73	9.79	7.10	6.94
	Cluster4	18.63	15.81	12.53	8.58	8.53
Percent of housing units that are mobile homes	Cluster1	5.13	7.22	8.99	7.58	6.14
	Cluster2	4.72	8.91	12.69	12.96	11.32
	Cluster3	4.19	9.51	14.48	15.57	13.99
	Cluster4	3.78	10.01	16.94	18.51	16.72
Percent of households with no telephone service available	Cluster1	3.52	5.79	3.86	1.58	2.64
	Cluster2	4.74	7.91	6.65	3.03	3.49
	Cluster3	6.01	9.61	9.04	4.20	3.96
	Cluster4	8.59	16.49	14.85	6.59	5.04
Percent of households with no automobiles /vehicles available	Cluster1	10.48	6.43	5.45	4.79	4.23
	Cluster2	13.68	8.72	7.73	6.56	5.52
	Cluster3	15.91	9.44	8.47	7.47	6.19
	Cluster4	18.90	11.14	10.65	9.28	7.39

Note: Cluster1: Persistent low vulnerability; Cluster2: Dynamic low-medium vulnerability; Cluster3: Dynamic medium-high vulnerability; Cluster4: Persistent high vulnerability.

Furthermore, we wonder to what extent the counties have changed their membership in different clusters. Table 5 shows how many counties have increased or decreased and how many

counties have remained unchanged in their social vulnerability in consecutive decades from 1970 to 2010. Cluster 1 and cluster 4 have more counties maintaining their social vulnerability states over time. It shows that counties with very low or very high social vulnerability tend to maintain their social vulnerability states over time. Counties in cluster 2 and cluster 3 are more volatile in changing their vulnerability states over time. In each decade, more than half of the counties have changed (increased or decreased) their social vulnerability states, even though the portion of counties in each social vulnerability state is relatively stable over time (Table 5). For example, many more counties in cluster 2 have changed their social vulnerability states (either increase or decrease) and only a small portion of counties have stayed the same level of social vulnerability in the consecutive decades from 1970 to 2010 (Table 5). However, the portions of counties in different social vulnerability states in cluster 2 appear to be relatively stable over time (Figure 4).

Table 5. Number of counties by changing social vulnerability status per cluster in consecutive decades

Clusters	Change of Vulnerability	1970-1980 (Period 1)	1980-1990 (Period 2)	1990-2000 (Period 3)	2000-2010 (Period 4)
Cluster 1	Up	10	19	6	108
	Stay the same	216	309	334	248
	Down	134	32	20	4
Cluster 2	Up	590	402	435	647
	Stay the same	384	538	653	458
	Down	544	578	430	413
Cluster 3	Up	318	250	197	183
	Stay the same	178	275	315	289
	Down	231	202	215	255
Cluster 4	Up	126	66	8	20
	Stay the same	293	383	424	312
	Down	43	13	30	130

3.2.6. Discussion and Conclusion

This study analyzes the spatial and temporal dynamics of social vulnerability of U.S. counties and examines how they evolve from 1970 to 2010. As the SoVI created at different times should not be directly compared, we implemented a methodology to standardize and cluster the indices over time. This study shows that U.S. counties exhibit four major trajectories of social vulnerability across the United States. These distinctive temporal dynamics also reflect on how local social vulnerability responds to the changing socio-economic and demographic characteristics across the United States since 1970. The counties with different dynamic categories have demonstrated distinctive spatial patterns. In accordance with the present results, a previous study projected that the socially vulnerable areas in 2010 would be concentrated along the U.S.-Mexico, counties that are adjacent to the lower Mississippi River, Pacific Southwest region, and the country's metropolitan areas (Cutter & Finch, 2008). Our analysis suggests that hazard mitigation and prevention efforts should pay more attention to those counties or areas that have persistent high social vulnerability as well as where social vulnerability has demonstrated large changes. Social vulnerability research to date has tended to focus on spatially explicit quantification of vulnerability at a particular point in time rather than the temporal trends. This project is the first longitudinal-transition study to provide quantitative long-term temporal trajectories and durations of the vulnerability status of individual counties from 1970 to 2010, expanding the study by Cutter and Finch (2008).

Social vulnerability has the same nature as many other social indicators as it is latent and multidimensional and cannot be directly measured. The social vulnerability index (SoVI) has been widely used as a proxy to represent the overall measurement of social vulnerability. The comparability of SoVI between different years has been plagued by inconsistencies in the

original variables, the data transformation/normalization methods, the unit of analysis (i.e., spatial scales), aggregation methods, and weighting schemes in creating the SoVI (Anderson et al., 2019; Jones & Andrey, 2007; Schmidtlein et al., 2008; Tate, 2012, 2013; Yoon, 2012). A recent study by Anderson et al. (2019) attempted to compare a hierarchically-constructed socio-ecological system vulnerability index, termed the Global Delta Risk Index, with the standard SoVI by counting how many census tracts change their vulnerability classes between the two indices and by mapping these class rank changes. But comparing the extent of divergence and convergence between the two indices is not an appropriate way to cope with different structural designs, epistemological frameworks, and aggregation methodologies. The methodology used in this study offers an alternative solution that is effective to 1) improve comparability of different vulnerability indices measured at different time points, taking into account the fundamental differences between various vulnerability indices, and 2) to study the spatial and temporal dynamics of social vulnerability. The proposed methodology can be applied to other social indicators. Beyond simply providing "point-in-time snapshots of vulnerability," this nationwide study at the county level provides the spatial and temporal evolution of the overall social vulnerability in the contiguous United States, showing generalized spatial and longitudinal patterns (Park & Xu, 2020). The study is still limited by lack of information on specific social conditions and local primary factors that drive higher levels of social vulnerability in a given region. Most studies using the SoVI approach cannot answer the question of the major driving social factors or the latent processes affecting social vulnerability at the local level (Yoon, 2012). Addressing key mechanisms of vulnerability in a local context is greatly needed to reduce vulnerability and to help policymakers and local communities make better-informed decisions.

The questions raised by this study can be approached by applying localized principal component analysis.

3.3. Local Scale – The Constituent Components and Local Primary Determinants of Social Vulnerability Index[2]

3.3.1. Objectives

The SoVI approach cannot explain the specific local social contexts that contribute to social vulnerability. The purpose of this subsection is to investigate the differential contributions of the components of SoVI and to examine the spatial and temporal dynamics of local factors of social vulnerability through a case study of the Houston–The Woodlands–Sugar Land Metropolitan Area. Geographically weighted principal component analysis (GWPCA) will be used to understand how local factors are distributed in space and how they have evolved over time since 1970.

3.3.2. Study Area

This study focused on The Houston-The Woodlands-Sugar Land Metropolitan Statistical Area (Greater Houston, hereafter), which is one of the most populous and rapidly growing metropolitan areas in the United States. Its population increased from 2,195,146 in 1970 to 7,051,556 in 2019, and the growth rate is 19.1% just from 2010 to 2019 (Balderrama et al., 2019). As of 2019, it consists of thirteen counties in Southern Texas near the US Gulf of Mexico. The Greater Houston area produced gross domestic product (GDP) of $490.1 billion in 2019, which placed it 7th place among the U.S. metropolitan areas (Balderrama et al., 2019). The median household income of the area was $64,688 in 2018, and the poverty rate was 14.5 percent in 2018, which was above the U.S. average of 13.1 percent (U.S. Census Bureau, 2018).

[2] Portions of this chapter have been published in the *Natural Hazards*, co-authored with Dr. Zengwang Xu

Its strong economy driven by the petroleum and medical industries has attracted a large influx of immigrants and domestic migrants (City of Houston, 2018).

The Greater Houston area has experienced rapid population growth and demographic diversification fueled by an array of social, demographic, economic, geographic, and urban governance factors (Fisher, 1989; Qian, 2010). In particular, the demographic diversity in the Greater Houston area is attributed to a large and burgeoning immigrant and migrant population over the past several decades. The Hispanic/Latino and Asian populations have more than doubled from 1980 to 2018. While the share of African American population has remained stable, the non-Hispanic white population has declined over time. Due to its proximity to the Gulf Coast, flat topography, and highly urbanized land use and land cover, the area has been plagued by many hazards, including hurricane wind and storm surge, flooding, air pollution, urban heat island effects etc. (Chakraborty, Grineski, & Collins, 2019; Harper, 2004; Streutker, 2003; Zhang, Villarini, Vecchi, & Smith, 2018). The area has undergone extensive land subsidence due to groundwater discharge and the oil and gas extraction operations, which leads to a greater risk of flooding (Stork & Sneed, 2002). Several infamous flooding events have severely damaged the area, such as tropical storm Allison in 2001, Houston's 'Tax Day Flood' in 2016, and Hurricane Harvey in 2017.

With the dramatic changes in social, economic, and demographic conditions along with the hazards it must confront, it is imperative to understand where and how the society is vulnerable, more importantly, what specific local social conditions have affected its local vulnerability. Studying social vulnerability in this area is in a pressing need to hazard mitigation along the US Gulf and Atlantic coasts. We hypothesize that the social vulnerability in this area

exhibits significant spatial heterogeneity in not only its relative magnitude but also the specific social determinants that underlie local vulnerability as well as its evolution over time.

3.3.3. Data and Methodology

The study begins with the overall social vulnerability in the area and how it evolves over time by computing the tract level SoVI using variables from the 1970, 1980, 1990, and 2000 decennial censuses, and the 2008-2012 and the 2013-2017 American Community Survey 5-year estimates. There is no consensus on what social variables have to be included in the SoVI. We adopt the social variables used in constructing the social vulnerability index created by the Center for Disease Control and Prevention (Flanagan et al., 2011). Among fifteen social variables, two of the variables (i.e., percent of population 5 years and older who speak English less than very well and percent of group quarter population) were excluded from our study due to skewed distributions and incomplete measurement over time. Thirteen social, economic, and demographic variables are selected and have been standardized to 2010 census tracts (Table 6).

Table 6. Variables selected from the 1970, 1980, 1990, and 2000 decennial censuses and the 2008-2012 and 2013-2017 American Community Survey 5-year estimates

Variables	Descriptions
PAGE5	Percentage of population under 5 years old
PAGE65	Percentage of population over 65 years old
PSPHCH	Percentage of single parent (male or female) householder, no spouse present with children under 18
PMINOR	Percentage of minority population (total of the following) 1970: Black or African American + Other (Before Substitutions and Allocations) 1980-ACS 2013-2017: Persons of Spanish Origin + Black or African American Alone + American Indian and Alaska Native Alone + Other
PPOVERTY	Percentage of population below poverty line
PUNEMP	Percentage of civilian labor force unemployed
PED12LES	Percentage of 25 years and older with less than high school education
PRENTER	Percentage of renters
MEDHHINC	Median household income (1970: Average family income)
PMOBILE	Percentage of housing units that are mobile homes

PHUBLT39	Percentage of housing units that were built 1939 or earlier
PNOTEL	Percentage of households with no telephone service available (1970: No television sets)
PNOVEH	Percentage of households with no vehicles

Following the standard social vulnerability index approach, this study also uses global PCA to calculate the overall SoVI using the sum of the PC scores. Both the values of the SoVI and its constituent PC scores are examined to understand the extent to which the SoVI values conceal the different combinations and variabilities of the constituent PC scores. The extent to which original social variables contribute to PCs is represented by the variables' loadings (i.e., correlation between the original variables and the components). The variables' loadings to PCs from the global PCA method are constant values that imply homogenous study-area-wide dependences between the PCs and the original variables. In other words, the dependence between the variable and the PC is the same everywhere across the study area, and this homogeneous dependency is termed stationarity (Demšar et al., 2013; Fotheringham, Charlton, & Brunsdon, 1998; Lloyd, 2010; Openshaw, Charlton, Wymer, & Craft, 1987).

Built on the stationarity assumption, the global PCA method does not take into account the heterogenous nature of variables at different locations. The PC scores from the global PCA method are the aggregated representations of several original social variables (Fotheringham & Brunsdon, 1999). The resultant SoVI is aggregated as the sum of scores of selected PCs, and this further generalizes and conceals the heterogenous contributions of the original variables to the SoVI at different spatial locations. The local spatial heterogeneity and dependence provide important insight on how social vulnerability is affected by different social conditions at the local level (Robinson et al., 2019). As the local version of the PCA method, the geographically weighted principal components analysis (GWPCA) is able to account for the spatial

heterogeneity of local social conditions in contributing to the social vulnerability at every spatial location (Gollini, Lu, Charlton, Brunsdon, & Harris, 2015; Lloyd, 2010).

GWPCA is the local version of the global PCA method and it applies the PCA method to the local neighborhoods of every location (Harris, Brunsdon, & Charlton, 2011; Harris, Clarke, Juggins, Brunsdon, & Charlton, 2015). GWPCA has been applied in many geospatial studies to explore the heterogeneous local structure. Some recent applications in geoscience and environmental studies investigated the local components of an air quality indicators (C. Wu, Hu, Zhou, Li, & Jia, 2019), heavy metal variability in soil (Fernández, Cotos-Yáñez, Roca-Pardiñas, & Ordóñez, 2018; Kumar, Lal, & Lloyd, 2012; H. Wang, Cheng, & Zuo, 2015), the distribution of flood vulnerability indicators (Chang & Chen, 2016), landslide susceptibility mapping (Sabokbar, Roodposhti, & Tazik, 2014), and land cover classification (Comber, Harris, & Tsutsumida, 2016). GWPCA has been widely adopted in social sciences to explore variations in the characteristics of the population of Northern Ireland (Lloyd, 2010), the heterogeneous local factors of the travel activity patterns of the elderly (Losada, Alen, Cotos-Yanez, & Dominguez, 2019), and the varying determinants of residential preferences in housing market segments (C. Wu, Ye, Ren, & Du, 2018). A growing body of literature has adopted GWPCA in the studies of social inequality in environmental health (Saib et al., 2015), urban deprivation (Mishra, 2018), energy poverty (Robinson et al., 2019), and quality of life (Murillo, Olmo, & Builes, 2019).

GWPCA begins by computing the local variance-covariance matrix ($\sum(u_i, v_i)$) for every spatial location i with coordinates (u_i, v_i). PCA is based on one global variance-covariance matrix ($\sum$), and GWPCA is based on variance-covariance matrices ($\sum(u_i, v_i)$) at every location:

PCA $$\sum = X^T X$$

$$\text{GWPCA} \qquad \sum(u_i, v_i) = X^T W(u_i, v_i) X$$

where X is the matrix consisting of n rows of observations and m columns of variables, (u_i, v_i) are the geographic coordinates of the i^{th} observation, and $W(u_i, v_i)$ is a diagonal matrix of weights determined by kernel functions that define local neighbors and spatial weights. Data observations at neighboring locations are weighted by a distance-decay kernel weighting function (e.g., exponential, Gaussian, and bi-square, etc.). For each location, its local principal components are derived by decomposing the locally-fitted variance-covariance matrix, the same way as the global PCA method decomposes the global variance-covariance matrix, as follows:

$$\text{PCA} \qquad \sum = \text{LVL}^T$$

$$\text{GWPCA} \qquad \sum(u_i, v_i) = L(u_i, v_i) V(u_i, v_i) L(u_i, v_i)^T$$

where $L(u_i, v_i)$ denotes a matrix of local eigenvectors and $V(u_i, v_i)$ a diagonal matrix of local eigenvalues at location i with coordinates (u_i, v_i). As the result, GWPCA generates loadings and component scores for every location based on data in its local neighborhood (Demšar et al., 2013; Gollini et al., 2015; Harris et al., 2011; Harris et al., 2015; Harris et al., 2016).

For a data matrix with n observations on m variables, the global PCA produces a set of at most m principal components and loadings for the whole study area, whereas GWPCA generates at most m principal components and loadings for each of the n observations/locations. The loadings at each location – local loadings – represent the contributions of the variables at the neighboring locations to the principal components at the location. Based on the local loadings, GWPCA makes it possible to examine at each location the extent to which the social variables in its neighborhood contribute to social vulnerability at the location, and especially, which variable

has the largest loading or contributes the most at each location, i.e., the primary determinant to the local social vulnerability (i.e., the 'winning' variable in GWPCA literature).

In order to utilize the GWPCA method appropriately, it is important to choose an appropriate kernel weighting method and bandwidth to define the local neighborhoods. The size of the kernel, so-called the kernel bandwidth, determines the size of local neighborhoods in the computation. If the bandwidth is too small, the GWPCA model will take into account a smaller number of local observations than that would make the GWPCA results reliable, whereas if the bandwidth is too large, the excessive number of local observations will be counted in the GWPCA, and its results are going to be close to the results of the global PCA (Wu et al. 2018). Hence, it is necessary to choose the optimal bandwidth that can contain sufficient local variability and avoid overgeneralization. Bandwidth selection can be achieved either by a user-defined fixed bandwidth or an adaptive bandwidth (using a fixed number of nearest neighbors via a cross-validation score); the adaptive bandwidth approach is more commonly used (Gollini et al. 2015; Harris et al. 2011). Our GWPCA method is based on a bi-square weighting function and adaptive bandwidths.

The major GWPCA results in this study are the primary determinants to local vulnerability, which are the social variables that contribute the most at each location. For every location (i.e., census tract in this study), GWPCA derives the primary determinant variable at every time point (i.e., 1970, 1980, 1990, 2000, 2008-2012, and 2013-2017). Thus, each location (or tract) can be characterized by a sequence of the primary determinants over time. Cluster

analysis is employed to explore how the sequences of primary determinants have changed in the study area over time.

Cluster analysis is commonly used to find patterns to group data; it is often conducted by maximizing the inter-cluster dissimilarity and minimizing the intra-cluster similarity (Aggarwal, 2014; Grubesic, Wei, & Murray, 2014; Murray & Estivill-Castro, 1998). The dissimilarity (similarity) between data observations is often calculated by using several distance metrics such as Euclidean distance, Manhattan distance, and Minkowski distance – all of these can only be applied to numerical variables. For data with categorical variables, Gower's distance can be used (Gower, 1971; Kaufman & Rousseeuw, 2009; Podani, 1999). The sequence alignment method can be employed only for categorical variables, such as the most influential social variables in this study (Needleman & Wunsch, 1970). As discussed earlier, the sequence alignment method evaluates the similarity or dissimilarity between two categorical sequences by Levenshtein edit distance, which is the cost to transform one sequence into another in terms of insertions, deletions, and substitutions (Levenshtein, 1966). In this study, we use the functions in TraMineR package in the statistical software R to calculate the minimal editing cost between the sequences of the primary determinants of any two tracts (Gabadinho et al., 2011). Ward's method is then applied to the minimum editing cost distance matrix to explore the clustering patterns of the sequences of primary determinants in the study area (Ward Jr, 1963). Figure 7 presents the flow of the overall research process.

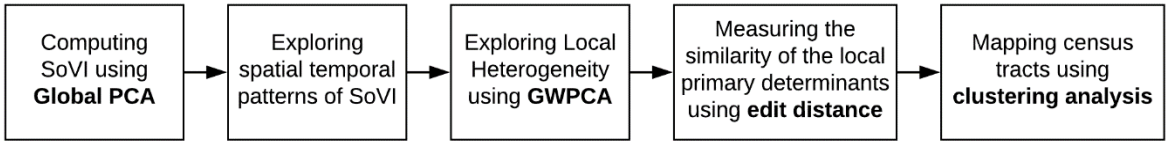

Figure 7. Overall methodology to study local factors of social vulnerability

3.3.4. Spatial and Temporal Patterns of SoVI and its Principal Components

We first examine the spatial and temporal patterns of the overall social vulnerability in the Greater Houston area by examining the SoVI and its constituent principal components (PCs). The Kaiser-Meyer-Olkin (KMO) statistic and the result of Bartlett test of sphericity indicated that the sample size of the dataset was suitable for PCA analysis. The results of the global PCA were then rotated using varimax rotation, which makes the extracted PCs more interpretable (Rencher & Christensen, 2012). Five PCs were extracted for each time point, and these PCs explain 76 to 84 percent of the total variance in the original variables (Table 7).

Table 7. The principal components of the SoVI during different time periods

Year	1970	1980	1990	2000	2008-2012	2013-2017
Percentage of total variance explained	79	84	84	81	77	76
Number of components	5	5	5	5	5	5
Major components (% variance explained)	1. Multiple vulnerable conditions (30) 2. High percentage of renter households& single parent households (15) 3. High percentage of elderly & low percentage of 5 years and younger (15) 4. Unemployment (10) 5. Mobile homes (10)	1. Multiple vulnerable conditions (38) 2. High percentage of the elderly & old buildings (15) 3. Less youth & high percentage of renter households(13) 4. Mobile homes (10) 5. Low median household income (9)	1. Multiple vulnerable conditions (38) 2. High percentage of the youth & low percentage of the elderly (13) 3. High percentage of old buildings (12) 4. Mobile homes (10) 5. High percentage of renter households & low median household income (10)	1. Multiple vulnerable conditions (37) 2. High percentage of the youth & low percentage of the elderly (12) 3. High percentage of renter households & low median household income (11) 4. High percentage of old buildings (11) 5. Mobile homes (10)	1. Multiple vulnerable conditions (30) 2. High percentage of households without telephone service & vehicles (15) 3. High percentage of youth & low percentage of the elderly (14) 4. Mobile homes (9) 5. High percentage of old buildings (8)	1. Multiple vulnerable conditions (29) 2. High percentage of youth & low percentage of the elderly (18) 3. High percentage of households without telephone service (11) 4. Mobile homes (10) 5. High percentage of old buildings (9)

Each PC is characterized by the social variables with large loading values. PC1 accounts for the most variance or is loaded with the variance from as many variables as possible. It correlates with multiple socially vulnerable conditions. For example, the PC1 for the 2013-2017 period correlates with several variables: percent of people in poverty, percent of unemployed civilian labor force, percent of households without a vehicle, percent of minority, percent of single parent households, low median household income, and percent of people with less than high school education. Other PCs correlate with fewer variables, and the number and variables can vary over time, for example PC2 for the 2008-2012 period positively correlates with the percent of households without a vehicle, the percent of households without telephone service, and the percent of renter households, but PC2 for the 2013-2017 period correlates with the percent of people 5 years and younger, the percent of single parent households, and the percent of minority racial/ethnic groups, and negatively correlates with the percent of people 65 years and older. This volatility results from changes in the social variables at different times. The last three PCs only correlate with one or two variables. Specifically, PC4 and PC5 mainly correlate with either percent of mobile homes or percent of older buildings. These two variables have quite different frequency distributions than other variables, and they are more skewed to a small value with a long tail. Most mobile homes are spatially distributed in the suburbs, and the older buildings are mainly located in the central city.

Figure 8 shows the spatial distributions of the SoVI in 1970, 1980, 1990, 2000, 2008-2012, and 2013-2017. The SoVI has shown persistent geographic patterns in the Greater Houston area. The most socially vulnerable areas are located in the inner-city and suburban outskirts, and between are the less vulnerable areas, forming a doughnut-shaped pattern. Although the specific

location and size of the annuluses are not the same at different time points, the general annulus pattern has been persistent since 1970.

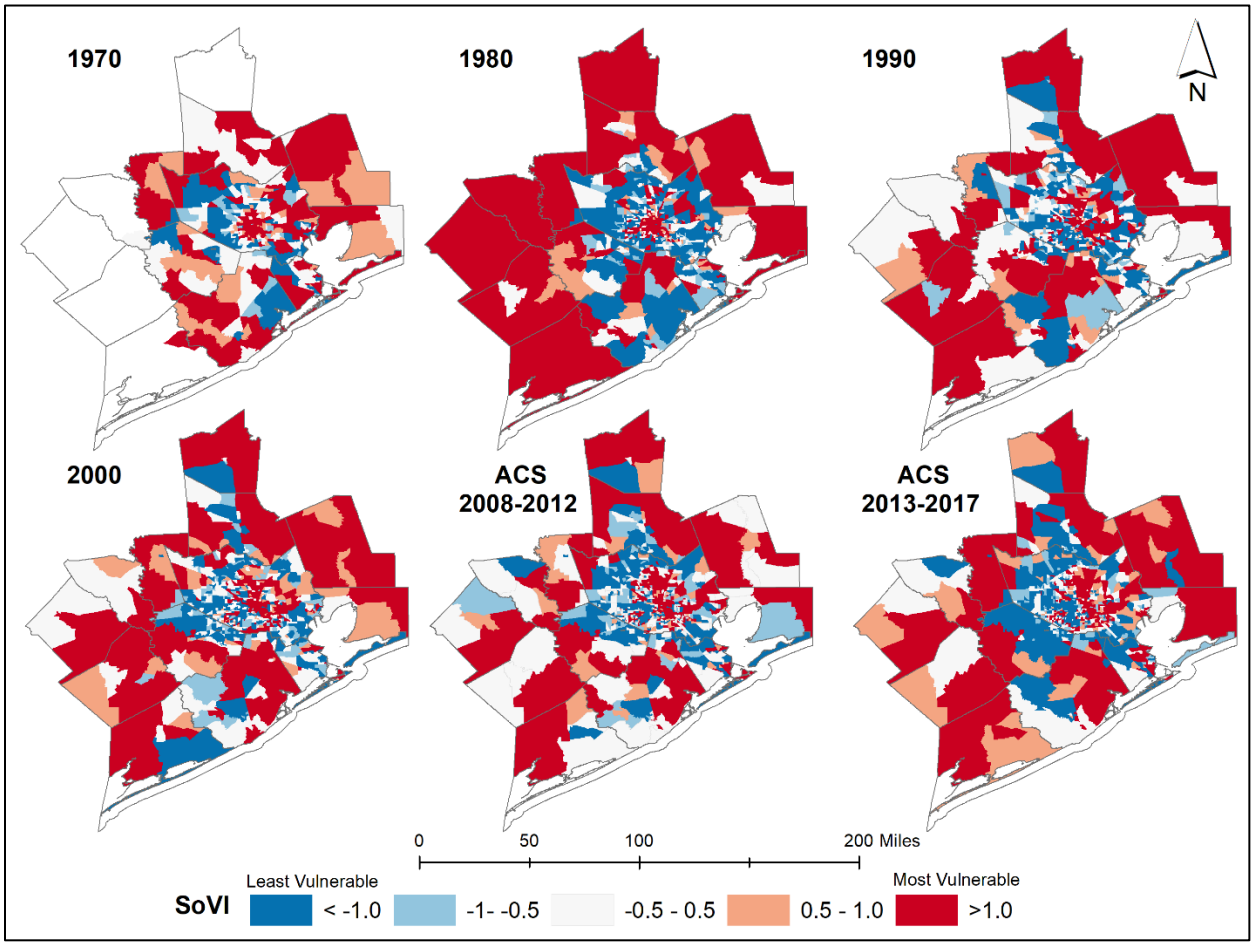

Figure 8. Spatial distribution of the social vulnerability index (SoVI) during different time periods

The central city area in Greater Houston has experienced chronic racial and ethnic segregation with a high concentration of poverty, and the majority of the population in this area is predominantly Hispanic and African American (O'Connell, 2016; O'Connell & Howell, 2016). East and south of the Inner Loop neighborhoods near downtown have transitioned from upper- and middle-income areas to lower-income neighborhoods since 1980. Meanwhile, suburban and coastal areas are composed of middle- or upper-class Whites and elderly retirees who prefer

suburban living or to reside near water (Crossett et al., 2013). Together, all these social demographic factors contribute to the persistent spatial patterns of social vulnerability.

3.3.5. The Differential Contribution of the Constituent Components of the SoVI

The SoVI is the sum of all the PC scores, and it cannot indicate the extent to which each constituent PC contributes to the overall sum. A high SoVI value can be the result of a high value for PC1 or other PCs. Figure 9 presents the value of all five PCs for the 2013-2017 period.

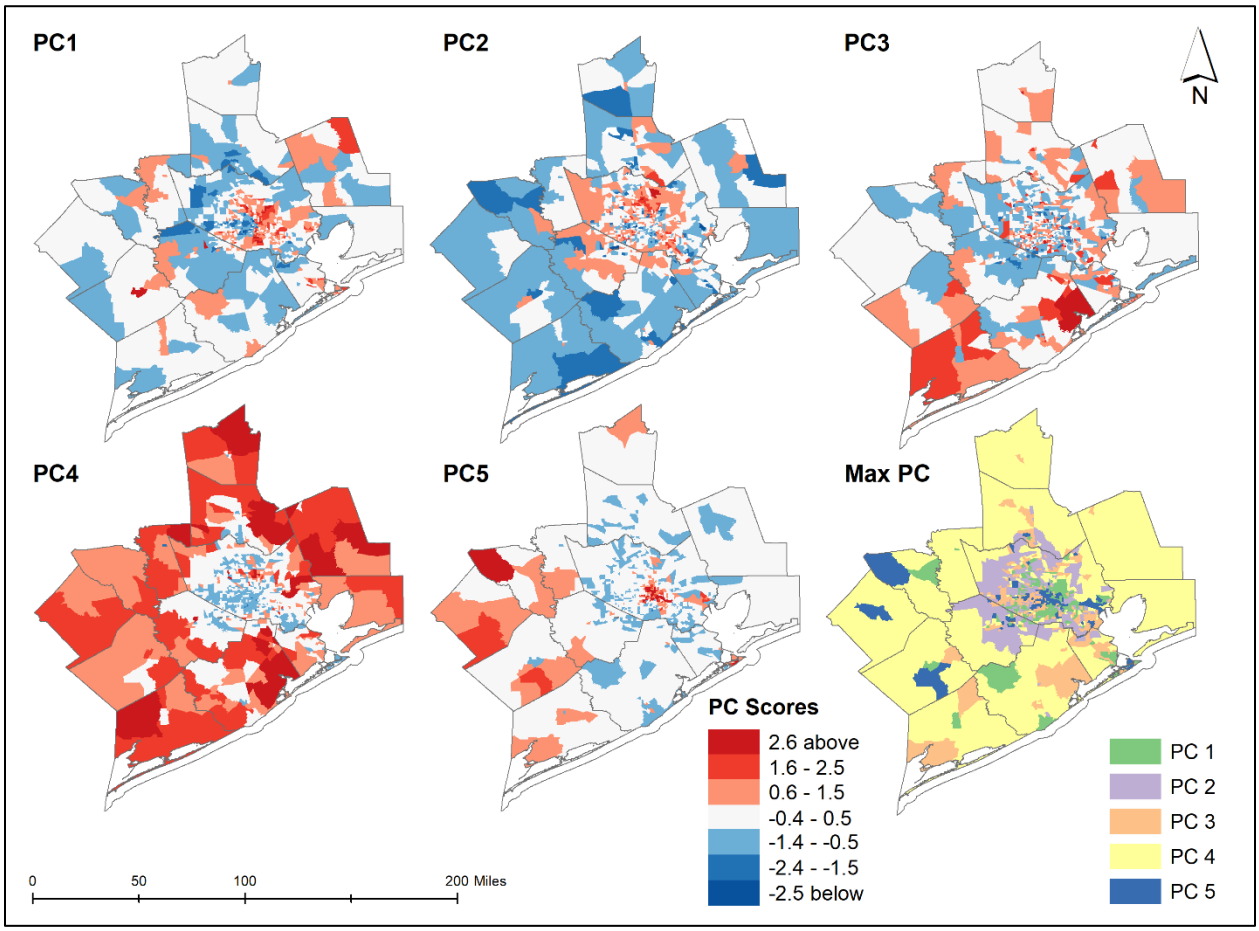

Figure 9. Spatial distributions of the principal component (PC) scores of the five constituent PCs (PC1: multiple vulnerable conditions, PC2: high percentage of youth and low percentage of the elderly, PC3: high percentage of households without telephone service, PC4: mobile homes, PC5: high percentage of old buildings) of the SoVI for the 2013-2017 period (PC1-PC5) and the distribution of the PCs that have the highest scores (Max PC)

Among the five PCs, PC1 accounts for the most variability in the original variables. For the 2013-2017 period, PC1 accounts for 29% of the total variability, and it is correlated with multiple original variables. High PC1 scores are mainly located in the inner Houston city, in the east of Harris County near Buffalo Bayou, and in some tracts in the suburbs. PC2 mainly correlates with a high percentage of youth and a low percentage of the elderly, and it also moderately correlates with single parent households and minority populations. PC3 mainly correlates with a high percentage of households without telephone service. PC4 correlates with a high percentage of mobile homes and PC5 correlates with a high percentage of old buildings.

The five PCs have different spatial distribution patterns, and each contributes to a layer of the spatial pattern of the SoVI in 2013-2017. Although PC1 accounts for the largest amount of variability in the original variables, the spatial distribution pattern of PC1 only contributes to some of the spatial distribution pattern of the SoVI, especially in the high vulnerability areas in the central city. This becomes more apparent when PC1 is contrasted to PC4, which only represents one variable – the percent of mobile homes – but has the highest PC score and contributes most to the high vulnerability of almost all suburban tracts (Figure 9 – Max PC). If the SoVI is used as the only measure of social vulnerability, the differential contributions of the specific PCs to the SoVI are going to be unknown. As shown by a scatter plot between all PCs and the SoVI in Figure 10, the variability of the PC scores become larger as the SoVI increases, and many of the tracts with high SoVI are due to high values in other PCs rather than PC1. This indicates the high overall vulnerability of those tracts is not only due to their overall social conditions, but also one or two specific conditions.

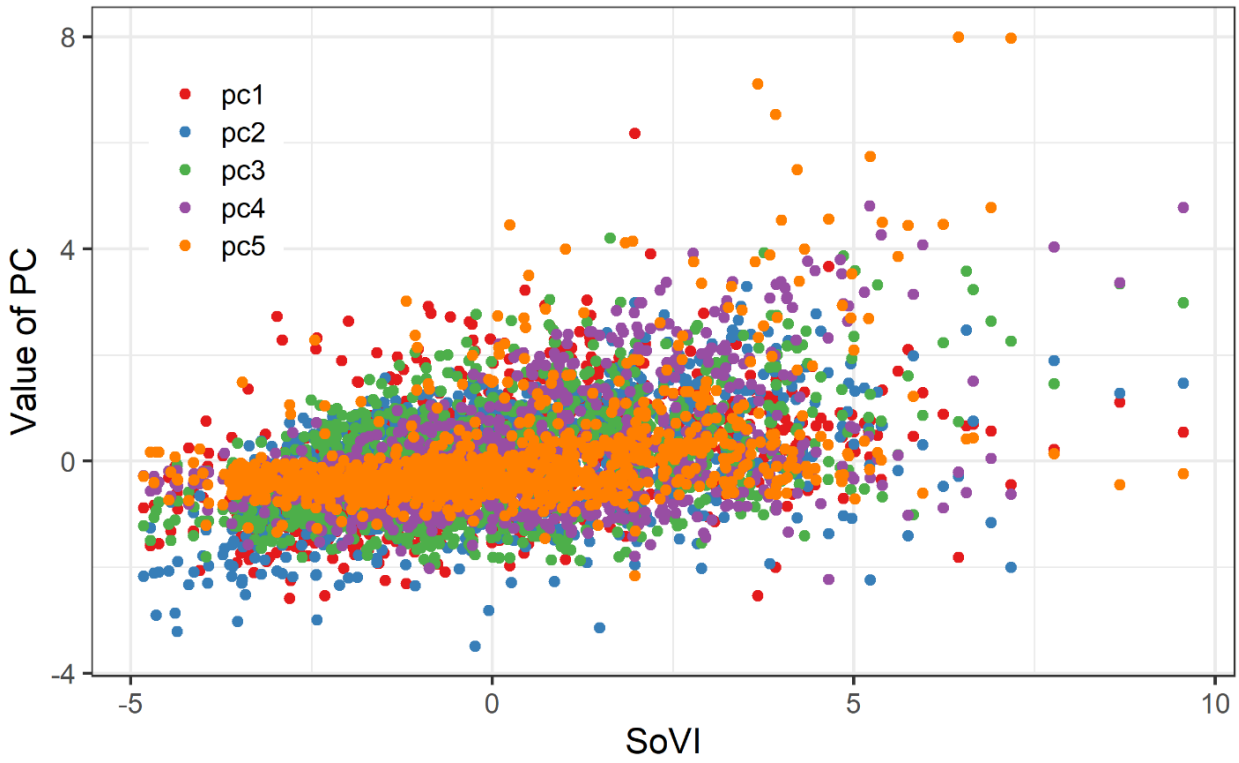

Figure 10. Scatter plot of the five PCs versus the SoVI in the 2013-2017 period

The values of the PCs and SoVI can only represent the relative magnitude of social vulnerability and cannot capture the contribution of specific social variables, especially at the local level. However, the GWPCA method can provide information about the contribution of original variables to the social vulnerability at each location. The GWPCA method in this study focuses on PC1 as it accounts for the most variability in the original variables and correlates with multiple original variables. The randomization test is conducted to verify if local eigenvalues vary across space so that the GWPCA is applicable (Harris et al., 2011). The Monte Carlo significance tests showed that the null hypothesis of local eigenvalue stationarity was rejected at a significance level of 0.05, which means that there exists significant spatial non-stationarity that warrants the use of GWPCA.

An important indicator of the performance of the PCA method is how much variance in the original variables the PCs account for. For example, the five PCs account for 76 percent of the variance in the original variables in the 2013-2017 period (Table 7). GWPCA produces its local geographically weighted principal components (GWPCs) for every location that accounts for local variability. Using GWPCA on the variables from the ACS 2013-2017, Figure 11 maps the cumulative local percentage of variance (PTV) of the top five local GWPCs that explain the most local variance. The local PTV indicates how much local variance can be explained by the local GWPCs for each tract. The local PTV ranges from 74.2 to 86.4 percent across the study area in 2013-2017. Most tracts have higher PTVs than 76 percent—the percentage of variance explained by the global PCA; only a small number of tracts have local cumulative PTV between 74.3 and 76 percent (colored in red on Figure 11). This implies that the locally-fitted GWPCA performs well in representing the variability in the original variables.

GWPCA produces locally-fitted components and loadings for each tract in the study area. We examine which social variable contributes to the local social vulnerability the most for each tract. The variable with the highest local loading is indicative of the greatest contribution of the variable to local social vulnerability, thus it is the primary determinant to local social vulnerability (Gollini et al., 2015; Harris et al., 2011). The primary determinants to PC1 are presented in Figure 12.

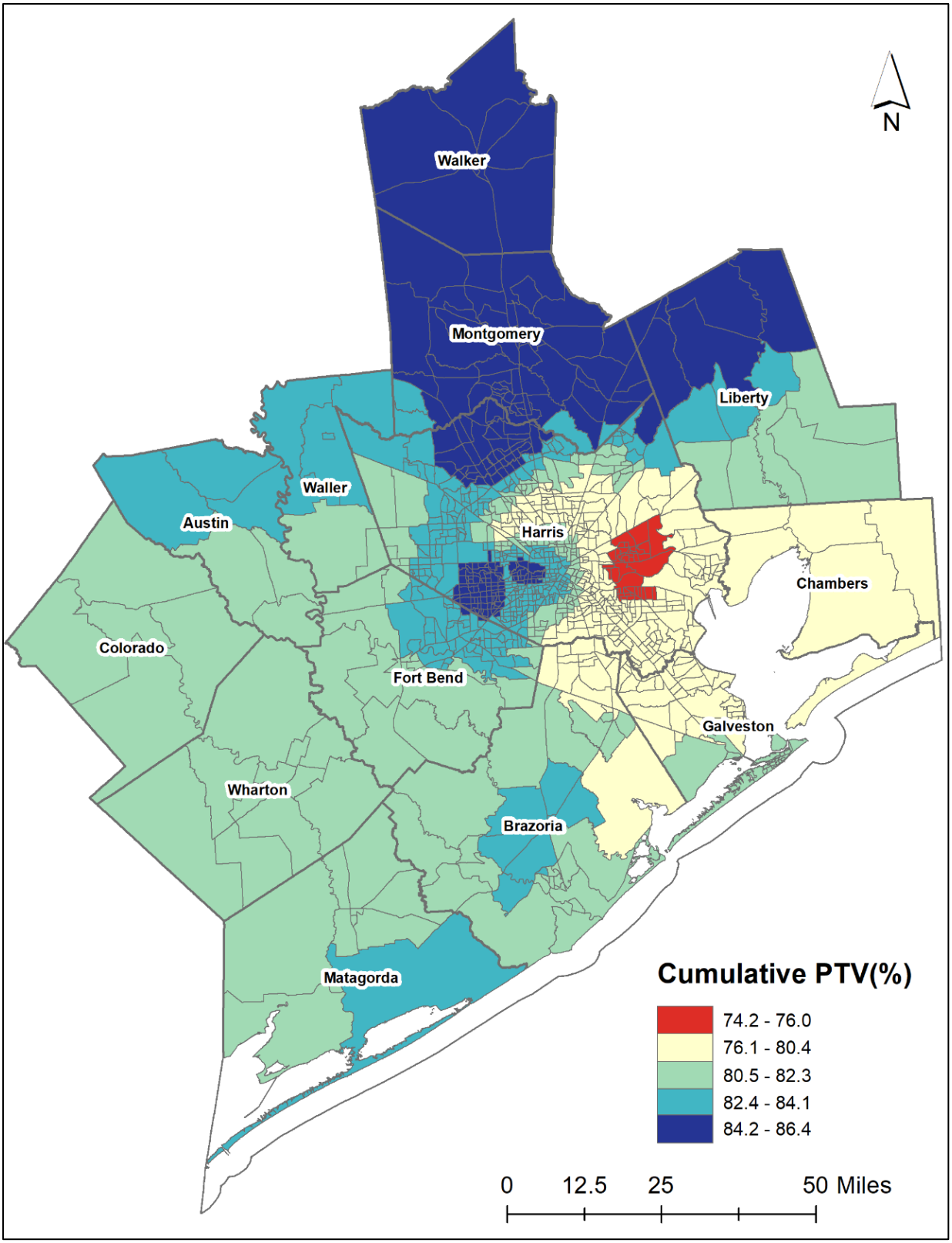

Figure 11. Cumulative local percentage of variance explained by top five GWPCs in the 2013-2017 period

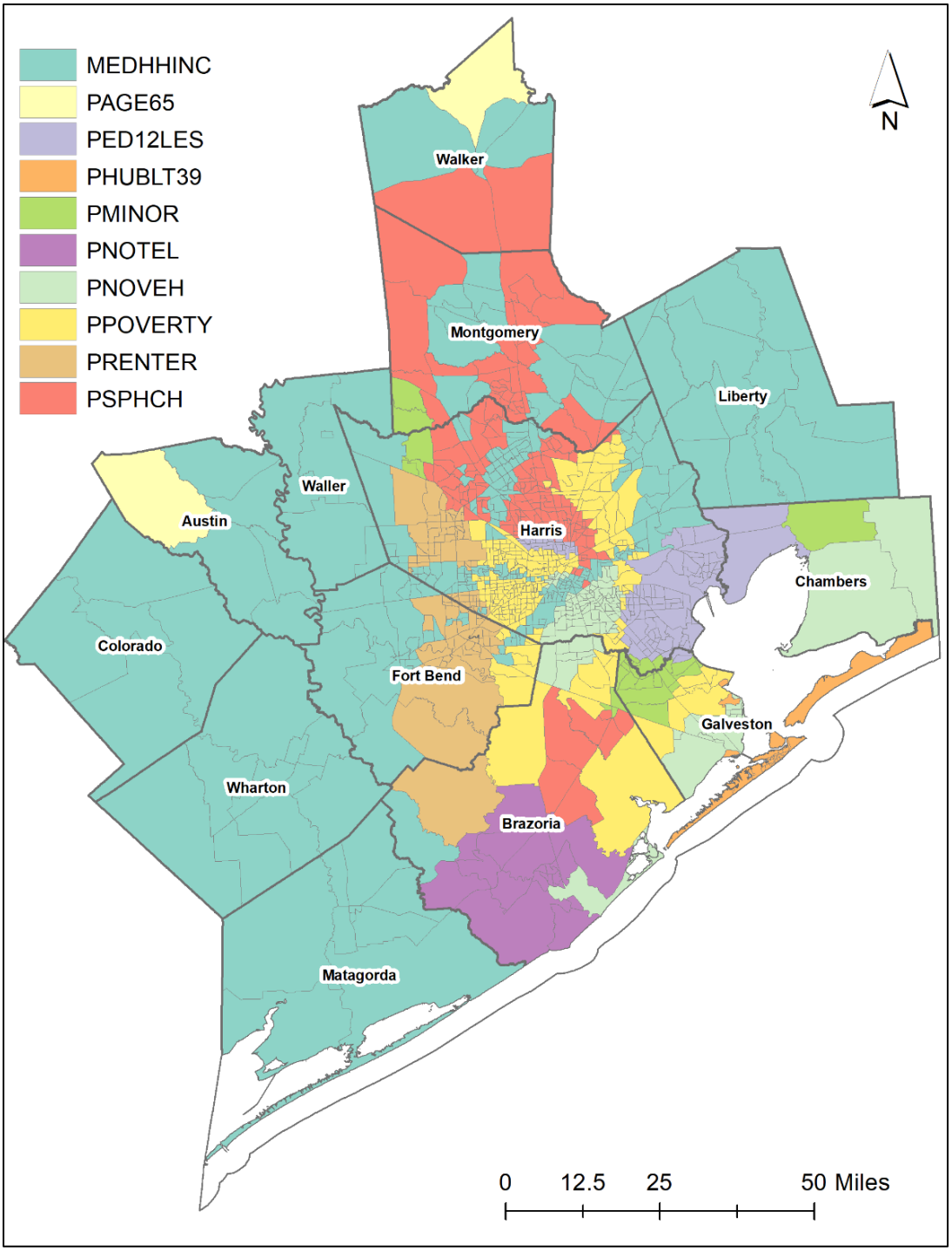

Figure 12. The primary local determinants of social vulnerability in the 2013-2017 period (MEDHHINC: median household income, PAGE65: percentage of population over 65 years old, PED12LES: percentage of 26 years and older with less than high school education, PHUBLT39: percentage of housing units that were built 1939 or earlier, PMINOR: percentage of minority population, PNOTEL: percentage of households with no telephone service available, PNOVEH: percentage of households with no vehicles, PPOVERTY: percentage of population below poverty line, PRENTER: percentage of renters, and PSPHCH: percentage of single parent householder with children under 18)

The primary determinants show great heterogeneity across the Greater Houston area. Ten out of thirteen of the variables are found to be the primary determinants in different parts of the Greater Houston area. Some variables are primary determinants for large geographical areas. For example, median household income is the primary determinant of local social vulnerability for large contiguous areas in the western and northern area. The percent of households in poverty, the percent of single parent households, and the percent of renter households are the primary determinants in moderately large patches of contiguous areas. These primary determinants reflect the heterogenous social conditions that drive local social vulnerability in different parts of the Greater Houston area.

3.3.6. Spatial and Temporal Patterns of the Local Primary Determinants of Social Vulnerability

The primary determinant of social vulnerability at a particular location can vary over time. To further understand how they have changed across the Greater Houston area, we conducted clustering analysis on the primary determinant variables to PC1 at different times. The clustering was based on the Levenshtein edit distance between tracts on their sequences of primary determinants. Several clustering algorithms were examined using the R package 'clValid' to determine a suitable clustering algorithm and an optimal number of clusters (Brock, Pihur, Datta, & Datta, 2008). Based on the elbow method and the intra-cluster similarity measures such as the Dunn index and silhouette width, the census tracts in the area were classified into five clusters using a hierarchical clustering method (i.e., Ward's method). The five clusters are shown in Figure 13.

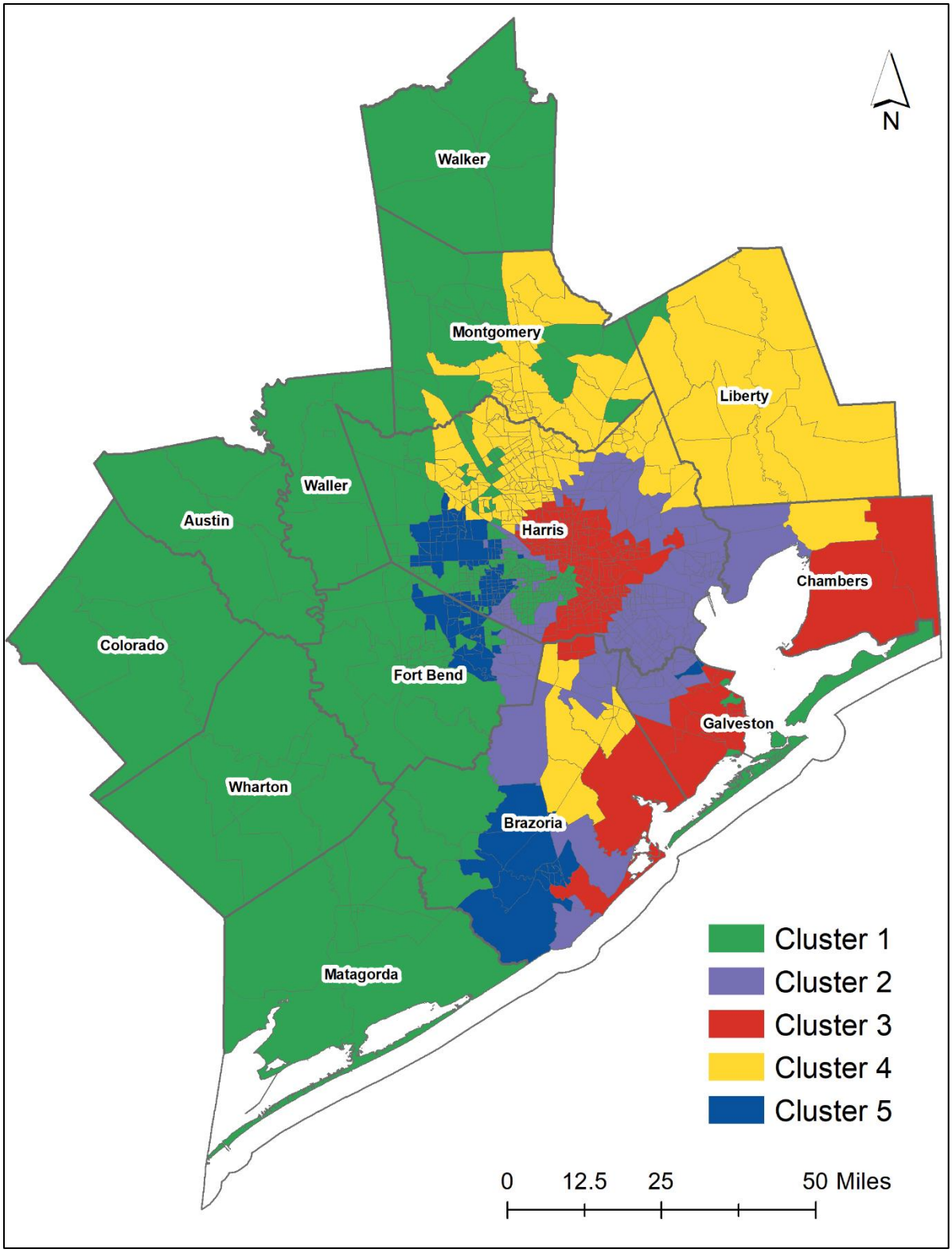

Figure 13. The five clusters of tracts based on their primary determinants in 1970, 1980, 1990, 2000, 2008-2012, and 2013-2017

Each cluster has its distinctive location in the Greater Houston area. As shown in Figure 13, cluster 1 is located in a large contiguous area mainly in the western Greater Houston area. Cluster 2 is mainly located in the eastern part of Harris County outside of the central city of Houston. Cluster 3 is located in the eastern part of the central city of Houston and part of the southwestern Greater Houston area near the Galveston Bay. Cluster 4 is mainly located in the northeastern suburbs. Cluster 5 is mainly located in western Harris County right outside of the City of Houston in part of northern Fort Bend County and part of Brazoria County.

Each cluster can be characterized by the primary determinant that the majority of its tracts hold. For the whole area and for each cluster, the primary determinants of tracts at different times are listed in Table 8. Over time, the median household income (MEDHHINC), percent of people in poverty (PPOVERTY), and percent of households without a vehicle (PNOVEH) have been the primary determinants for the majority of census tracts across the Greater Houston area (Table 8). The degree of the majority of these variables varies from 25% (278/1104 in 2013-2017) to 58% (645/1104 in 2008-2012). All three variables are closely related to economic disadvantage. For the majority tracts in cluster 1, cluster 2, and cluster 3, the primary determinants have been persistent over time: median household income (MEDHHINC) in cluster 1, percent of people in poverty (PPOVERTY) in cluster 2, and percent of households without a vehicle (PNOVEH) in cluster 3. For the majority of tracts in clusters 4 and 5, there are a greater number of fluctuations in the primary determinants over time, indicating frequent changes. For tracts in cluster 4, there are four primary determinants over time, i.e., percent of people in poverty (PPOVERTY), percent of children 5 years and younger (PAGE5), median household income (MEDHHINC), and percent of single parent households (PSPHCH). For tracts in cluster 5, the primary determinants are the percent of people in poverty (PPOVERTY), percent of

children 5 years and younger (PAGE5), median household income (MEDHHINC), and percent of renter households (PRENTER).

Table 8. The primary determinants to PC1 for the majority of tracts across the Greater Houston area and in different clusters at different time points

Areas	1970	1980	1990	2000	2008-2012	2013-2017
The Whole Study Area	MEDHHINC (405/1060)	PNOVEH (285/1104)	PPOVERTY (286/1104)	MEDHHINC (427/1104)	PPOVERTY (645/1104)	MEDHHINC (278/1104)
Cluster 1	MEDHHINC (176/259)	PAGE5 (120/299)	MEDHHINC (139/299)	MEDHHINC (165/299)	MEDHHINC (155/299)	MEDHHINC (170/299)
Cluster 2	MEDHHINC (78/223)	PPOVERTY (65/223)	PPOVERTY (115/223)	PED12LES (95/223)	PPOVERTY (214/223)	PPOVERTY (94/223)
Cluster 3	PNOVEH (180/237)	PNOVEH (197/237)	PNOVEH (170/237)	PNOVEH (77/237)	PPOVERTY (217/237)	PNOVEH (86/237)
Cluster 4	PPOVERTY (68/195)	PAGE5 (78/195)	PPOVERTY (72/195)	MEDHHINC (140/195)	PSPHCH (143/195)	PSPHCH (124/195)
Cluster 5	MEDHHINC (63/146)	PRENTER (105/150)	MEDHHINC (78/150)	PAGE5 (60/150)	PPOVERTY (85/150)	PRENTER (76/150)

Note: The number in parentheses signifies the number of tracts with the primary determinants / total number of tracts, respectively.
*MEDHHINC = median household income; PAGE5=percent of 5 years old and younger; PPOVERTY=percent of people under poverty; PED12LES=Percent of 25 years and older with less than high school education; PNOVEH=percent of households without a vehicle; PSPHCH=percent of single parent households; PRENTER=percent of renters; PRENTER = percent of renter households.

We also plot the frequency of the primary determinants of all tracts in each cluster in Figure 14. Each cluster has a unique frequency distribution of the primary determinants. It is apparent that the median household income (MEDHHINC) is the primary determinant in cluster 1. A moderate number of tracts have the percent of 5 years and younger (PAGE5) in 1980, and percent of people in poverty (PPOVERTY) during the 2008-2012 and 2013-2017 periods. In cluster 2, the primary determinant of around 90% of its tracts is the percent of people in poverty (PPOVERTY) between 2008 and 2012. The percent of people with low levels of educational attainment (PED12LES) also have a high frequency beginning in 1980. In cluster 3, the percent

of households without a vehicle (PNOVEH) is the primary determinant for all the time periods except the 2008-2012 period when the percentage of people living in poverty (PPOVERTY) is the primary determinant. In cluster 4, the percent of single parent households (PSPHCH) is the primary determinant of the majority of tracts during the 2008-2012 and 2013-2017 periods. During other periods, the percent of 5 years and younger (PAGE5), percent of minority (PMINOR), median household income (MMEDHHINC), percent of people in poverty (PPOVERTY) are the primary determinants for large numbers of tracts in cluster 4. In cluster 5, the percent of renter households (PRENTER) is the primary determinant for a larger fraction of tracts. The percent of people in poverty (PPOVERTY), median household income (MEDHHINC), and percent of 5 years and younger (PAGE5) are the primary determinants for large portions of tracts at different times in cluster 5.

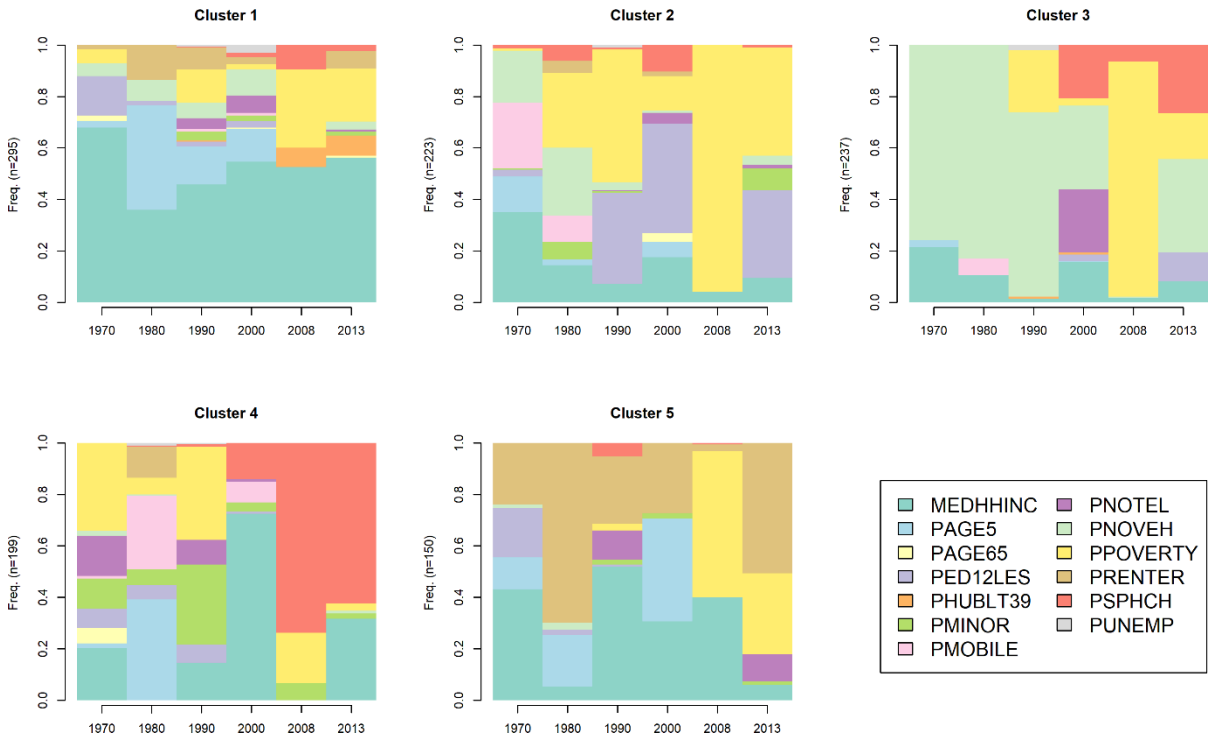

Figure 14. The frequency distribution of the primary determinants over time in each cluster

The primary determinant of a tract can vary over time. Each tract can be characterized by a sequence of primary determinants at different times, i.e., 1970, 1980, 1990, 2000, 2008-2012, and 2013-2017. This cluster analysis is based on the dissimilarity between the sequences of primary determinants of tracts. To understand the prominent sequences in each cluster, the top ten most frequent sequences in each cluster are plotted in Figure 15. These top ten most frequent sequences cumulatively account for different percentage of tracts in different clusters: 32.9% in cluster 1, 46.6% in cluster 2, 48.9% in cluster 3, 44.2% in cluster 4, and 48.7% in cluster 5. In cluster 1, the most frequent sequence is MEDHHINC (1970) → PNOVEH (1980) → MEDHHINC (1990) → MEDHHINC (2000) → PHUBLT (2008) → PHUBLT (2013), which shows that the sequence has median household income (MEDHHINC) in 1970, percent of households without a vehicle (PNOVEH) in 1980, MEDHHINC again in 1990 and 2000, and percent of housing units that were built 1939 or earlier (PHUBLT39) in both 2008-2012 and 2013-2017 periods. Some clusters have different sequences, while others have a fluctuating frequency of primary determinants each year. For example, the most frequent sequence in cluster 3 has the percent of households without a vehicle (PNOVEH) as the primary determinant in 1970, 1980, 1990, and 2000. The overall impression from Figure 15 is that there is significant change over time of the primary determinants.

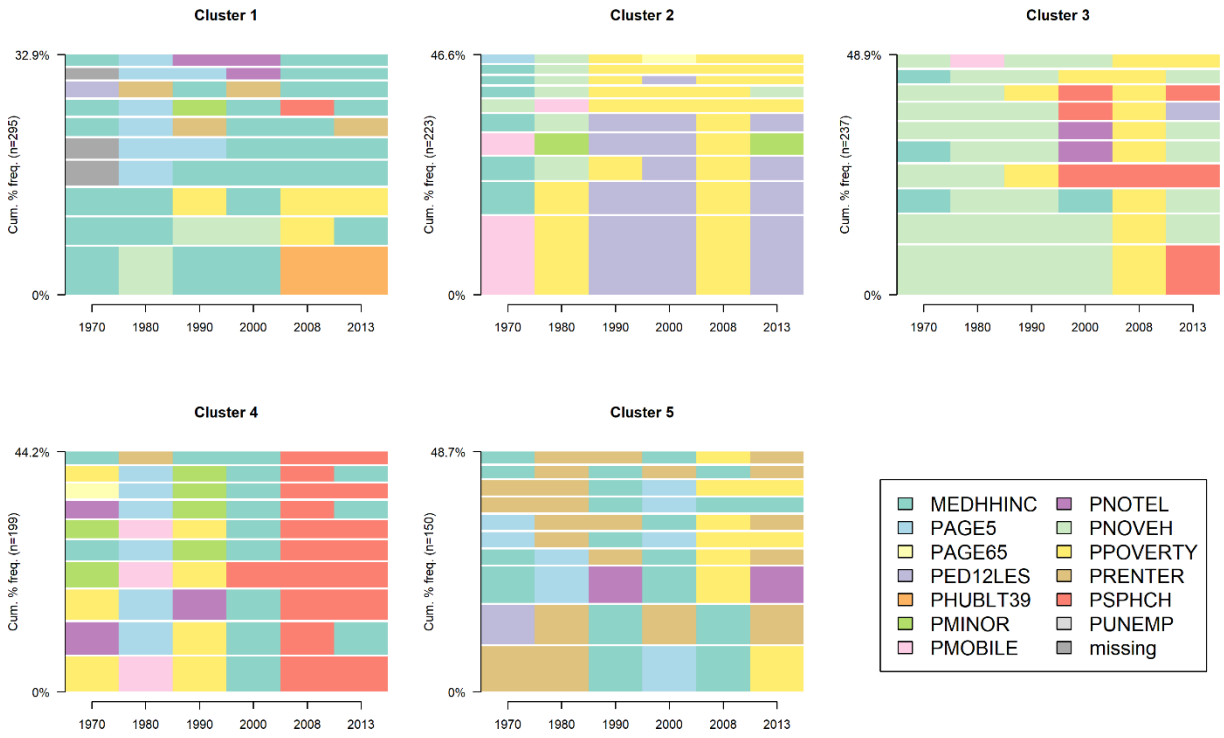

Figure 15. The top ten frequent sequences of the primary determinants over time in each cluster

In order to examine the degree of change, we summarized the number of tracts that have changed (or not changed) their primary determinants in consecutive time periods in Table 9. For the whole Greater Houston area, there are always more tracts that change their primary determinants than those that have not in consecutive periods. The number of tracts that have changed their primary determinants is 6 times greater than those that have not changed from 2000 to the 2008-2012 period. Among the five clusters, tracts in cluster 1 and cluster 3 are relatively stable. In other clusters, there are significantly more tracts that change their primary determinants, for example, all except 6 tracts in cluster 5 have changed their primary determinants from 2000 to the 2008-2012 period.

We also aimed to examine the most prominent transitions of the primary determinants over time. In Table 10, we summarize the primary determinant transitions in consecutive time

periods. For the whole Greater Houston area, from 1970 to 1980 and 1980 to 1990, the most frequent observed sequence is from PNOVEH to PNOVEH for both periods, i.e., there are more tracts that remain PNOVEH than any other sequences. The rest of the transitions in other time periods are PPOVERTY → MEDHHINC, MEDHHINC → PSPHCH, and PPOVERTY → PPOVERTY. For cluster 1, most tracts remain in MEDHHINC (median household income) than change to other primary determinants between years since 1970. For cluster 2, the major transitions are between PPOVERTY and PED12LES, i.e., between percent of people in poverty and percent of people with education less than high school. For cluster 3, the major transitions are between PNOVEH and itself or PNOVEH and PPOVERTY, i.e., the percent of households without a vehicle and percent of people in poverty. In clusters 4 and 5, the transitions involve more diverse primary determinants, such as PSPHCH (percent of single parent households) and PRENTER (percent of renter households). As such, it is evident that clusters 1, 2, and 3 have shown persistent transition patterns, while clusters 4 and 5 have shown more varying transitions.

Table 9. The number of tracts that have (or not) changed their primary determinants in consecutive time periods

Areas	Change of the most influential variable	1970 – 1980	1980 – 1990	1990 – 2000	2000 – 2008*	2008 – 2017**
The whole study area	Not changed	279	308	314	148	455
	Changed	781	796	790	956	649
Cluster 1	Not changed	89	103	102	77	170
	Changed	170	196	197	222	129
Cluster 2	Not changed	11	14	97	34	85
	Changed	212	209	126	189	138
Cluster 3	Not changed	146	139	72	19	54
	Changed	91	98	165	218	183
Cluster 4	Not changed	6	18	26	12	114
	Changed	189	177	169	183	81
Cluster 5	Not changed	27	34	17	6	32
	Changed	119	116	133	144	118

Note: ACS 2008-2012 5-year estimates*, ACS 2013-2017 5-year estimates **

Table 10. The most frequent transitions of the primary determinants between consecutive years (or periods)

Areas	1970→1980	1980→1990	1990→2000	2000→2008*	2008→2017**
The whole study area	PNOVEH→ PNOVEH (146/1060)	PNOVEH→ PNOVEH (137/1104)	PPOVERTY→ MEDHHINC (114/1104)	MEDHHINC→ PSPHCH (163/1104)	PPOVERTY→ PPOVERTY (192/1104)
Cluster 1	MEDHHINC→ MEDHHINC (89/259)	MEDHHINC→ MEDHHINC (55/299)	MEDHHINC→ MEDHHINC (74/299)	MEDHHINC→ MEDHHINC (72/299)	MEDHHINC→ MEDHHINC (104/299)
Cluster 2	PMOBILE→ PPOVERTY (42/223)	PPOVERTY→ PED12LES (59/223)	PED12LES→ PED12LES (73/223)	PED12LES→ PPOVERTY (93/223)	PPOVERTY→ PPOVERTY (85/223)
Cluster 3	PNOVEH→ PNOVEH (143/237)	PNOVEH→ PNOVEH (137/237)	PNOVEH→ PNOVEH (71/237)	PNOVEH→ PPOVERTY (76/237)	PPOVERTY→ PNOVEH (85/237)
Cluster 4	PPOVERTY→ PMOBILE (27/195)	PMOBILE→ PPOVERTY (49/195)	PPOVERTY→ MEDHHINC (49/195)	MEDHHINC→ PSPHCH (129/195)	PSPHCH→ PSPHCH (108/195)
Cluster 5	MEDHHINC→ PRENTER (34/146)	PRENTER→ MEDHHINC (66/150)	MEDHHINC→ PAGE5 (48/150)	MEDHHINC→ PPOVERTY (41/150)	PPOVERTY→ PRENTER (44/150)

Note: MEDHHINC = median household income; PAGE5=percent of 5 years old and younger; PPOVERTY=percent of people under poverty; PED12LES=Percent of 25 years and older with less than high school education; PNOVEH=percent of households without a vehicle; PSPHCH=percent of single parent households; PRENTER=percent of renter households. ACS 2008-2012 5-year estimates*, ACS 2013-2017 5-year estimates **.

3.3.7. Discussion and Conclusion

The inductive design of SoVI using global PCA and the associated aggregation process tend to obscure spatial effects, making it difficult to capture which social indicators contribute the most to overall social vulnerability at a particular place. As a result, the SoVI score cannot elucidate the primary contributors to vulnerability and subtle geographical nuances that influence overall social vulnerability (Anderson et al., 2019; Morse, 2004; Robinson et al., 2019; Rufat, 2013; Yoon, 2012). Preliminary work on understanding the specific vulnerability factors was undertaken by Rufat (2013). His work identified the spatial distribution of each socio-economic indicator profile (i.e., spectra graphs) and compared them with the average values of the study area in an effort to unravel the specific drivers of vulnerability—called "spectra of vulnerability." However, this study did not take into account spatial interactions of the area being studied. In the same vein, Robinson et al. (2019) investigated the relative influence of social indicators on vulnerability to energy poverty in England to disentangle each global component and its spatial distribution using GWPCA.

To date, there has been no application of GWPCA to social vulnerability to natural hazards. This study has examined the contributions of the constituent components of the SoVI. Although the SoVI is intended to measure the overall degree of social vulnerability, a significant portion of areas with high SoVI are composed of components representing only one or two specific social conditions. We found that the overall social vulnerability in the Greater Houston area, as measured by the SoVI, has exhibited persistent spatial patterns since 1970. The central city and suburban outskirts in the Greater Houston area are more socially vulnerable as they have high SoVI values. But the spatial patterns of the SoVI are not equally constituted by the

components of the SoVI. In particular, the high social vulnerability of suburban areas is mainly the result of one principal component that highly correlates with the percent of mobile homes.

We have also examined the spatial and temporal patterns of the local primary determinants of social vulnerability by using the geographically weighted principal components analysis (GWPCA) and sequence alignment analysis-based clustering method. The application of GWPCA allows us to see that the local primary determinants of social vulnerability have exhibited prominent spatial and temporal patterns. The median household income, percent of households without a vehicle, and percent of people in poverty are the three primary determinants that have been held by most tracts in the Greater Houston area since 1970.

In addition, results of this study indicate that five clusters of primary determinants in the Greater Houston area change over time. Clusters 1, 2, and 3 are mainly dominated by median household income, percent of people in poverty, and percent of households without a vehicle, respectively. This is consistent with the demographic trend of the City of Houston where the population has experienced high poverty alongside a significant growth of immigrants and minority populations, and high unemployment rates (O'Connell & Howell, 2016). Clusters 4 and 5 have larger variation in their primary determinants over time. All the primary determinants that are held by most tracts in the clusters and throughout the Greater Houston area reflect that disadvantages in economic situation, mobility, and family structure are the most influential factors contributing to social vulnerability. For clusters 4 and 5, the primary determinants of the local social vulnerability change more often than clusters 1, 2, and 3. The temporal patterns of the local primary determinant variables of social vulnerability exhibited a substantial change over time. More than half of the tracts in the Greater Houston area change their local primary determinants in consecutive time periods. The most frequent change of the primary determinants

in consecutive time periods varies per cluster. In cluster 1, the most frequent change is from median household income to itself, suggesting the dominance and persistence of this variable in this cluster. Cluster 3 has a similar persistent pattern, but the variable is the percent of households without a vehicle. The other clusters involve more variables changing over time.

The present study has been the first attempt to explicitly examine the extent of temporal variation in local primary determinants of the social vulnerability index from 1970 to 2010 using Greater Houston as a case study. The insights gained from this study may enable effective resource allocation by identifying local contributing factors to social vulnerability.

In addition to offering specificities in reducing social vulnerability, the local primary determinants to the social vulnerability shed light on the potential qualitative processes that underlie the changing social vulnerability across space and over time. Many social indicators are similar to the aggregate composite indicators (e.g., resilience, deprivation, collective efficacy, social cohesion, etc.) like the SoVI. They are useful in simplifying complex social phenomena, but very often they are found to be too simplified for resource allocation and decision and policy-making. The methodology adopted in this study shows the possibility of local spatial statistical methods in helping bring more local realism and specificity to these social indicators. With the increasing availability of data from different sources, a larger set of variables can be incorporated in constructing aggregate composite indicators. Although this study only used thirteen variables, they still form the basis of the social vulnerability index representing socio-economic status, household composition and disability, minority status and language, and housing and transportation (Flanagan et al., 2011). There is not a consistent agreement on how many and which variables should be included in a social vulnerability index, but a higher number of

variables does not guarantee a reliable and meaningful index (Spielman et al., 2020; Strode et al., 2020).

The primary determinant variables found in this study show that only a few variables are the primary determinants and that they are very persistent in certain parts of the study area. GWPCA is a local spatial statistical method that performs the principal components analysis on a sub-dataset for each location. Although GWPCA has wide applications, it carries the common caveats of the local spatial statistical methods, such as overlapping statistical tests, so its usage and interpretation are more exploratory rather than confirmatory. However, the local spatial statistical methods that account for spatial heterogeneity and dependence show its strength in contributing useful insight in social indicator research.

3.4. Summary

The purpose of this chapter was to address two criticisms of the social vulnerability index (SoVI) at both the national and local scale: (1) social vulnerability has not been characterized as with spatial and temporal dynamics in a systematic and quantitative manner, and (2) the SoVI conceals the heterogeneous local contributors. This chapter proposed a methodological framework to advance the SoVI in an effort to understand systematic temporal variation of social vulnerability at the national scale for the conterminous United States and the local primary determinants contributing to the overall social vulnerability in Greater Houston as a case study. Applying the sequence alignment analysis coupled with the SoVI, this study has shown that the U.S. county-level social vulnerability exhibits four distinctive temporal variations from 1970 to 2010, revealing areas of persistently low/high vulnerability and areas with dynamically changing vulnerability statuses that either increase or decrease over time. In addition, the application of GWPCA can be used as an alternative way to track down the most influential social determinants

that constitute the SoVI index. Temporal trends of the local primary determinants of social vulnerability index can be beneficial in understanding what socioeconomic conditions are pervasive and consistently affect vulnerability in a particular region over a long-term period of time. These pragmatic approaches adopted in this study have significant implications for practitioners and local stakeholders in monitoring vulnerable areas being studied and establishing potential hazard mitigation plans.

The analytic framework proposed in this chapter, nonetheless, is still based upon the spatial aggregation of the social vulnerability in which its core purpose is to identify the generalized pockets of high social vulnerability across multiple/all hazards (Beccari, 2016; Flanagan et al., 2018; Tellman et al., 2020; Yoon, 2012). Each hazard has its unique characteristics in terms of physical phenomena and its consequential damage. However, the majority of studies using the SoVI approach has served as the basis for providing an overall social vulnerability profile in the event of all-natural hazards rather than being a hazard-specific approach. Since the occurrence of natural hazards still carries accidental and random components, it is necessary to understand what areas have been historically damaged by a certain hazard risk to provide a fuller picture of hazard preparedness.

Despite the fact that the SoVI is a useful instrument for detecting the "outliers or anomalies" where there is relatively high vulnerability, the ecological fallacy—a type of inference fallacy when the interpretation of results about individuals are deduced from aggregate data measured at multiple geographic scales—is part of the indicator-based approaches (Beccari, 2016; Gall, 2007; Wood et al., 2010). The local primary determinants from GWPCA are complementary in explaining what social factors play a major part in producing the overall social vulnerability at a certain place. Yet, to fully understand *who* is vulnerable is still questionable

solely based upon the SoVI approach. In conjunction with the SoVI, vulnerability research should take into consideration the population distribution and demographic composition to answer who is at greater risk of exposure to a certain natural hazard, termed “demographic differential vulnerability” (Muttarak, Lutz, & Jiang, 2015). In this respect, the remaining chapters of this dissertation focus on hurricane hazards to investigate what population groups have resided within the hurricane-impacted areas over time in the United States.

Chapter 4. Hurricane Damage along the U.S. Gulf and Atlantic Coasts from 1950 to 2018

4.1. Introduction

U.S. coastal populations face the risk of hazards such as hurricanes, storm surges, sea-level rise, and coastal erosion. Estimating exposure to hurricane risk is a basic step in comprehending geophysical vulnerability of coastal communities (Cutter, 2001). To date, numerous studies have assessed hurricane vulnerability on a case-by-case basis, focusing on the most devastating hurricane events that have caused enormous societal losses. Such case-specific studies do not necessarily show the long-term effects of hurricane risks in coastal regions and provide a limited picture in assessing the comprehensive vulnerability to hurricane hazards over time. One longitudinal study by Logan and Xu (2015) modeled hurricane-related hazards to capture spatial patterns of actual hurricane exposure that have occurred from 1950 to 2005. Despite the importance of long-term research in hurricane vulnerability, there remains a paucity of longitudinal studies that systematically examine vulnerability in terms of demographic changes along the U.S. Gulf and Atlantic Coasts. The majority of damage and loss of life are associated with storm surges and high winds in the wake of hurricanes, and impacts have been unevenly distributed across the U.S. during the past several decades. Figure 16 shows the trajectories of all hurricanes and tropical storms that reached the U.S. East Coast, Florida, and Gulf Coast area from 1950 to 2018. The objective of this chapter is therefore to estimate the geographic distribution of hurricane hazards in the United States by modeling the extensive hurricane-related damage (i.e., storm surge and wind damage) from 1950 to 2018. Specifically, this chapter is designed to answer the following research questions: (1) What are the spatial extent and intensity of storm surge inundation and wind damage caused by hurricanes along the

Gulf and Atlantic Coasts in the United States from 1950 onwards? and (2) What regions have been particularly hard hit by hurricanes in the U.S. coastal counties over the past decades since 1950?

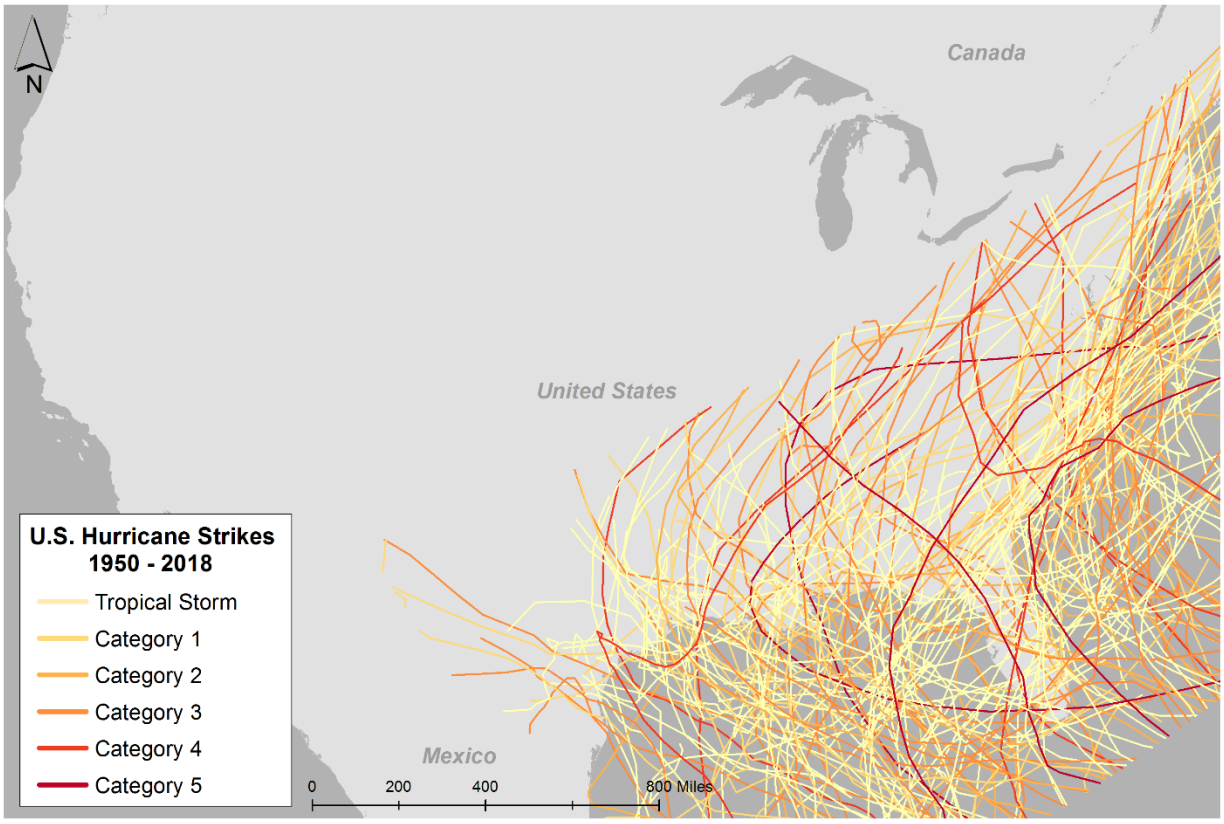

Figure 16. Historical hurricane and tropical storm tracks that made landfall along the U.S. Gulf and Atlantic coasts from 1950 to 2018

4.2. Data and Methodology

Since the historical geospatial data of hurricane impacts are seldom available, it is necessary to reconstruct to what extent past and recent hurricanes have affected coastal regions. This chapter intends to determine the geographic extent of storm surges and wind damage over an extended period of time from 1950 to 2018 to identify the comprehensive locational vulnerability to hurricane impacts. The modeled results from every hurricane are then aggregated

to a single unified spatial surface, reflecting the long-term hurricane impacts across the entire coastal areas for decades. The resultant unified geographic extent of all hurricane-related damage is based on 190 hurricanes and tropical storms during the study period from 1950 to 2018, serving as a baseline to Chapter 5's examination of vulnerability to hurricane damage among different segments of the population.

In estimating hurricane-related damage, the public hurricane database (known as the revised Atlantic hurricane database, HURDAT2) was employed in this study to identify the areas that are susceptible to frequent major hurricanes. The HURDAT2 is the second-generation hurricane database maintained and updated annually by the U.S. National Oceanic and Atmospheric Administration (NOAA) at the National Hurricane Center (NHC). This database can be obtained from the NHC Data Archive and contain the best-estimated track records of all historical hurricanes, tropical storms, and subtropical storms of the Atlantic basin, including the Gulf of Mexico and Caribbean Sea since 1851. Each storm can be identified by its name and identifier number with detailed information such as date, time, position that geocoded the center of the storm (latitude and longitude), intensity (i.e., maximum sustained wind in knots), central pressure, and size (Landsea & Franklin, 2013; Landsea, Franklin, & Beven, 2015). These parameters are used to compute the storm surge heights and wind damage resulting from hurricanes by considering hurricane gust factors.

Topographic data or digital elevation models (DEM) are also crucial in determining storm surge inundation because the shape of the terrain is highly related to how water flows and drains along and off a surface. The primary dataset used in this study is the U.S. Geological Survey (USGS) National Elevation Dataset (NED), which is seamless elevation data covering the conterminous United States at different spatial resolutions (Zachry, Booth, Rhome, &

Sharon, 2015). In this study, the 1/3 arc-second (approximately, 10 meters) DEM dataset is selected for coastal inundation mapping. Tide data is also required to generate a water surface as an input value in storm surge modeling. The initial water level for each hurricane can be found at the nearby tide station referring to the hurricane path observed 18 hours before nearest approach (or landfall) in most storm situations (Jelesnianski, Chen, & Shaffer, 1992; Logan & Xu, 2015). The table below provides the source of the data required in estimating the areas affected by storm surges and wind damage from 1950 to 2018.

Table 11. Data sources for hurricane damage modeling

Data	Source
The revised Atlantic hurricane database (HURDAT2)	National Hurricane Center Data Archive (https://www.nhc.noaa.gov/data/)
National Elevation Dataset	USGS The National Map Viewer (https://apps.nationalmap.gov/viewer/)
Tide, currents, and water levels	NOAA Tides and Currents (https://tidesandcurrents.noaa.gov/)
Sea, Lake, and Overland Surges from Hurricanes (SLOSH) Model Display Program	National Hurricane Center (https://www.nhc.noaa.gov/surge/slosh.php)

4.3. Estimation of Storm Surge Inundation

In an attempt to overcome data scarcity in historical GIS hurricane data, this study adopts a hydrodynamic model, called Sea, Lake, and Overland Surges from Hurricanes (SLOSH) in obtaining the spatial extent and intensity of storm surge. The SLOSH model is currently being used by NHC for real-time forecasting of potential hurricane storm surges across the entire seaboard of the United States (Glahn et al., 2009; Jelesnianski, Chen, Shaffer, & Gilad, 1984; Lin et al., 2010). A major advantage of the SLOSH model is its ability to reproduce the historical hurricane storm surges based on the HURDAT2 dataset. The accuracy of the estimated surge

height is known to be within ± 20% of the observed water heights (Forbes, Rhome, Mattocks, & Taylor, 2014; Jelesnianski et al., 1984; K. Smith & Petley, 2009).

The SLOSH model is a two-dimensional numerical coastal model that computes the maximum water heights considering the dynamic flow of water over land and water based on pre-determined grid cells referred to as a basin. Currently, there are 32 basins covering the entire US Atlantic and Gulf of Mexico Coasts, Hawaii, Puerto Rico, Virgin Islands, and the Bahamas. All hurricanes and tropical storms that made landfall along the coastal regions can be modeled with the operational basins as shown in Figure 17. If a hurricane impacted a larger extent of the area, multiple basins are considered in the modeling procedure.

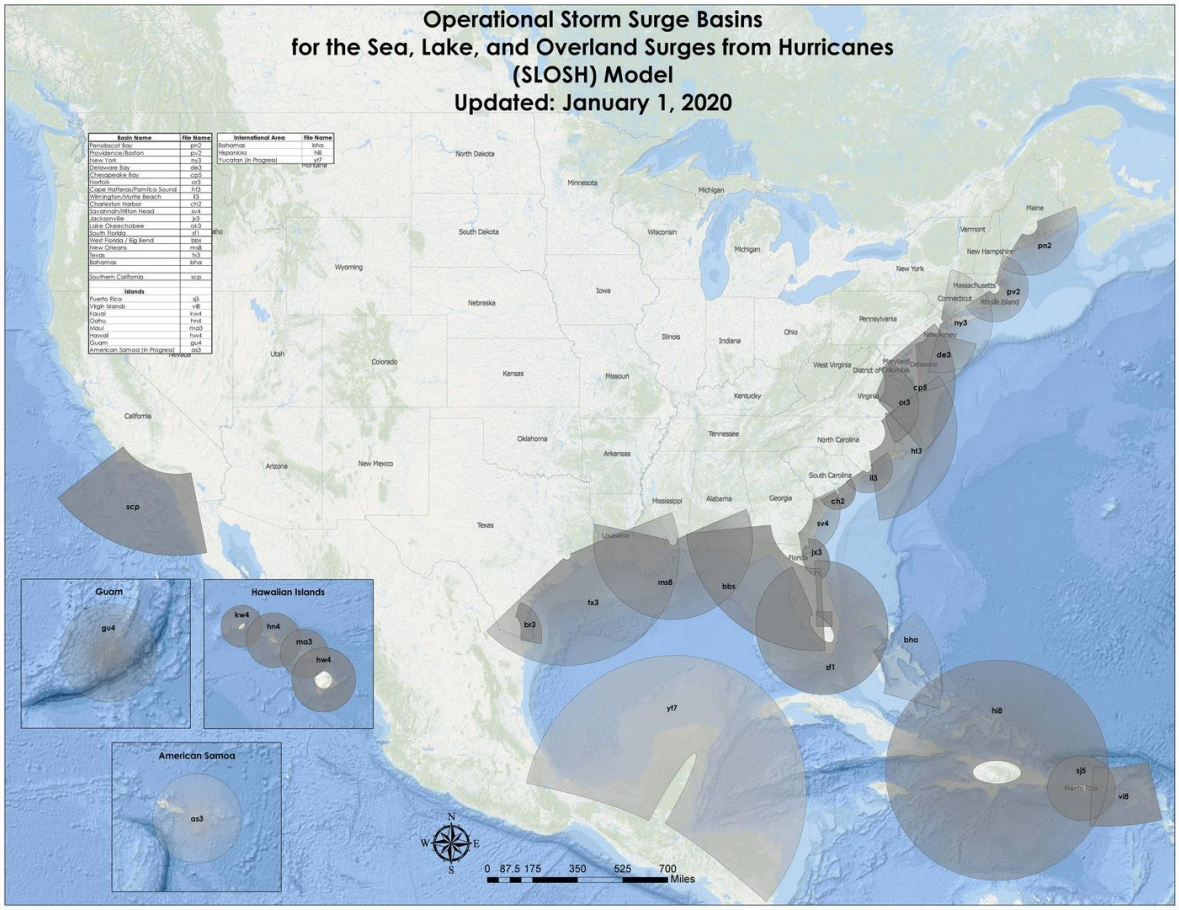

Figure 17. The coverage of the SLOSH model

Depending on the region, the basins have different shapes (mostly, polar or hyperbolic/elliptical) composed of thousands of grid cells, and these are one of the primary inputs with the meteorological parameters that must be entered in the modeling process (Conver, Sepanik, Louangsaysongkham, & Miller, 2008). The closer to the primary area of interest such as a bay or a region immediately adjacent to the coastline, the finer the resolution of the grid cells. Meanwhile, the spatial resolution of the grid cells is coarser in the deep open oceans due to a low significance in simulation. The basins integrate geographical characteristics of the particular area along the coasts that influence storm surge such as topography, shoreline structure, levees, bathymetry of ocean areas, and continental shelves (Forbes et al., 2014). Modeling storm surge requires the following meteorological parameters as input parameters to generate the wind field that drives the storm surge inundation: storm track positions (i.e., latitude and longitude at 6-hour interval), intensity (i.e., storm central pressure at 6-hour interval), radius of maximum wind (RMW, i.e., size—the distance between the center of a storm and the location where the strongest wind generates at 6-hour interval), forward speed, and landfall time (Jelesnianski et al., 1984; Mercado, 1994). Considering these input parameters coupled with a selected basin, the SLOSH model can determine the flow of storm surge across the surface and then estimate the maximum envelope of water in each basin grid during a storm's life cycle.

Spatial analysis can be conducted to derive the inundation extent and the depth of a storm surge using simulated water height from the SLOSH model and DEM data. It is important to note that each dataset refers to a different vertical datum; the SLOSH model output references the National Geodetic Vertical datum 1929 (NGVD29); the initial tidewater level refers to Mean Lower Low Water (MLLW); the elevation data is based on the North American Vertical datum of 1988 (NAVD88). All elevations are based on different vertical data and cannot be directly

used for spatial analysis. Therefore, it is required to maintain a consistent vertical datum between the estimated storm surge inundation height and the terrain elevation data using a transformation to derive the depth of a storm surge accurately. The SLOSH model does not include the wave components on top of the surge, and thus the astronomical tides can be added to the model results (Frazier, Wood, Yarnal, & Bauer, 2010; Glahn et al., 2009; Houston, Shaffer, Powell, & Chen, 1999; Logan & Xu, 2015; Maloney & Preston, 2014). As a result, the maximum surge water height generated from the SLOSH model can be converted to a GIS file format to create an interpolated surface.

Figure 18 represents the coastal regions that have been exposed to the impact of one foot or higher of storm surge since 1950. The result is consistent with the NOAA/National Weather Service/National Hurricane Center Storm Surge Unit's storm surge inundation map (Zachry et al., 2015). Storm surge damage is highly localized along coastal areas. Overall, a stretch of the Gulf Coast from South Texas to the Florida panhandle has borne the brunt of storm surge damage over time. Southeastern Louisiana (especially, the lower Mississippi River delta region), Alabama, Mississippi, and the Northwestern Panhandle of Florida have been hard hit by the most intensive storm surges more than twenty-one times with the maximum frequency of thirty-nine for the past several decades. Western Louisiana, Southwestern Florida, and West-Central Florida have also experienced frequent exposure to storm surge impacts. In the Southeastern coastal regions, the Charleston area in South Carolina, the Outer Banks, and the coastal counties near Brunswick, New Hanover, Pender, and Onslow Counties have been affected by storm surges at least eleven times. In contrast, the Mid-Atlantic region has been relatively less affected by storm surge inundation. Particularly, the Chesapeake Bay area—especially the southeastern shore of Virginia (Hampton Roads region) and the southern tip of Delmarva Peninsula—have been

flooded by storm surges at least ten times. It is not unusual to observe fairly frequent storm surge inundation in the Eastern Long Island regions (Nassau and Suffolk County) and southwestern Connecticut. New England regions have also been subject to coastal inundation for decades. These regions are increasingly becoming more susceptible to hurricane strikes due to climate change and sea-level rise (Boon, 2012; Cutter et al., 2007; Sallenger, Doran, & Howd, 2012).

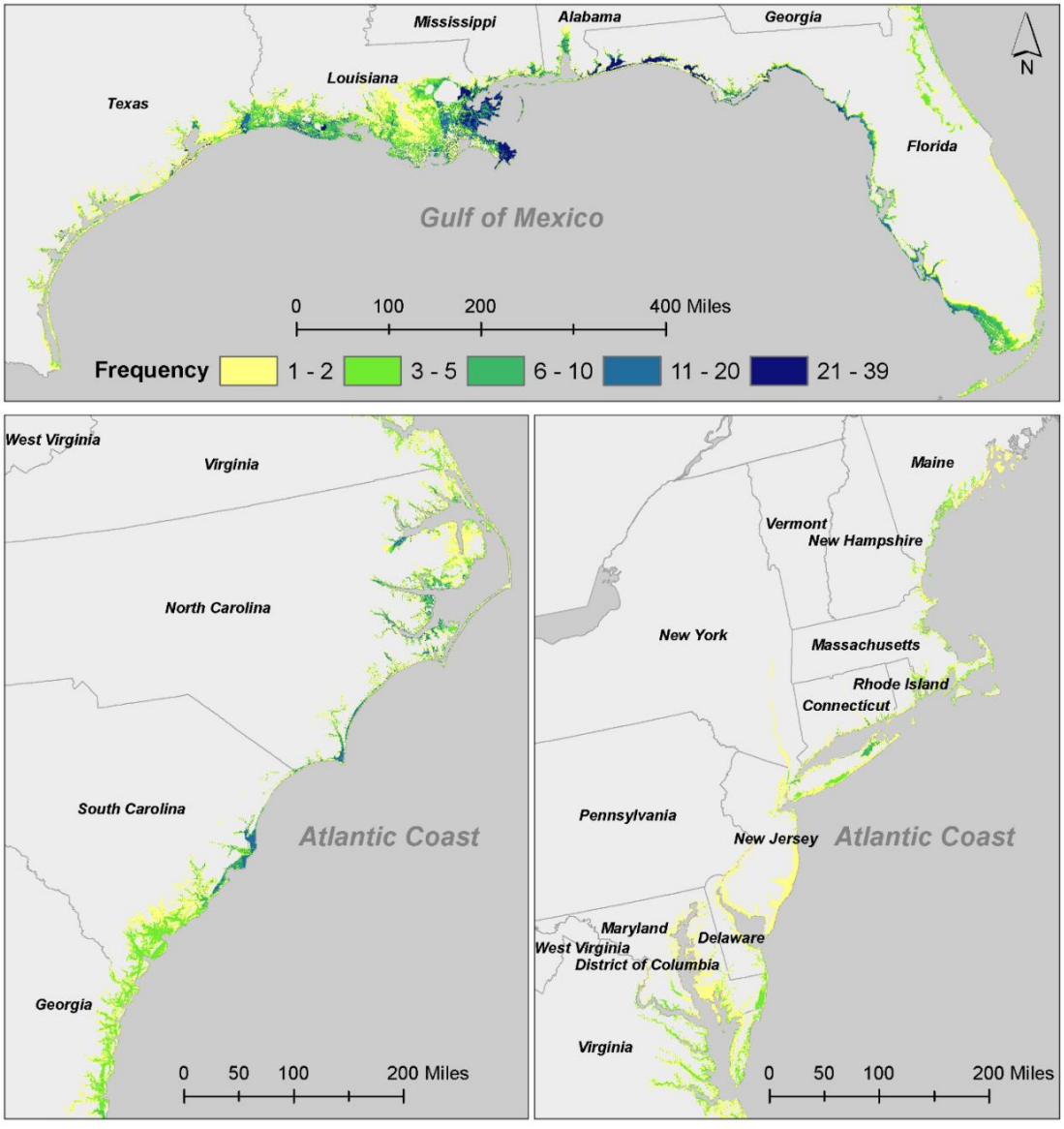

Figure 18. Modeled frequency of storm surge inundation of one foot or higher based on hurricanes and tropical storms from 1950 to 2018

4.4. Estimation of Wind Damage

Strong hurricane winds often cause severe structural damage to infrastructure, residential structures, and commercial structures (K. Smith & Petley, 2009). This study adopts a simple meteorological model (HURRECON), which is based on published empirical studies of hurricanes, to reconstruct the intensity of wind damage by each hurricane. The HURRECON model was developed to estimate the basic structure of a storm's surface wind conditions such as sustained wind velocity, peak gust velocity, and wind direction of movement. This model also uses the meteorological parameters[3] of a storm (i.e., storm track and wind speed) as input data. It also requires a rectangular geographic file (i.e., 16-bit IDRISI raster file format) to distinguish the land cover type (water or land) in estimating the surface wind speed and direction. The raster grid should be equally divided per each cell to produce a more accurate modeling result. The parametric equations are well documented in the literature (Boose, Chamberlin, & Foster, 2001; Boose, Serrano, & Foster, 2004; Logan & Xu, 2015). In this model, the predicted wind damage is adjusted for hurricane wind field estimation and then classified into the modified Fujita scale classes (no damage, F0, F1, F2, F3)—originally proposed by Fujita (1971) to characterize the wind intensity and damage by tornadoes—by correlating the maximum quarter-mile wind speed with wind damage intensity (Boose et al., 2004). The HURRECON model can generate the prediction of wind damage for an individual site as a table or for the entire area of interest as an IDRISI raster format, which is compatible with TerrSet (formerly IDRISI) software.

[3] The estimation of hurricane wind is based on the same parameters used in previous empirical study that modeled historical hurricanes along the Gulf Coast (Logan & Xu, 2015). Different parameters may result in more accurate estimations for storms that made landfall on the Atlantic coast.

The HURRECON-modeled results are compiled to show a more complete picture of wind damage for the entire coastal regions on the Fujita scale since 1950 (Figure 19). Hurricane wind rapidly becomes weaker as the storms make landfall along the coast as a consequence of their interaction with coastal geomorphic characteristics and the loss of heat. Occasionally, hurricanes can travel hundreds of miles deep into the interior counties after landfall, intensifying its power. Hence, the areas affected by hurricane wind are not just limited to the immediate vicinity of coastal regions, moving further inland (Emrich & Cutter, 2011; Kruk, Gibney, Levinson, & Squires, 2010).

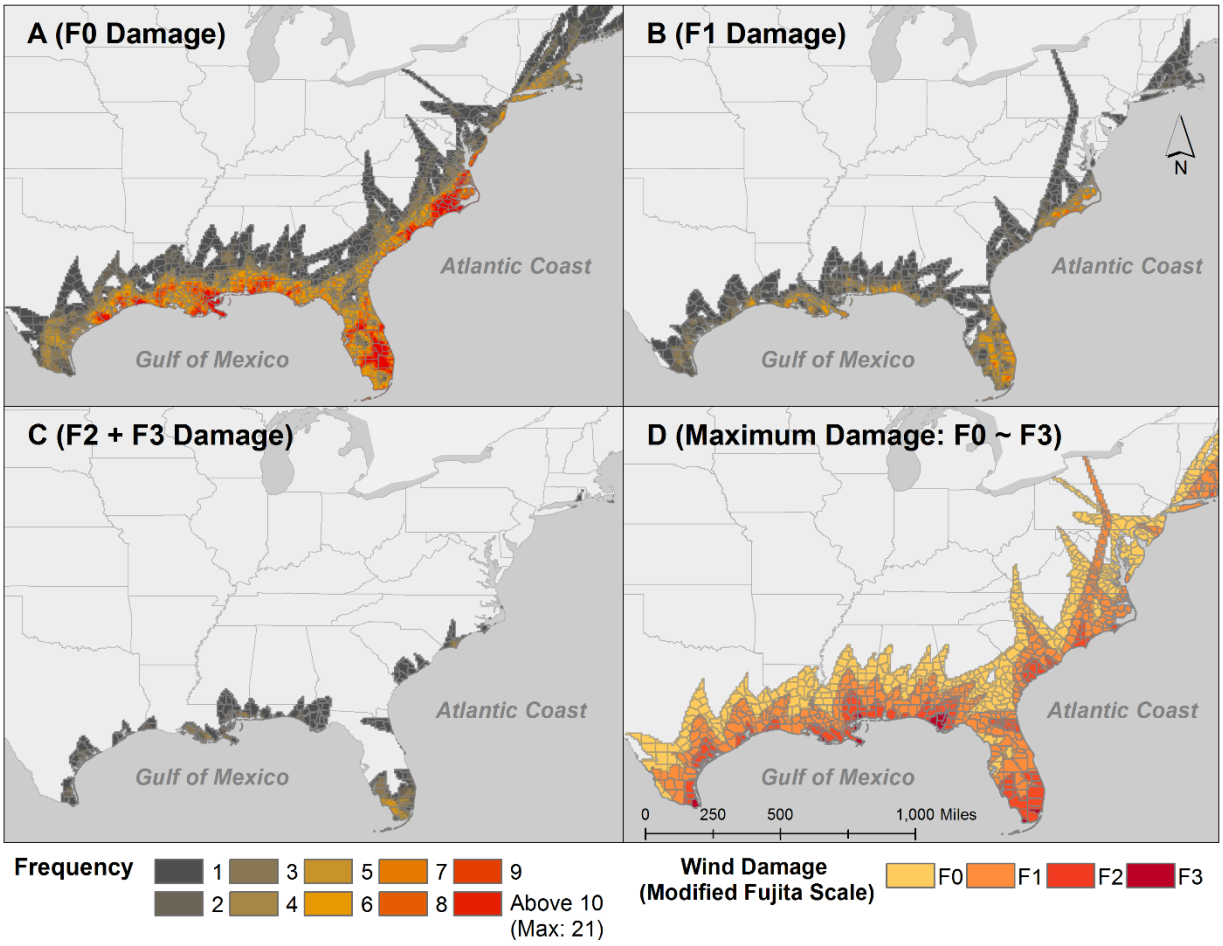

Figure 19. Modeled wind damage frequency and intensity from 1950 to 2018

Panel A shows the spatial extent of hurricane risk in which a total of 759 counties have experienced F0 wind damage (the loss of leaves and branches) over time stretching from Southeast Texas to the far stretches of Maine. The counties within 100 miles of the coastline have been exposed to F0 wind strengths more than 5 times. Panel B reveals the areal extent of F1 damage (scattered blowdown), and 478 counties have been exposed to F1 strength wind forces. As can be seen from Panel C, the areas exposed to F2 or F3 (extensive blowdown) wind strengths are concentrated along and including the coastal regions of North Carolina, South Florida, and the Gulf of Mexico. As expected, F0- and F1-intensity winds traveled further inland compared to F2- and F3-scale winds that are more localized along the coastline (Panel D). The areal extent of hurricane-driven storm surge is geographically concentrated along the coastal shoreline counties, whereas hurricane winds tend to affect the inland areas to a larger extent, penetrating deep into the inland areas of the United States. This is more apparent in northeastern states.

4.5. Summary

Hurricanes pose the risk of great damage to the coast and to society. Physical or locational vulnerability can be assessed based on the impacts, magnitude, frequency of natural hazards, and geographical proximity to the source of natural hazards (Cutter, 2001; Logan & Xu, 2015). The purpose of this chapter was to determine the geographic extent of the area impacted by hurricane damage and to examine regional variation in frequency and intensity of damage from 1950 to 2018 along the U.S. Gulf and Atlantic Coasts. The modeled outputs of all hurricanes were aggregated into a singular geographic area to show long-term historic cumulative damage over the past six decades. As a result, 759 counties were found to be the hurricane at-risk zones that have experienced at least one instance of hurricane damage during

the study period, which will be my study area in the following chapter. The next chapter, therefore, moves on to discuss what population groups have been more or less susceptible to hurricane hazards within the hurricane-prone areas.

Chapter 5. Social Vulnerability to Hurricane Hazards: The Changing Demographics within Hurricane At-Risk Areas

5.1. Introduction

According to the hazards of place model, social vulnerability to natural hazards or environmental risks arises not only from physical or locational vulnerability but also from the close linkage between the environment and the underlying social processes (Cutter, 1996). Socioeconomic and demographic characteristics of people, including age, gender, race/ethnicity, income levels, level of education, and employment status, etc. can affect vulnerability. Most studies have focused scholarly attention on measuring the relative level of social vulnerability, adopting the place-based SoVI approach at different local scales focusing on a single hurricane hazard (C. G. Burton, 2010; Clark et al., 1998; Finch, Emrich, & Cutter, 2010; Flanagan et al., 2011; Myers et al., 2008; C. Wang & Yarnal, 2012).

The adverse impact of natural hazards can be compounded by human occupancy and the ability of people and places to cope with and to mitigate the effect of natural hazards (Barnett & Adger, 2018; Martine & Guzman, 2002; Muttarak et al., 2015). In recent years, there has been an increasing amount of literature on population change, composition, and the interplay of population dynamics and vulnerability (Donner & Rodríguez, 2008; Fussell et al., 2017; Logan, Issar, & Xu, 2016; Logan & Xu, 2015; Marandola & Hogan, 2006; Schultz & Elliott, 2013). Population changes and composition can transform risk or a hazardous event into catastrophic natural disasters. Although population composition and distribution are interwoven with social vulnerability, intersectional theory has not been incorporated into the understanding of demographic dynamics and the study of vulnerability. The degree of vulnerability is not solely contingent on a single-axis demographic factor (e.g., older adults and children). Rather, it is

produced as the consequence of the interconnectedness of other demographic factors such as race, sex, age, and social class (Kuran et al., 2020). As a proxy to better understand differential demographic vulnerability, this chapter also investigates which demographic subgroups are at risk of hurricane damage, as detailed in chapter 4, by incorporating an intersectional approach from 1970 to 2018. Specifically, this study aims to unravel which populations are increasingly or decreasingly exposed to the hurricane damage over time within hurricane-prone regions considering population dynamics. The findings of this research can assist policymakers and local community stakeholders in supporting disaster emergency planning and evacuation strategies in a meaningful manner.

5.2. Study Area

This study focuses on the coastal counties that have experienced at least one instance of hurricane-related damage between 1950 and 2018 along the Gulf of Mexico and Atlantic Coasts in the United States (Figure 20). Coastal counties, as defined in this study, are geographically restricted to the Gulf of Mexico coastline and the eastern Atlantic Coast of the United States (i.e., the North Atlantic Basin region), excluding the Pacific Coast and the Great Lakes region, providing a baseline for describing the human settlement of the hurricane-impacted coastal shorelines (Ache, Crossett, Pacheco, Adkins, & Wiley, 2015; Crossett et al., 2013; NOAA Office for Coastal Management, 2021; Strobl, 2011).

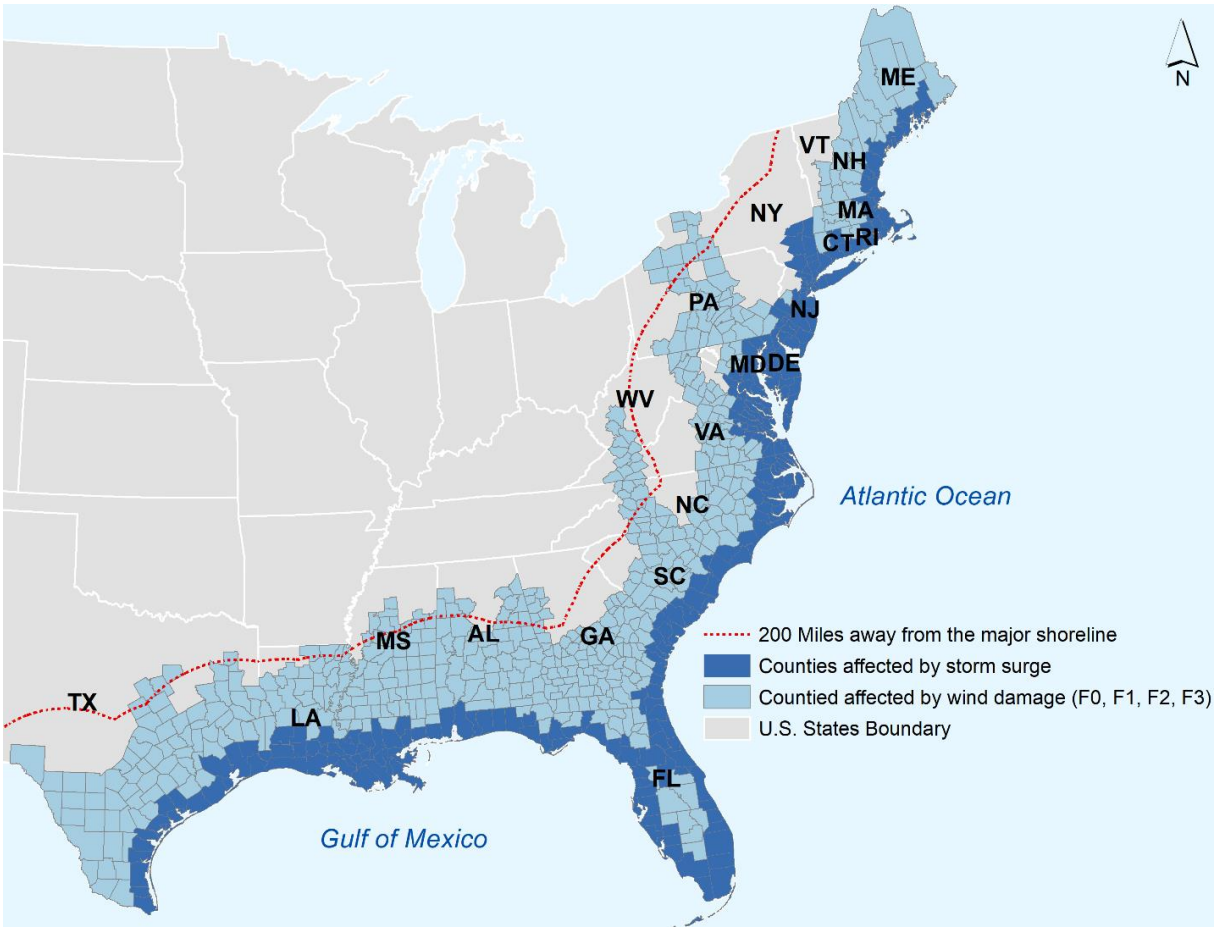

Figure 20. The study area in the U.S. Gulf and Atlantic Coasts (759 coastal counties)

Combining the spatial extent of hurricane damaged areas of F0, F1, F2, and F3 wind and storm surge, the spatial coverage of this study area consists of 759 counties over 22 states. The aggregated geographic extent of all hurricane-related damage shows a generalized and standardized pattern with no seasonal or random variation across time and space (Logan & Xu, 2015). The affected coastal counties in the Gulf Coast cover the majority of counties that are affected by hurricanes, up to approximately 200 miles from coastal shorelines. Meanwhile, the affected coastal counties of the Atlantic Coast are located up to 400 miles from the coast, reaching further inland than the Gulf Coast. The whole study area is used to calculate the share of the population groups that are exposed to storm surge inundation and wind damage (F0, F1, F2, and F3) within residential areas described in the following subsections.

5.3. Data and Methodology

Land-cover dataset – This study investigates at-risk populations in residential areas of hurricane-prone areas using land-use and land-cover type to calculate the percentage of residential areas in each county/census tract that have been affected by storm surge and wind damage (i.e., damage fraction, hereafter). To ensure non-residential land use areas are excluded in calculating the fraction, this study integrates nationwide land cover data from the National Land Cover Database (NLCD) for the following years: NLCD 2001, 2006, 2008, 2011, 2013, and 2016 (Homer et al., 2020; Pozzi & Small, 2005; Yang et al., 2018). A longitudinal study of temporal change of land-cover patterns by Homer et al. (2020) reported that as much as 5.6 percent of the United States' 29,000km^2 has been developed over the last 15 years. By incorporating the long-term land-cover dataset, it is possible to take into account land-use change and rapid urban/suburban sprawl. For the purpose of analysis, 4 categories of developed/built areas are selected among the 16 land cover classification categories in this study (Table 12).

Table 12. National Land Cover Database classification (developed/built areas)

Land Cover Class	Classification Description
Developed, Open Space	Areas with a mixture of some constructed materials, but mostly vegetation in the form of lawn grasses. Impervious surfaces account for less than 20% of total cover. These areas most commonly include large-lot single-family housing units, parks, golf courses, and vegetation planted in developed settings for recreation, erosion control, or aesthetic purposes.
Developed, Low Intensity	Areas with a mixture of constructed materials and vegetation. Impervious surfaces account for 20% to 49% percent of total cover. These areas most commonly include single-family housing units.
Developed, Medium Intensity	Areas with a mixture of constructed materials and vegetation. Impervious surfaces account for 50% to 79% of the total cover. These areas most commonly include single-family housing units.
Developed High Intensity	Highly developed areas where people reside or work in high numbers. Examples include apartment complexes, row houses and commercial/industrial. Impervious surfaces account for 80% to 100% of the total cover.

Source: Multi-Resolution Land Characteristics (MRLC) Consortium (https://www.mrlc.gov/)

Population dataset – Using the damage fraction of storm surge and wind damage (measured by Fujita scale – F0, F1, F2, F3) coupled with population data, we can obtain the number of people that have been exposed to hurricane risks over the past five decades. For the areas affected by wind damage, this study incorporates the U.S. Intercensal County Population Data (1970-2018). For storm surge areas, census tract data from the decennial census and American Community Survey (ACS) can yield the localized impact of storm surge inundation (Logan & Xu, 2015). Both the county-level data and census-tract level population data are stratified by age, gender, race, and Hispanic origin in which race is classified into different number of categories depending on the year of data. Recently, a growing consensus believes that intersectionality can be an analytical tool to uncover qualitative differences in vulnerability and resilience within groups (Kuran et al., 2020). In this study, demographic population data are stratified by age, gender, race, and Hispanic origin to further examine how the extent of vulnerability varies among different segments of populations (e.g., white male elderly, white female elderly, black male elderly, black female elderly).

Gender plays a role in vulnerability with females being more susceptible to natural hazards than males causing differential impacts (e.g., mortality rates, causality rates) in the aftermath of natural hazards (Cutter et al., 2003; Wisner et al., 2004). The concept of "gendered disaster vulnerability" helps in understanding how gender functions with other demographic characteristics (e.g., class, race/ethnicity, age) in shaping social vulnerability (Enarson & Meyreles, 2004; Llorente-Marrón, Díaz-Fernández, Méndez-Rodríguez, & Gonzalez Arias, 2020; Neumayer & Plümper, 2007; Parida, 2015). Initially, this study hypothesized that there would be a significant difference between the males and females in estimating at-risk populations. However, it was found that their population tends to have similar patterns. For this

reason, demographic data are only stratified by four race categories (non-Hispanic White, non-Hispanic Black, non-Hispanic Others, and Hispanic) and five age groups as follows – age group 1 (0-4 years), age group 2 (5-19 years), age group 3 (20-34 years), age group 4 (35-64 years), and age group 5 (65 years and older).

To allocate population to each hurricane-damaged zone, this study calculated a damage fraction using zonal raster operations. GIS zonal analysis calculates descriptive statistics (e.g., sum, count, mean, mix/max, standard deviation, etc.) and evaluates different raster datasets for a specified zone (Dong, Sadeghinaeenifard, Xia, & Tan, 2019). Zonal statistics were implemented to obtain the damage fraction for each zone using multiple raster datasets—residential land cover from the NLCD data and the estimated hurricane damage results from chapter 4. The results of the zonal analysis calculated the total number of residential cells that are affected by hurricane damage and the total number of residential cells for each county or census tract, respectively. Based on these two values, the damage fraction was calculated and then multiplied with the stratified demographic data to estimate how many people have been in high-risk hurricane zones within residential areas. The specific procedure is described in the flow chart (Figure 21). Data management and analysis were performed using ArcGIS 10.7 and statistical software R.

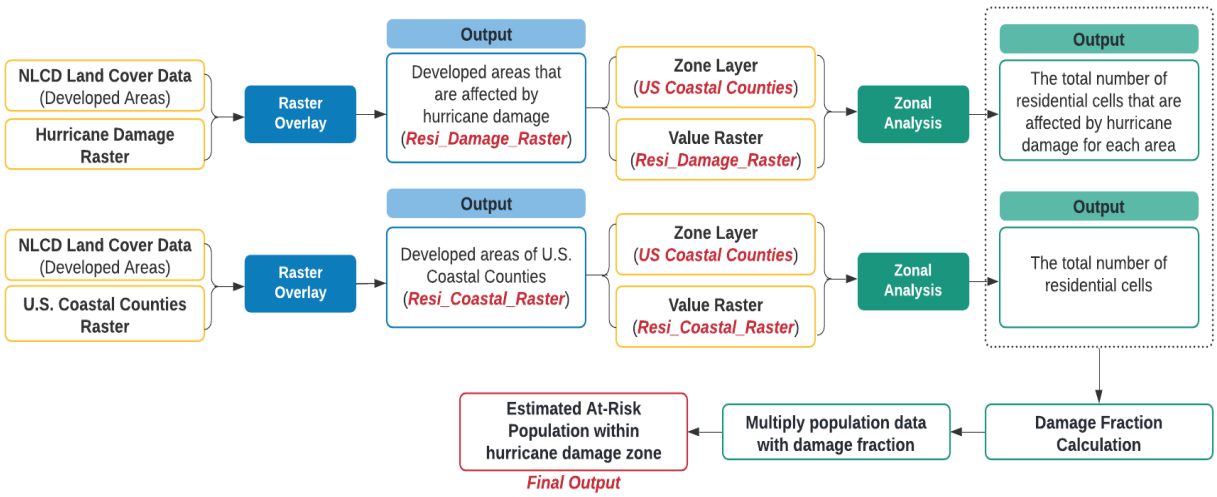

Figure 21. Data processing procedure for estimating at-risk populations

This study measured both the percentage of populations residing in varying degrees of hurricane damage zones in the United States and their share of the population within the study area over time. The percentage refers to the ratio of one age-race group in the affected area to the total population in the affected area, and the share denotes the ratio of one age-race group in the affected area to the total population of that group in the study area. As defined in section 5.2, the study area is the combined geographical areas of storm surge damage and F0 wind damage in the U.S. coastal region, encompassing all counties that have been affected by some category of hurricane damage (i.e., 759 counties). Calculating the age-race specific percentages ($ARSpP$) and age-race specific share ($ARSpS$) can be expressed in the following forms:

1) The percentage of populations affected by each hurricane damage category:

$$ARSpP = \frac{P_{ij}}{\sum P_{ij}} \times 100$$

where $\sum P_{ij}$ is sum of all race-age groups in the specific hurricane damaged area and P_{ij} is the total population of a race-age specific group i (e.g., non-Hispanic White age group 1) affected by

a hurricane damage category j (i.e., storm surge damage or wind damage by each category F0, F1, F2, F3). The age-race specific percentage of populations affected by each hurricane damage category is calculated as the ratio of one age-race group in the affected area to the total population in the affected area.

2) The share of populations affected by each hurricane damage category:

$$ARSpS = \frac{P_{ij}}{P_{iq}} \times 100$$

where $P_{iq}$is the total population of a specific race-age group in the study area (q) and P_{ij} is the total population of a race-age specific group i affected by a hurricane damage category j in the study area (i.e., 759 counties).

Based on the percentage and the share of populations affected by each hurricane damage category, this study seeks to understand how each population subgroup stratified by race and age groups has changed within the most hurricane-prone areas in the U.S. coastal counties from 1970 to 2018.

5.4. At-Risk Populations in the Hurricane-Prone Coastal Counties

How many people have been living in the U.S. hurricane coastal counties (i.e., 759 coastal counties as shown in Figure 20) from 1970 to 2018? Before delving into the demographic changes of coastal populations, it is important to understand how the U.S. national population and its growth rate have been changing over time. The graph below presents the U.S. population growth over the past 50 years (Figure 22). The national population was about 204 million in 1970 with the population growing exponentially over time, reaching 327 million in 2018. This increase can be attributed to the influx of immigrants in the 1980s and 1990s (Heisler &

Shrestha, 2011). While there have been uptrends in national population growth between 1970 and 2010, in general, the yearly rate of population growth has slowed to an all-time low of 0.62% per year in 2018, possibly due to the 2008 recession, low fertility rate, and severe immigration restrictions in more recent years (Frey, 2021).

In this study, coastal counties are defined as counties that border the Gulf of Mexico coastline and the eastern Atlantic Coast of the United States, excluding the Pacific Coast. In these coastal counties, population growth has largely mirrored the national trend during the same period. The coastal counties are more overcrowded than the nation as a whole, and they are expected to grow in the future (Crossett et al., 2013). The total number of people living in coastal areas was 73 million in 1970, growing by a total of 100 million people between 1970 and 2000 (Figure 23). Although the population growth rate consistently declined after 2000, along with the national trend, there was a 63 percent increase in the coastal population from 1970 to 2018, exceeding 119 million in 2018. The population density of coastal counties is substantially greater than inland counties (Crossett et al., 2013; Crowell et al., 2010). The coastal populations are facing multiple threats, such as climate change and coastal hazards, exposing 36.5 percent of the U.S. total population to increasingly vulnerable situations (Figure 24). Along with rapid population growth and an economic construction boom, the coastal populations has been racially diversified, thereby further exacerbating their vulnerability to hurricane hazards in the coastal counties over time (D. T. Cohen, 2018; Cutter et al., 2007).

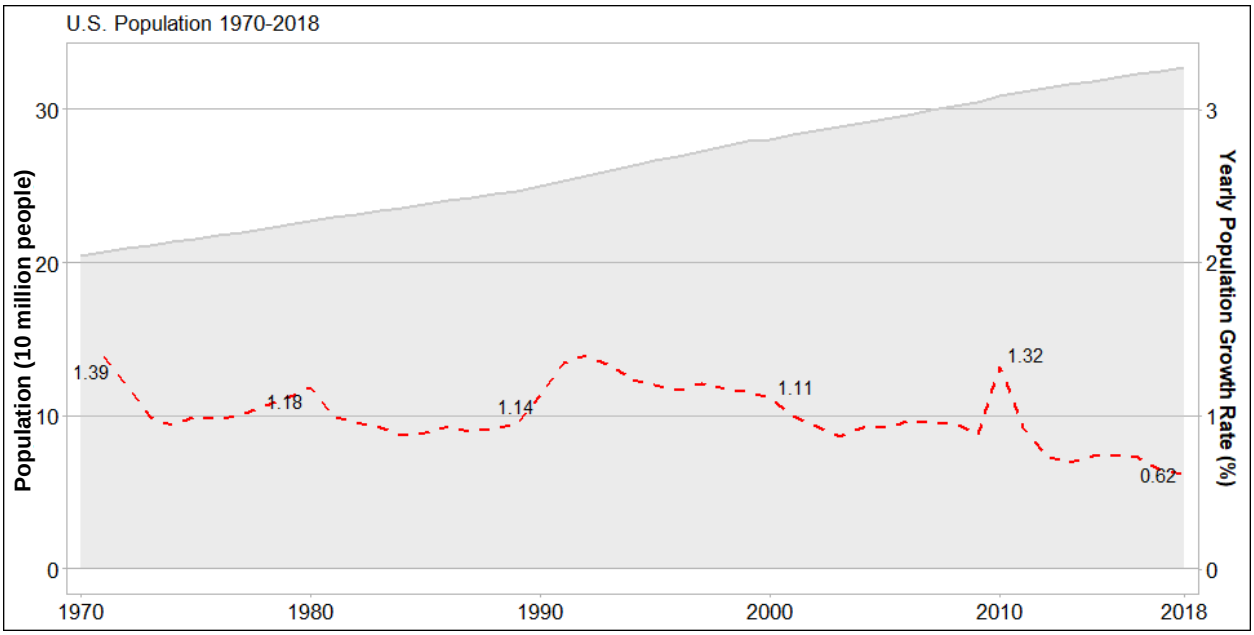

Figure 22. The national trend of the U.S. total populations and growth rate

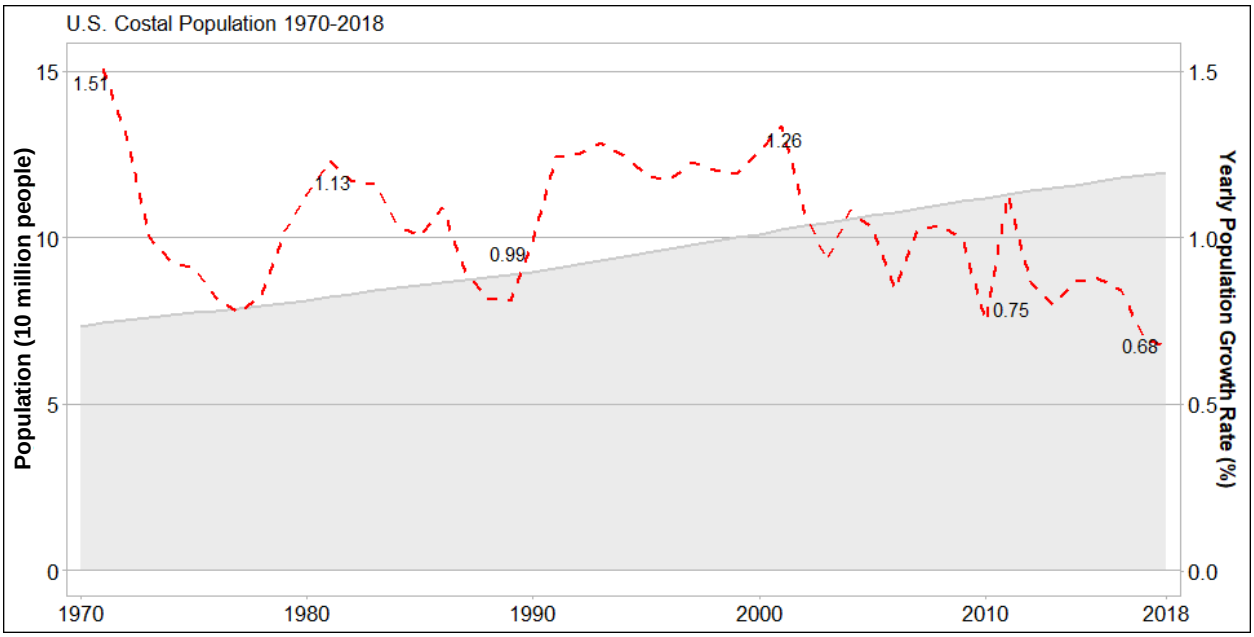

Figure 23. The population trend of the coastal counties and growth rate*

* Coastal counties, as defined in this study, are geographically restricted to the Gulf of Mexico coastline and the eastern Atlantic Coast of the United States (i.e., the North Atlantic Basin region), excluding the Pacific Coast and the Great Lakes region

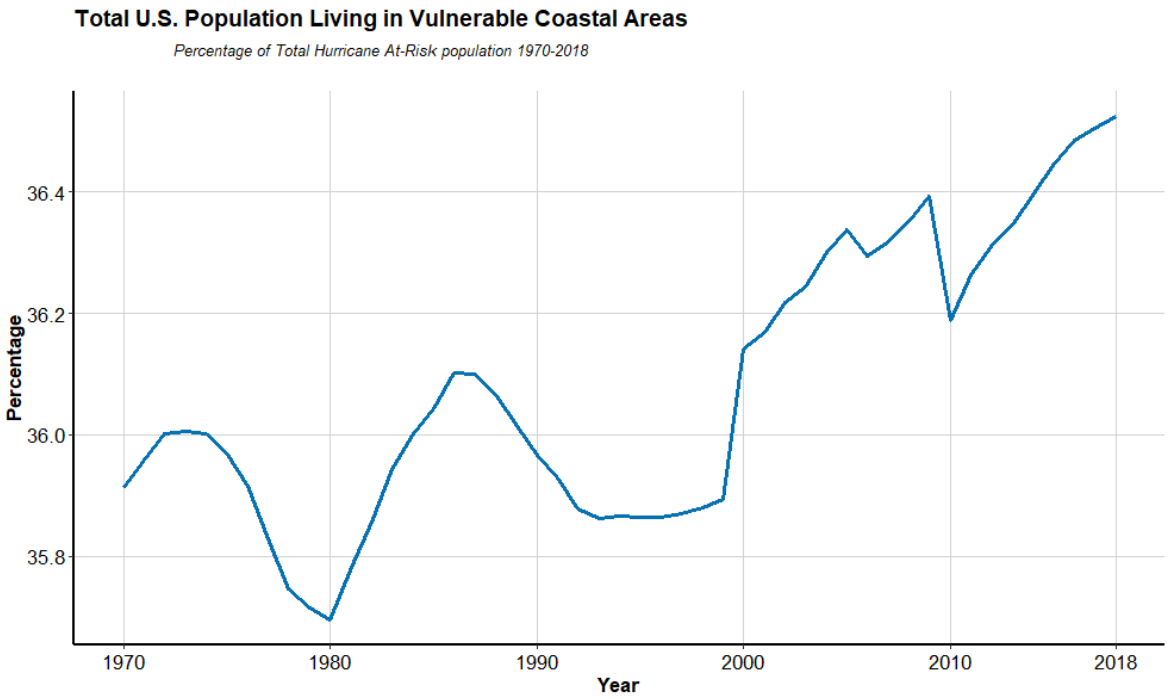

Figure 24. The percentage of the total U.S. population living in coastal counties*

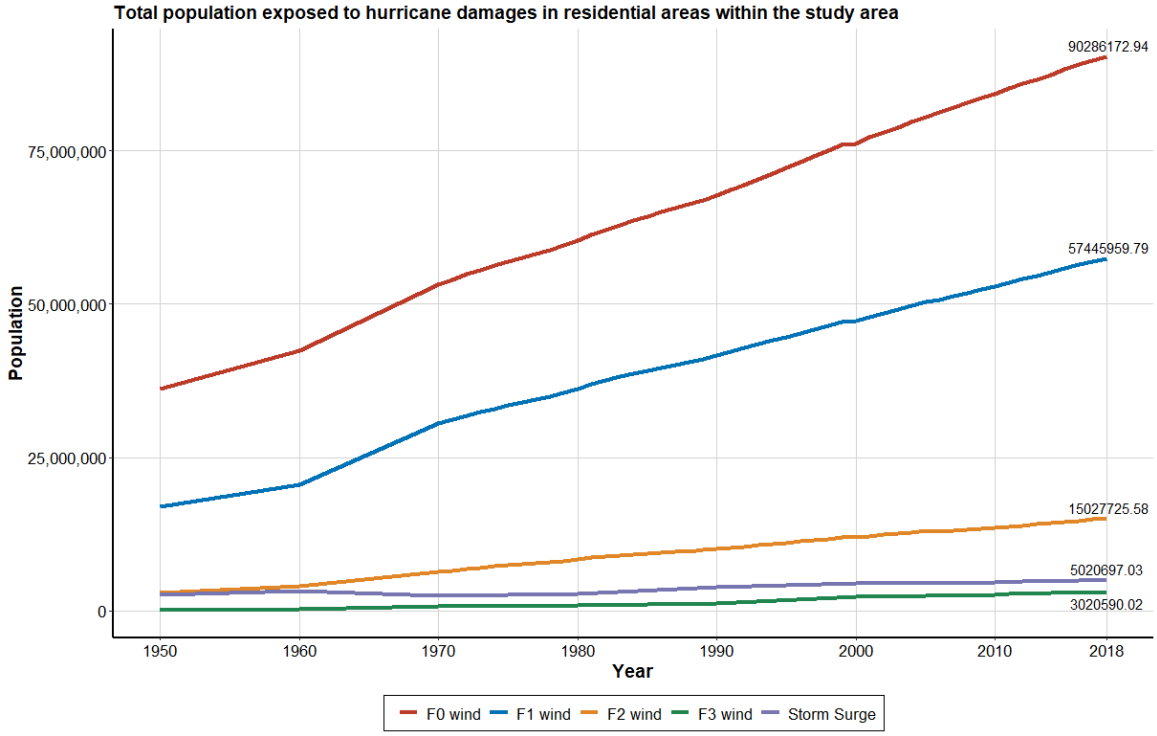

Figure 25. Total population exposed to hurricane damage in the study area from 1950 to 2018

* Coastal counties, as defined in this study, are geographically restricted to the Gulf of Mexico coastline and the eastern Atlantic Coast of the United States (i.e., the North Atlantic Basin region), excluding the Pacific Coast and the Great Lakes region

Figure 25 presents how many people have been exposed to hurricane-related damage in absolute terms. It is apparent that the total population has continuously increased within each hurricane affected area from 1950 to 2018. Wind damage is separated into different categories based on intensity (i.e., F0, F1, F2, and F3). While some of this growth might be due to the national trend, there is higher exponential growth trend in F0 and F1 areas than the national trend. Approximately, 165 million people are affected by some degree of wind damage during the study period. Generally, the intensity of hurricanes weakens when they interact with coastal geomorphic characteristics and lose their energy source (i.e., warm ocean waters). However, tropical storms and hurricanes can travel hundreds of miles deep into interior counties after landfall and the remnants of hurricanes may occasionally intensify their power. Therefore, the affected areas are not just limited to the immediate vicinity of coastal regions, extending hundreds of miles from the immediate coastal shorelines (Figure 27). In contrast, storm surge damage and F3 wind are highly localized along coastal areas as shown in Figure 26 and Figure 27. From the graph above (Figure 25), we can see that 5 million people resided in the residential areas that are affected by storm surge damage and 3 million people resided in high intensity of wind (F3 scale) areas as of 2018.

To summarize, the overall demographic trends within hurricane impacted areas reveal that the coastal populations are faster growing than the national average, and this migration puts more people at greater risk of hurricane hazards. This poses a challenge to policymakers to make more informed decisions in mitigating coastal vulnerability to hurricane hazards. In addition to the national demographic profile of coastal populations, it is imperative to further investigate what population groups have become progressively more susceptible to storm surge and wind damage over time.

5.5. At-Risk Populations in Different Hurricane Damage Categories

This section aims to unravel the vulnerability of people by applying the demographic data stratified by race and age groups to the geographic boundaries of each hurricane damage category (i.e., storm surge inundation, wind damage by Fujita scale). Rather than solely considering the unitary axes of a demographic category (e.g., race, gender, age, socioeconomic status, etc.,) independently, this study adopts a descriptive inter-categorical approach (i.e., cross-coded categories) that can help us understand how intersected demographic categories shape vulnerability (Bauer & Scheim, 2019; Kuran et al., 2020; Muttarak et al., 2015). Since the coastal areas exposed to storm surge and F3 wind damage are highly concentrated along the coastal shoreline (Figure 26), this study uses the decennial census (1970, 1980, 1990, 2000) and the American Community Survey (ACS) 5-year estimates (2014-2018) at census tract level. On the other hand, hurricane winds produce widespread damage both in coastal counties and inland counties. Considering such a larger extent of wind-driven hurricane impacts, this study analyzes county-level population estimates within the contours of F0, F1, and F2 wind-damaged areas. As mentioned in section 5.3, the demographic data are divided into sub-groups according to race and five age groups: age group 1 (0-4 years), age group 2 (5-19 years), age group 3 (20-34 years), age group 4 (35-64 years), and age group 5 (65 years and older). However, the starting year of the specific race recording differs by race category and the unit of analysis. At census tract level, the Other race category and Hispanic origin are available beginning in 1980 and 2000, respectively. Prior to 1990 at county level, the race categories available are white, black, and Other with no Hispanic origin. The Other race category and Hispanic origin are available from 1970 and 1990 at county level, respectively.

5.5.1. Populations At-Risk from Storm Surge Inundation

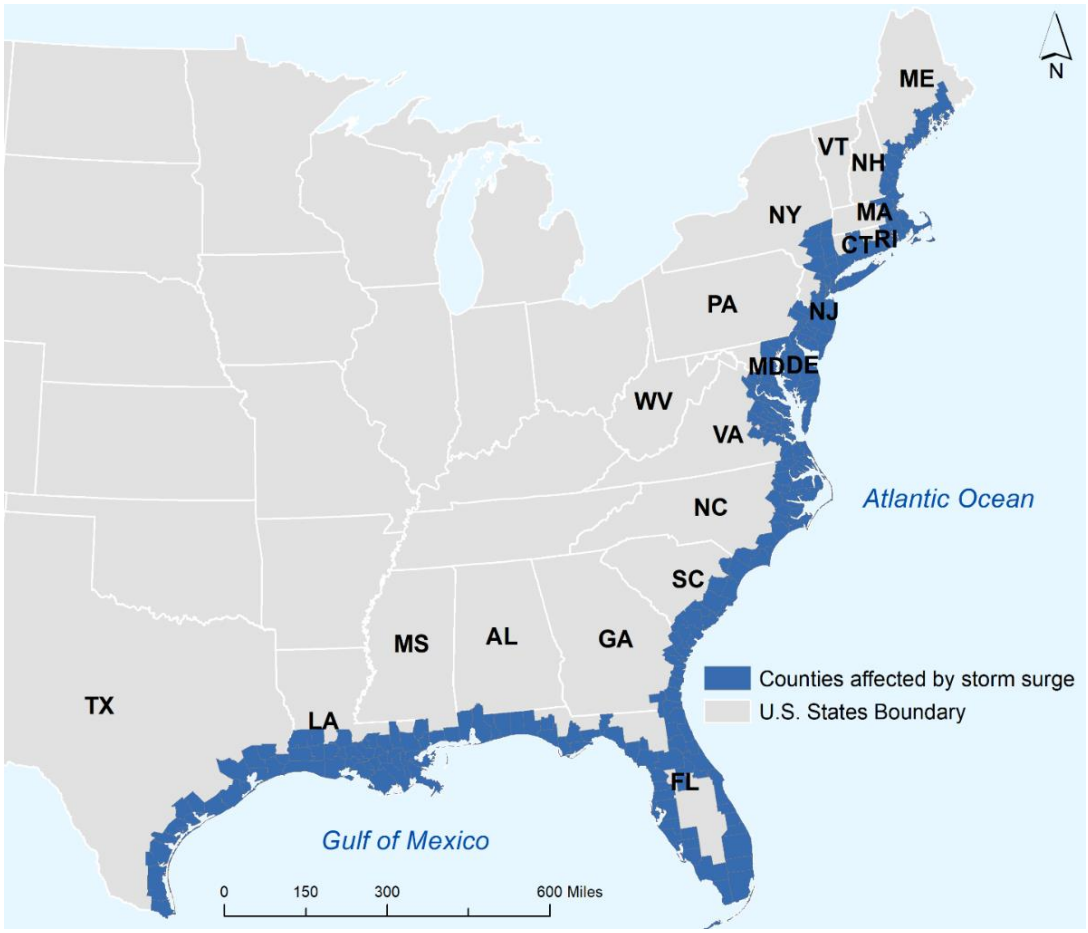

Figure 26. The coastal counties affected by storm surge

Percentage of people living in storm surge damaged areas – As shown in Figure 26, most counties damaged by storm surges over the study period are located along the coastal shoreline, within an area of 409,652 km^2. Figure 27 is a breakdown of the racial and age composition affected by storm surge damage during the study period. Out of all the categories, age group 3 has occupied the largest proportion among all race categories. The white population consistently accounts for the largest proportion of the affected population. However, the white age group 3 has been declining steadily since 1980. Notably, among all racial groups, white age group 5 has been steadily increasing since 2010. The black population mirrors the trends of the white population. As of 2018, the black age group 5 has overtaken age group 2 as the second largest

proportion among the black population. Although the Other category only occupies a small proportion of the overall percentage, the middle-aged adults (age group 3 and age group 4), and older adults (age group 5) have increased continuously over time. In addition, the Hispanic population tends to remain stable with no distinctive demographic shifts, beginning with its classification in 2000.

Share of people living in storm surge damaged area – In terms of share of the storm surge affected population (Figure 28), age groups 4 and 5 account for the highest share across all other racial-age groups. This is possibly due to the preference of the older generation to live in coastal communities by purchasing second-homes for recreational opportunities or retirement destinations. Overall, the share of the population living in storm surge affected areas has decreased across all age and racial groups since 1970. From 1970 to 1990, the black and Other populations were the most affected by storm surges, however, since 1970[4] both of these population groups have been declining. In contrast, the white population and Hispanic population have been relatively consistent, only marginally decreasing beginning in 2000. This indicates that whites and Hispanics have greater vulnerability but also greater resiliency when compared to the black and Other populations. Storm surge affected areas tend to have higher residential property values due to the proximity to waterfront, and cost of insurance in these areas tends to be more expensive than inland areas (Bin, Kruse, & Landry, 2008; Logan & Xu, 2015). This can lead to minority populations being financially displaced from these areas. These results show an inverse pattern of social vulnerability occurring with whites, presumably rich people, being more vulnerable than minority populations, excluding the Hispanic population.

[4] Since 1980 for the Other population group

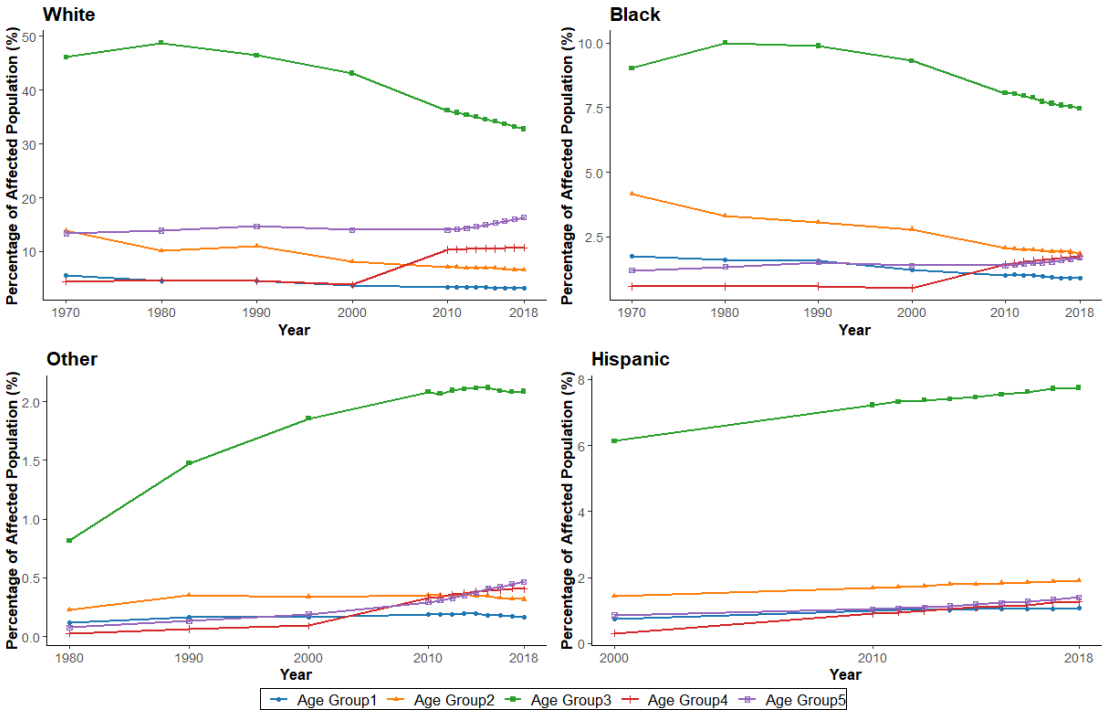

Figure 27. Demographic trends in the areas exposed to storm surge inundation among different population groups stratified by race and age groups (percentage)
**Note: The start of the specific race category recording at census tract level: Other (1980), Hispanic origin (2000). The decennial census is used until 2010, and the ACA data are used beginning in 2010.*

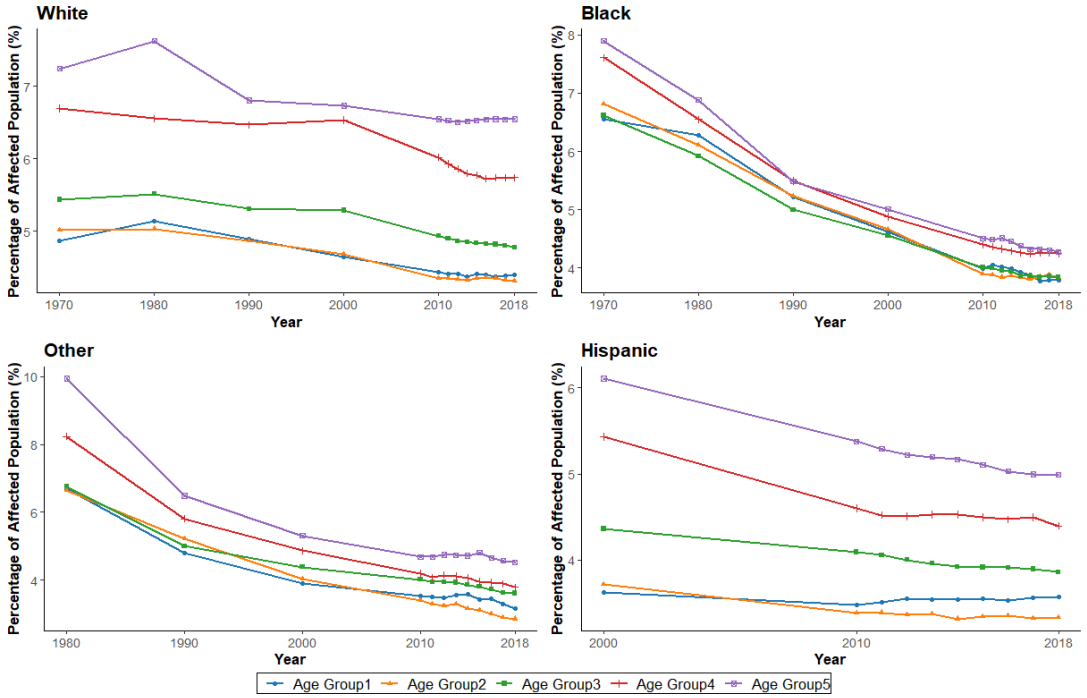

Figure 28. Demographic trends in the areas exposed to storm surge inundation among different population groups stratified by race and age groups (share)
**Note: The start of the specific race category recording at census tract level: Other (1980), Hispanic origin (2000). The decennial census is used until 2010, and the ACA data are used beginning in 2010.*

5.5.2. Populations At-Risk to F0 Wind Damage

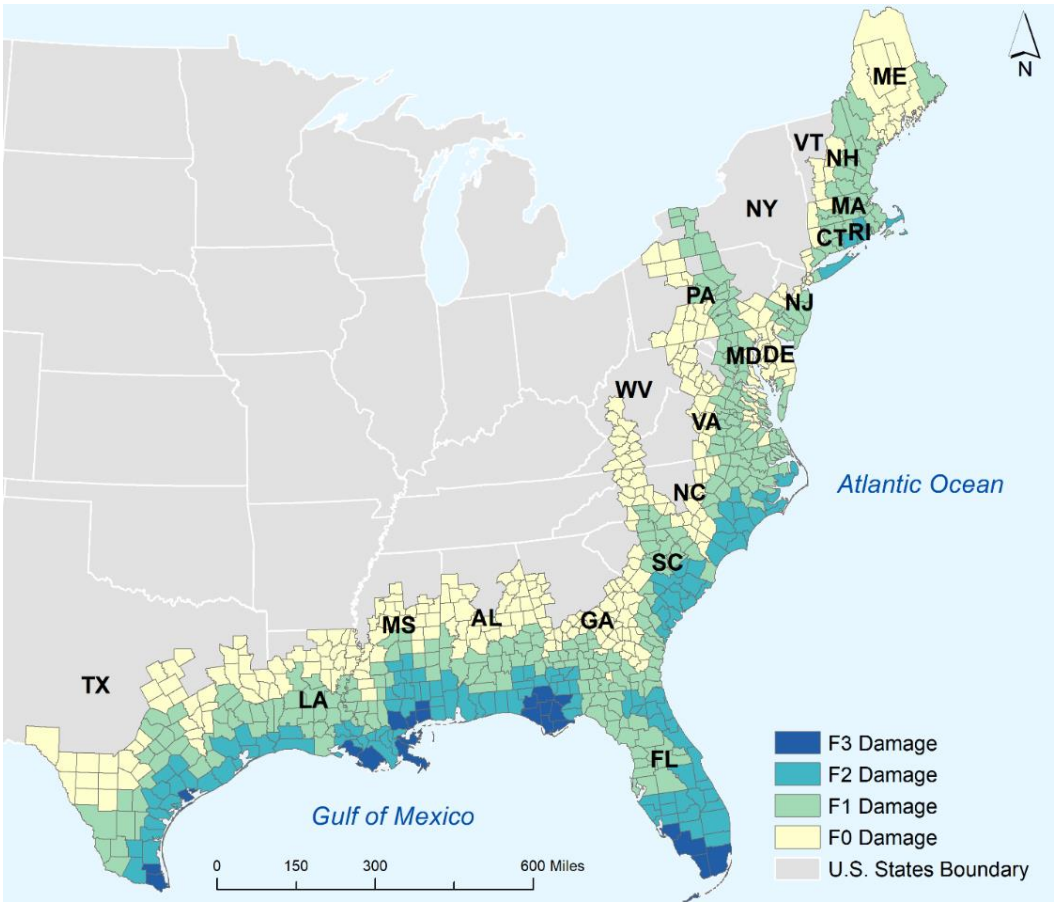

Figure 29. The coastal counties affected by wind damage according to Fujita scale (F0, F1, F2, and F3): **Note: F0: minor damage to buildings/trees, F1: houses damaged, and single or isolated groups of trees blown down, F2: houses unroofed or destroyed and extensive tree blowdowns, F3: houses blown down or destroyed and most trees down*

Percentage of people living in F0 wind-damaged areas – As can be seen from the map (Figure 29), F0 affects the largest portion of the study area, 1,298,585km^2. The areas affected by F0 wind ranges from 120 miles to more than 300 miles away from the coastlines, and they are less exposed to the more damaging effects of hurricanes. As shown in Figure 30, prior to 1990, age group 2 was the largest proportion affected among the black population, and age groups 2, 3, and 4 shared equal proportion among the Other and Hispanic categories. Beginning in 1990, age group 4 occupies the largest proportion of the population across all racial groups. According to the U.S. Census Bureau, the proportion of people 65 years and over (i.e., age group 5) declined

nationally between 1990 and 2000 (Hetzel & Smith, 2001). However, in the F0 affected area, the proportion of age group 5 did not demonstrate this national trend, instead it remained stable among the white and black population. The proportion of the elderly showed an increasing trend among Other and Hispanic racial groups. Beginning in 2010, age group 5 has seen a higher rate of growth among all racial groups, demonstrating an aging population in F0 inland counties. Notably, Hispanic and other racial groups have been consistently increasing their share of the percentage throughout the study period. This uptrend also coincides with the steady decline of most of the age groups within the white population. These general demographic trends are consistent among F0, F1, and F2 areas, with the percentages being nearly identical (Figures 30, 32, 34).

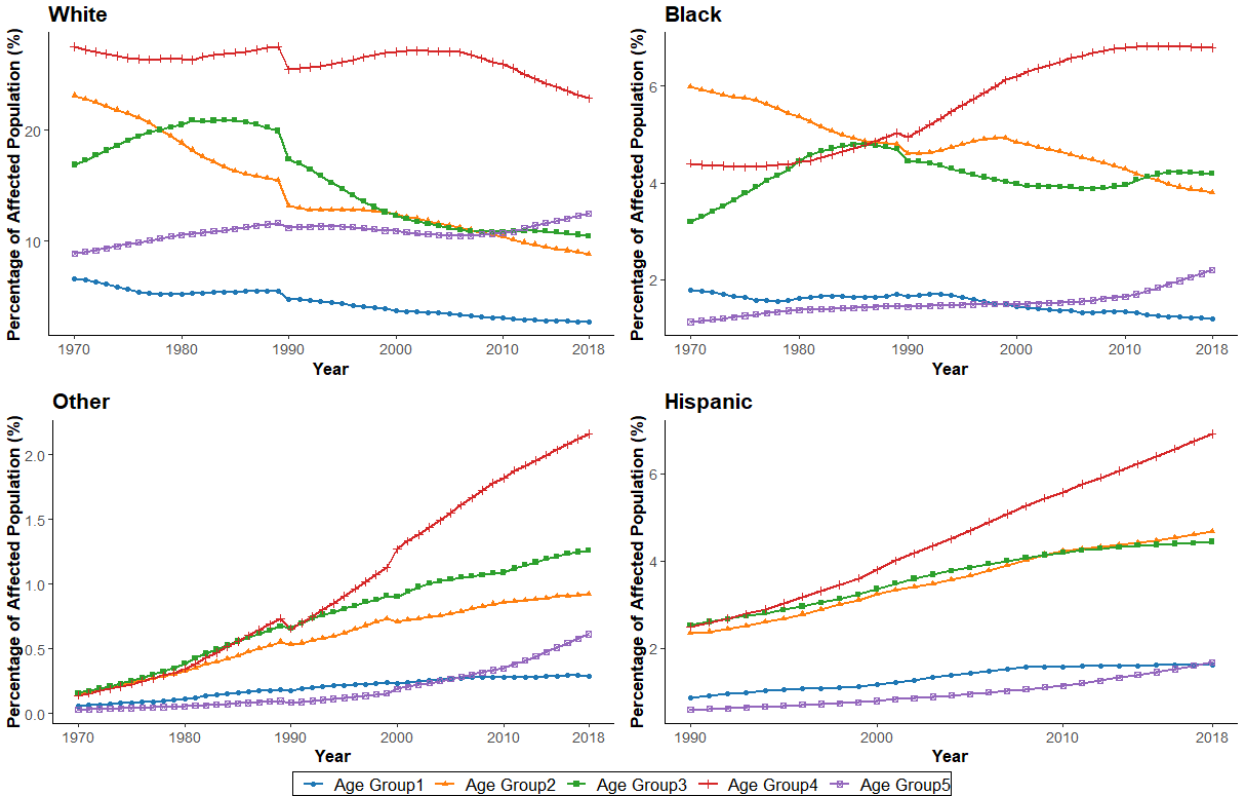

Figure 30. Demographic trends in the areas exposed to F0 damage among different population groups stratified by race and age groups (percentage)
**Note: The start of the specific race category recording at county level: Other (1970), Hispanic origin (1990)*

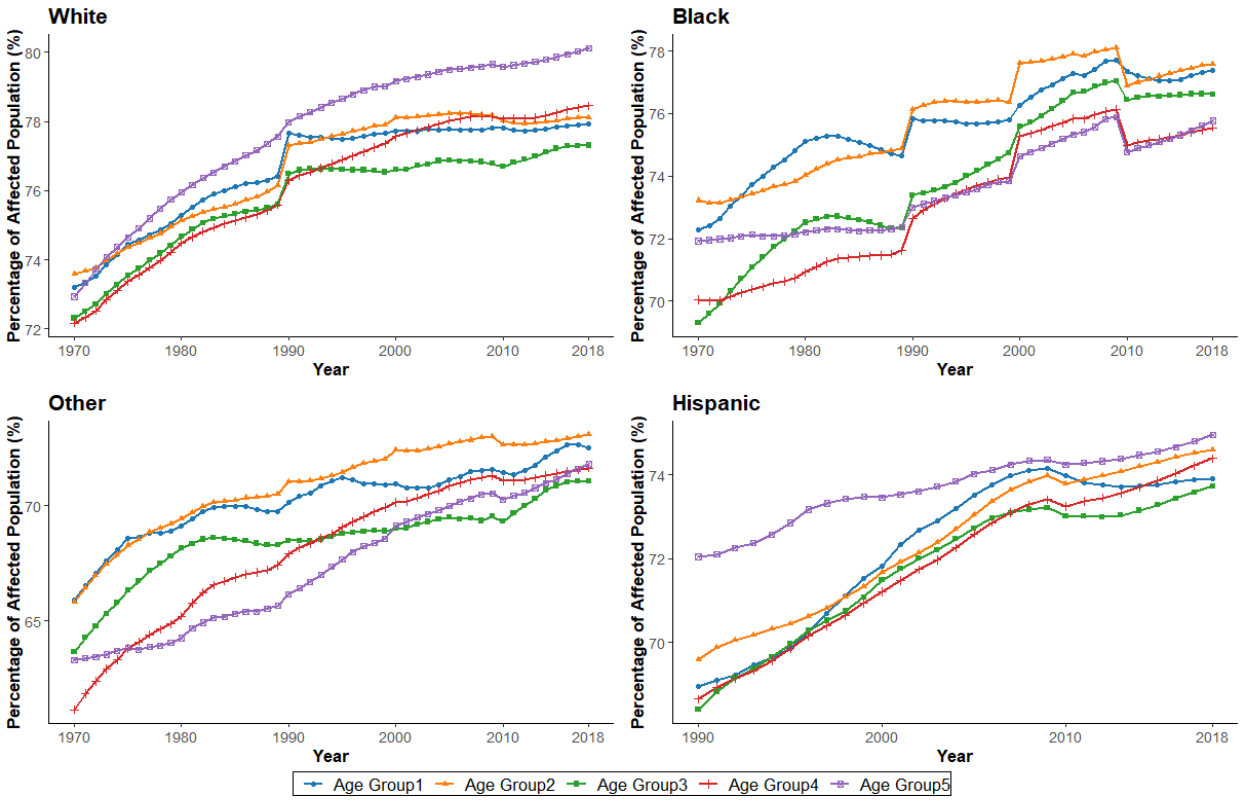

Figure 31. Demographic trends in the areas exposed to F0 damage among different population groups stratified by race and age groups (share)
**Note: The start of the specific race category recording at county level: Other (1970), Hispanic origin (1990)*

Share of people living in F0 wind-damaged areas – In 1970, there was no significant difference in the share of age groups of white populations (Figure 31). However, as time goes on, the share of age group 5 split off from the other cluster of age groups, occupying about 3 percent more of the share than the other age groups. This coincides with the increasing trend of age group 5 among the proportion of affected populations. Although, the black and white populations have a similar affected share within the F0 affected areas, there is an inverse pattern between the age distribution of the white population and the black population. That is to say, age groups 4 and 5 occupy the smallest share among the age groups of the black population, whereas age groups 4 and 5 are the highest shares among the white affected population. Age groups 1 and 2 (children and teenagers) occupy the largest share among other age groups of the black population consistently from 1970 to 2018. Within the white population, these age groups account for the

third and fourth highest share among the other age groups and are clustered around age group 4. The other racial category tends to show a similar trend in age group as the black population. The Hispanic racial category is somewhat similar to the white racial group. However, age groups 1 through 4 cluster toward age group 5 in Hispanic population over time, whereas age group 1 through 4 are clustering away from age group 5 in the white population.

5.5.3. Populations At-Risk from F1 Wind Damage

Share of people living in F1 wind-damaged areas – F1 wind affects a slightly smaller geographic area, 817,360km^2, falling within 90 miles to 200 miles from the coastal shorelines, which is mostly rural (Figure 29). The population distribution and growth tend to have similar trends, corresponding to the inland counties affected by F0. Since both the percentage and the share of F1 have a similar population distribution and growth over time as F0 (Figure 32), this section mainly focuses on the share.

The share of all age groups of the white population steadily increased from 1970 to 1990, but then age groups 1, 2, 3, and 4 started to level off in 1990 and remained steady. The exposure of white age group 5 has been continually increasing over time among the F1 affected population. The black and white populations share the same inverse relationship among age groups as the F0 affected population. The other racial group shares the same characteristics as the F0 distribution, mimicking the black population (Figure 30). Notably, the share of age group 5 of the Hispanic population steadily increased from 1990 until 2000 and then remained stable over time, reaching up to 56 percent in 2018. All the other Hispanic age groups have experienced continuous growth from 1990 to 2018. Overall, F0 and F1 have very similar distributions and trends among the affected population.

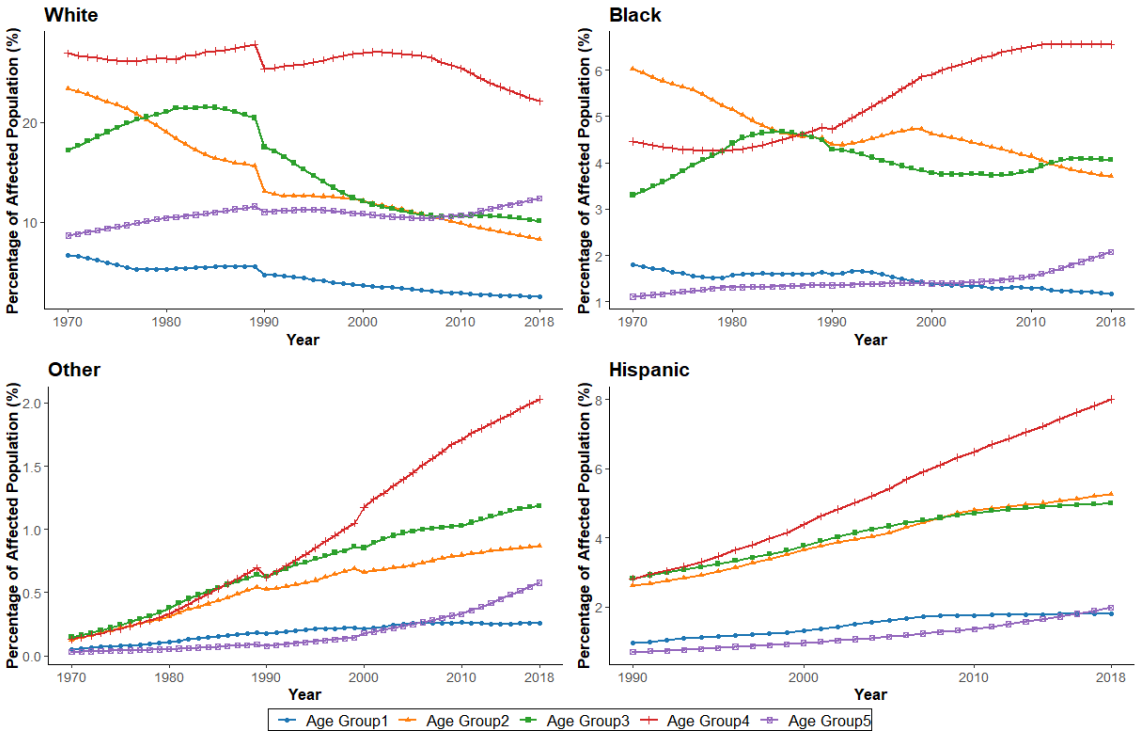

Figure 32. Demographic trends in the areas exposed to F1 damage among different population groups stratified by race and age groups (percentage)
**Note: The start of the specific race category recording at county level: Other (1970), Hispanic origin (1990)*

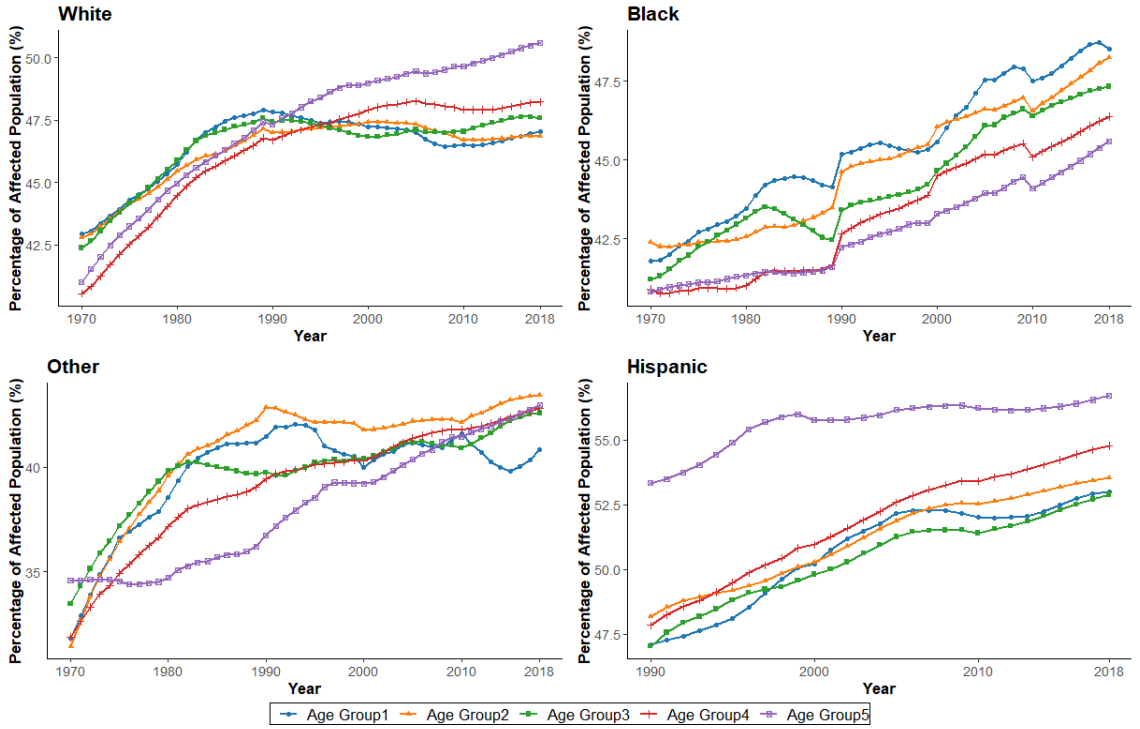

Figure 33. Demographic trends in the areas exposed to F1 damage among different population groups stratified by race and age groups (share)
**Note: The start of the specific race category recording at county level: Other (1970), Hispanic origin (1990)*

5.5.4. Populations At-Risk from F2 Wind Damage

Share of people living in F2 wind-damaged areas – F2 wind damage is more localized along the coasts in areas with hurricane landfall events within an area of 311,142km^2, composed of mostly urbanized areas (Figure 29). As mentioned earlier, population distribution of F2 damaged areas resembles F0 and F1 areas in terms of percentage (Figure 34), and thus this subsection addresses the population in terms of its share of the population in the study area.

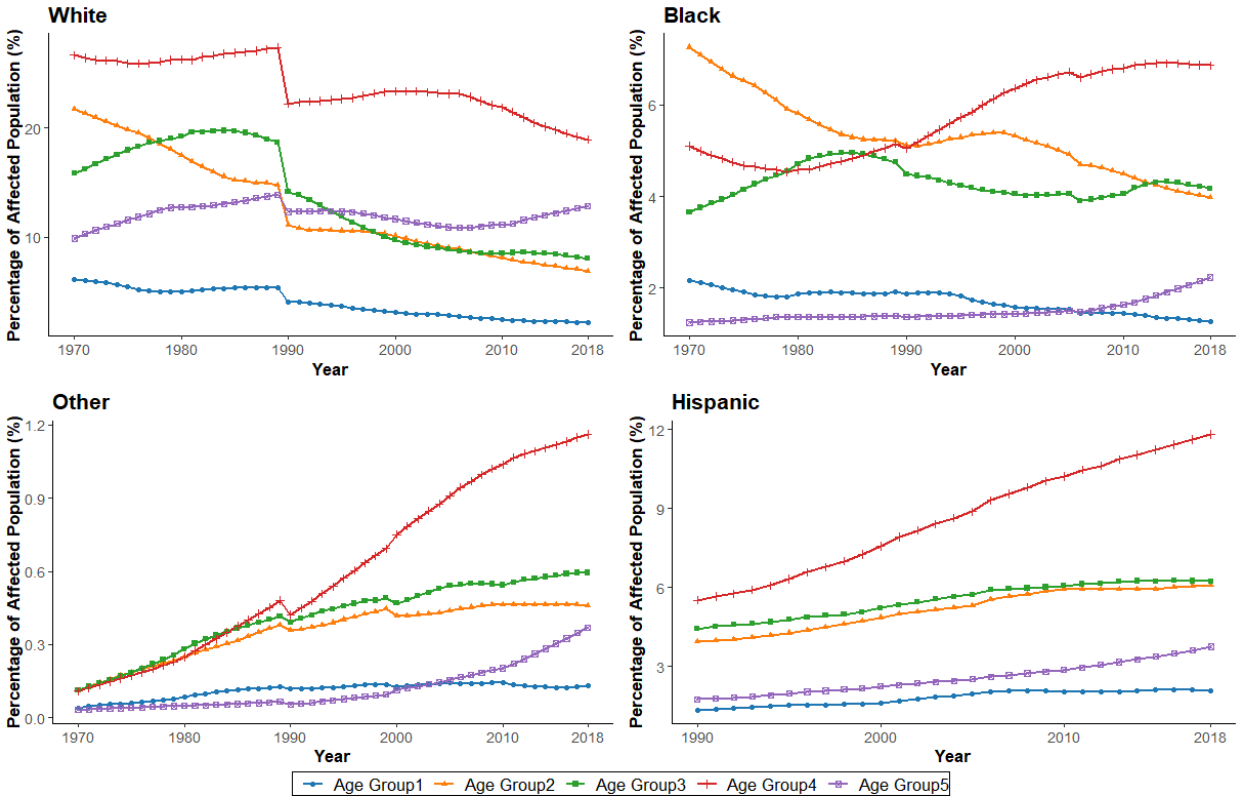

Figure 34. Demographic trends in the areas exposed to F2 damage among different population groups stratified by race and age groups (percentage)
**Note: The start of the specific race category recording at county level: Other (1970), Hispanic origin (1990)*

As shown in Figure 35, the share of age groups 1, 2, and 3 among the white and Hispanic population has historically experienced less F2 wind damage. The share of white elderly people is significantly higher than other age groups within the white population over time. Since 1990,

there has been about a 3 percent point gap between age group 5 and the other age groups within the white population.

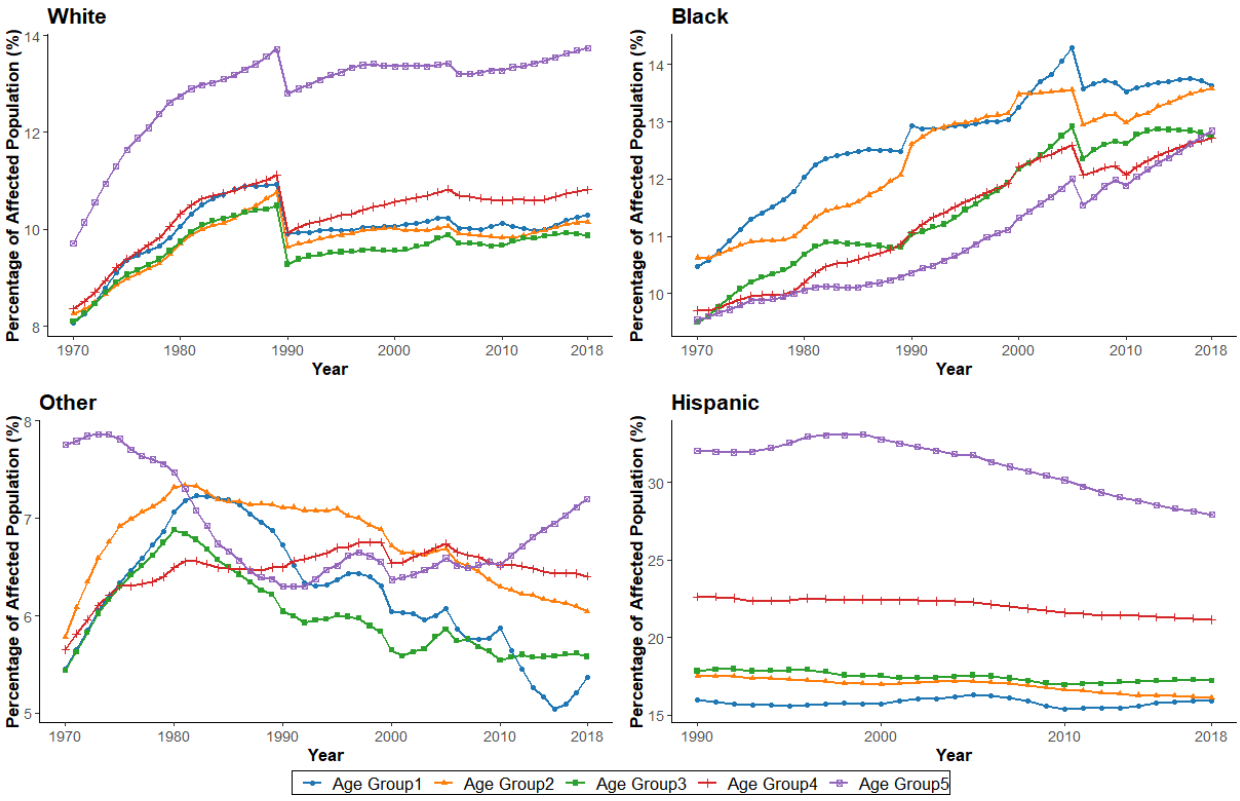

Figure 35. Demographic trends in the areas exposed to F2 damage among different population groups stratified by race and age groups (share)
**Note: The start of the specific race category recording at county level: Other (1970), Hispanic origin (1990)*

Overall, the black population demonstrates similar patterns and distributions as the previous wind damage categories. However, there is a significant dip among all age groups between 2005 and 2006. This might be related to the displacement of the black population following Hurricanes Katrina and Rita during the 2005 hurricane season. Consistent with previous empirical studies (Do Yun & Waldorf, 2016; Frey & Singer, 2006; Myers et al., 2008; Paxson & Rouse, 2008), these two intense hurricanes significantly impacted the black population, causing an approximately 1 percent decline in the number of black people living within the F2 at-risk areas. This dip can also be observed among the white population. However,

the impact was minimal, and the population quickly recovered in the following years. There is no evidence of these events impacting the Hispanic population. It is unclear whether or not these two hurricanes made an impact on the Other racial group as many of their age groups were already in decline during this period. Remarkably, the Hispanic population has the largest share among all racial groups, a two-fold increase compared to white population. This disparity becomes more evident within the F3 wind-damaged area.

5.5.5. Populations At-Risk from F3 Wind Damage

Percentage of people living in F3 wind-damaged areas – The areas affected by F3-scale wind damage comprise only 23 counties within an area of 53,000km^2, generally concentrated around New Orleans Louisiana, the Florida panhandle, the southern tip of the Florida peninsula, and along the southeastern US-Mexico border in Texas (Figure 29). Figure 36 and Figure 37 provide the breakdown of racial and age composition affected by F3 wind damage during the study period in percentage terms and absolute terms, respectively. As of 2018, the white population cumulatively makes up about 50 percent of the affected population living in F3 affected areas. This is likely due to the high property value along the coastal areas. The Hispanic population cumulatively accounts for about 40 percent of the affected population exposed to F3 wind damage in the same year. In contrast, the other two categories (i.e., the black and the Other racial groups) only make up a small percentage of the overall composition. Among all racial groups, age group 3 dominates all other age groups. This is presumably because the F3 areas are located adjacent to coastal shorelines where there are mostly urban coastal metropolitan areas such as Matamoros–Brownsville on the Mexico-US border, Greater New Orleans in Louisiana, and Naples and Panama City in Florida. Taking into account the recording of Hispanic populations in

2000, the age-racial composition of the affected population remains consistent throughout the study period.

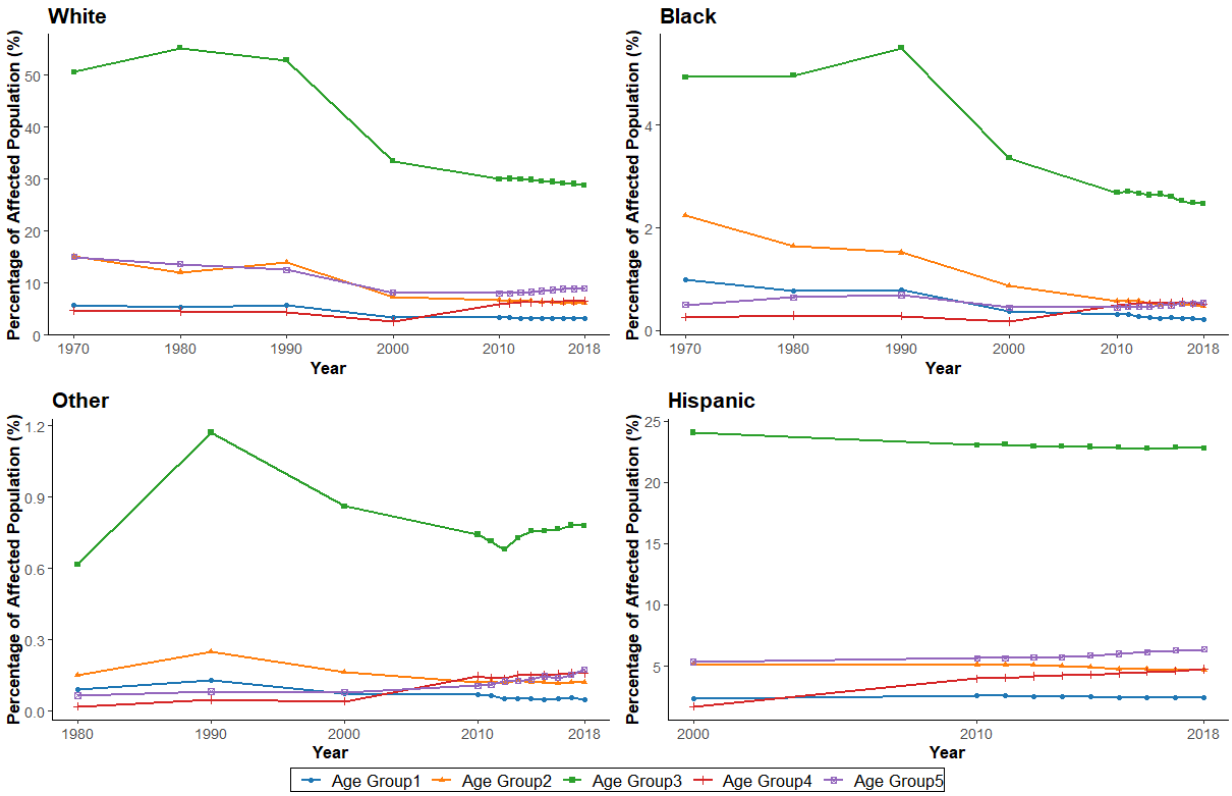

Figure 36. Demographic trends in the areas exposed to F3 damage among different population groups stratified by race and age groups (percentage)
**Note: The start of the specific race category recording at census tract level: Other (1980), Hispanic origin (2000). The decennial census is used until 2010, and the ACA data are used beginning in 2010*

Share of people living in F3 wind-damaged areas – In terms of share, only a small percentage of the white, black, and Other population groups live within F3 damaged zones (Figure 37). Interestingly, the share of the Hispanic population living in these high-risk areas ranges from 5 percent for age group 1 all the way to 15 percent for age group 5 in 2018. Despite the risk, a large share of the Hispanic population lives within these 23 counties, whereas only a small share of all other racial groups lives in these areas. Even though a large absolute number of white people are affected by F3 wind, shown through the percentage (Figure 36), this amount accounts

for roughly 2 percent of each age group living in the study area. In addition, the share of the white population living in the affected area has increased roughly one percent between 1970 and 2018. In contrast, the share of black, Other, and Hispanic have decreased roughly by one percent during the study period. This implies that the white population is more adaptable and resilient to high-intensity hurricanes. On the other hand, minority populations are not as well-equipped to handle storms of high intensity, leading to an exodus from these high-risk areas.

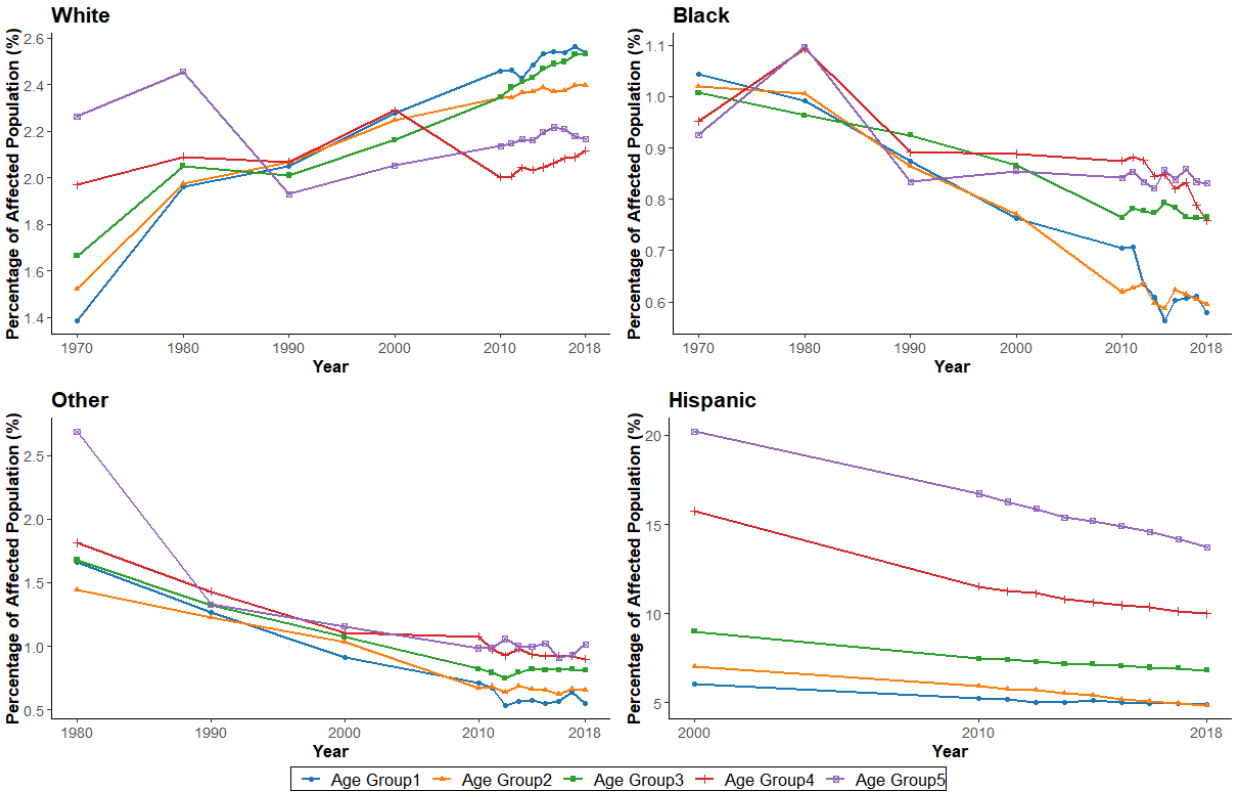

Figure 37. Demographic trends in the areas exposed to F3 damage among different population groups stratified by race and age groups (share)
**Note: The start of the specific race category recording at census tract level: Other (1980), Hispanic origin (2000). The decennial census is used until 2010, and the ACA data are used beginning in 2010.*

5.5. Discussion and Conclusion

This study integrates the estimation of storm surge and wind damage based on historical hurricanes from 1950 to 2018 to explicate demographic differential vulnerability in the U.S. Gulf

and Atlantic coasts. Although it is known that land-cover change is closely associated with human settlement and population density (Pozzi & Small, 2005), no previous study has incorporated the residential land-use characteristics in estimating the demographic changes of at-risk populations. To fill this void, the present study was designed to explore how the overall population has been affected by hurricane impacts within the residential areas along the Atlantic and Gulf coasts. Hurricane hazards did not affect all population subgroups in the same way. The second aim of this study was to disentangle how different demographic intersectional group memberships (e.g., white young adults, white elderly people, black young adults, black elderly people, etc.) stratified by race and five age groups shape vulnerability across intersecting population subgroups.

This study finds that a greater share of white and Hispanic populations are exposed to hurricane storm surges than black and Other populations. In addition, the middle-aged and the elderly population (i.e., age groups 4 and 5) take up the highest share across all other racial-age groups. These findings are consistent with that of Logan and Xu (2015) who also identified the white and the elderly population as being the most vulnerable group to storm surge damage along the U.S. Gulf Coast during the period 1950-2005. In regard to the wind damage, F0, F1, and F2 have the same age and race distribution among the affected population in terms of percentage. Even as the spatial extent of wind damage shrinks, the racial and age makeup of the affected population remains the same. In terms of share, there is a growing population trend across all the racial-age groups within the F0, F1, and F2 affected areas in general. This is attributable to the large extent of hurricane wind damage, encompassing most of the study area. It appears that the demographic trend follows the national trend. In accordance with the literature, there is a demographic dip between 2005 and 2006 among African American

population in particular, possibly due to substantial residential displacement following Hurricanes Katrina and Rita. Another interesting finding is that the share of Hispanic population is the highest among racial groups within the F3 wind-damaged area. This demographic trend is aligned with the Hispanic population growth within the F3 damaged area especially in Texas and Florida (Hernández & Moreno-Fernández, 2018).

Knowing what population groups are at greater risk of hurricanes is important. This approach may help us to understand what population groups have had to take the brunt of adverse effects of hurricanes and how demographics have changed within the hurricane-prone areas. However, the results of this study do not distinguish between natural population changes and those that are caused by hurricanes. These results, therefore, need to be interpreted with caution. This study is a descriptive inter-categorical intersectional approach rather than an analytical intersectional approach (Bauer & Scheim, 2019), since it cannot identify the causal processes of hurricane damage and the extent of hurricane-induced residential mobility and natural migration. For most events that are not severe enough to immediately displace people, the effect might not be as direct and explicit (Fussell et al., 2017; Hunter, 2005). There are still many unanswered questions about the extent of inflow and outflow of the population between pre-disaster and post-disaster periods (i.e., actual hurricane-induced residential mobility) and return migration patterns. Future research should investigate hurricane-induced forced migration by applying analytic statistical models and using micro datasets.

Chapter 6. Conclusion

6.1. Summary and Significance

This dissertation is fundamentally based upon the hazards of place (HOP) model and the social vulnerability index (SoVI), which have long traditions in geographic social vulnerability scholarship. Although widely accepted by scholars, the SoVI-based research is still in need of methodological improvement to further advance vulnerability science (Fekete, 2019). The research presented in Chapter 3 was undertaken to propose complementary methods to address the shortcomings of the SoVI approach in two ways.

The social vulnerability index derived from different time points cannot be used to reveal the temporal trajectories of social vulnerability. An alternative solution is to standardize the indices measured at different time points and to create sequences indicating vulnerable status at each time point in order to find the areas having a similar progression of vulnerability. By applying the sequence alignment analysis and cluster analysis, this study investigated how the social vulnerability of U.S. counties has evolved across space and time from 1970 to 2010. The results show that U.S. counties exhibit four major features in their temporal dynamics and pathways of the social vulnerability progression across the United States: the counties with persistent low vulnerability status, those counties with dynamically low-medium vulnerability status, the counties with dynamically medium-high vulnerability status, and the counties with persistently high vulnerability status. The insights gained from this study may be of assistance to policymakers in monitoring temporal changes of vulnerability and developing long-term mitigation hazard strategies, paying particular attention to those areas that have persistently high social vulnerability and continuously fluctuate. Understanding the temporal paths of vulnerable statuses across different time points can be beneficial in understanding where and when to take

actions to reduce disaster social vulnerability and enhance resilience (Cutter, Burton, & Emrich, 2010).

The SoVI is a highly aggregated index composed of multiple layers of social-demographic variables. Despite the usefulness of this composite index in encapsulating the multidimensional nature of social vulnerability, it tends to smooth out the extreme values of social variables and local interactions in designing the SoVI (Fekete, 2012; Jones & Andrey, 2007; Rufat, 2013; Rufat et al., 2015). In terms of policy implications, this poses some problems in that it cannot determine the local primary determinants or agents that contribute to overall social vulnerability. To address this problem, this study demonstrates the application of geographically weighted principal component analysis to identify the contributions of the integral components of SoVI and the local primary determinants that contribute to social vulnerability. The approach suggested in this study will prove useful in scrutinizing the "black box" of the SoVI by specifying which local primary factors have contributed to the output of overall social vulnerability (Fekete, 2019). The derived local primary determinants can provide additional information about the underlying social processes that underlie the transitions of social vulnerability across space and time. In addition, the methods used for this study may be applied to other social indices such as social resilience index or quality of life index as an alternative way to provide the elements that lie hidden from the composite indices.

However, while these two methods complement the social vulnerability approach, they do not take into consideration the properties of physical hazards and the differential demographic populations specifically affected. In Chapter 4 and Chapter 5, this research narrowed down the scope of vulnerability to hurricanes and tropical storms to address hazard-specific social vulnerability. Extending the existing literature by Logan and Xu (2015), this study estimates the

spatial extent and intensity of hurricane wind and storm surge damage of all hurricanes that made landfall along America's hurricane coasts from 1950 to 2018 (Cutter et al., 2007). The spatial extent and intensity of historical hurricanes that have affected the Gulf and Atlantic coastal areas revealed that storm surge damage in these areas extends up to approximately 41,000km^2 and the largest extent of wind damage (F0) extends to approximately 1,300,000km^2. This project is the first comprehensive investigation of hurricane vulnerability encompassing the Atlantic and Gulf Coasts stretching from Texas to Maine. The extensive results of the hurricane modeling were aggregated into a single surface, representing longitudinal risk of hurricanes. By integrating the past and recent hurricane damage over long periods of time, the results delineated the high risk of hurricane zones more accurately than arbitrarily defining the study areas. The findings from this study can provide a fundamental basis for understanding the risk of exposure and demographic vulnerability to hurricane-related damage of the coastal regions at a national scale.

In order to determine demographic characteristics of the people most impacted by storm surges and strong winds, Chapter 5 identified generalized patterns of demographic changes that are subject to hurricane hazards. Based on the geographic extent of hurricane at-risk zones and land-use data, this study performed zonal analysis to further examine how many coastal populations are exposed to hurricane-related damage within the residential areas. Specifically, this study attempts to identify which population subgroups are most at risk to hurricane hazards according to the hurricane damage categories—storm surge damage and F0/F1/F2/F3 wind damage. Adopting an inter-categorical descriptive intersectional approach, the demographic datasets employed in this study were stratified by race and five age groups. The demographic variables were cross-coded (i.e., white age group 1~5, black age group 1~5, Other age group 1~5, Hispanic age group 1~5) to take into account how social-demographic identities affect

people's vulnerability and resilience to hurricane hazards. Based on the share of population, the results suggest that different groups have been impacted differently over time with white and Hispanic, middle-aged, and the elderly population (i.e., age groups 4 and 5) being more exposed to storm surge damage. In terms of wind damage, white and Hispanic populations tend to have similar trends among all wind damage categories, excluding F3, identifying age groups 4 and 5 as the groups most exposed among these categories. Within the areas affected by F3, Hispanic age groups 4 and 5 are the population groups subject to the most intense wind damage. The population change of Hispanics has been shown to be neutral, neither increasing nor decreasing over time. The share of white has been increasing, whereas the share of black and Other has been declining over time, implying that the white population is more resilient than the other racial groups. Black and Others are likely to leave the high-risk areas of F3 wind, migrating to inland counties, as the increasing trend of their population share indicates. Hurricane damage might act as a push-factor, pushing the groups with fewer economic resources from heavily impacted areas. Based on these results, we can conclude that the minority population groups (black, Other, and Hispanic) are more impacted by hurricane-related damage than the white population. Disaster policies and government recovery plans should therefore aim to make these population groups more resilient in the future, providing more resources to the hardest hit groups living in the most exposed counties. Although this study is exploratory and descriptive, the results provide detailed insight into vulnerability (Kuran et al., 2020; Ryder, 2017).

As discussed earlier, the SoVI approach has received much criticism due to its oversimplification and generalization. This can lead to misinterpretation of the mapping results of SoVIs, especially when making an inference about individuals from this aggregated measurement (Beccari, 2016; Fekete, 2012; Wood et al., 2010). Since the SoVI is composed of

multiple socio-demographic variables, it is difficult to pin down the specific population groups that are situated in vulnerable conditions and *who* they are. It simply draws a conclusion that people within the highly vulnerable areas are all vulnerable to the same degree with no consideration of demographic characteristics (race/ethnicity, age, gender, or class). The SoVI also tends to blur the actual demographic composition of an affected area, often neglecting the heterogeneity of the studied populations. For example, within storm surge damaged areas, white elderly people are at the highest risk, however, since the SoVI does not consider the white elderly population in creating the index, this subgroup is likely to be ignored. Moreover, the changing racial/ethnic composition and diversification of U.S. demographics also complicate this assessment (Frey, 2018). This study highlights the importance of demographic analysis in conjunction with the SoVI approach to offer a more nuanced picture of population vulnerability (Marandola & Hogan, 2006; Muttarak et al., 2015).

In conclusion, this dissertation lays the groundwork for comprehensive social vulnerability research by rethinking the shortcomings of the critical 'HOP' framework and the SoVI approach. According to Morse (2004, p.156), "they [the social indices] are only meant to help with an initial analysis of the phenomenon being studied." Despite its caveats, the SoVI is still useful in identifying vulnerable areas in a quantifiable manner at the initial stage of assessment. While all the approaches proposed in this study still have some limitations, they are pragmatic and complementary to the HOP model and the SoVI approach. The broad implication of this integrated approach is that it can be beneficial for stakeholders and decision makers in capturing the temporal dynamics and the primary local drivers of social vulnerability as well as the specific vulnerable population groups. Despite its exploratory nature, this dissertation demonstrates how demographic changes can be incorporated into social vulnerability research to

untangle the specific population subgroups facing the risk of hurricane hazards. The analytical framework suggested in this study is interdisciplinary and can enrich the approach to vulnerability assessment to natural hazards by converging geographic and demographic perspectives.

6.2. Future Research

This study was limited by the absence of the validation of the SoVI-based vulnerability analysis due to scarcity of relevant data such as mortality data, property damage, population displacement, and residential mobility data within the hurricane-affected area at the national level (Rufat et al., 2019; Tate, 2012). Especially, exploring the demographic changes within the hurricane at-risk areas was purely descriptive; it was not possible to determine a causal relationship between long-term hurricane damage and population change. Future studies need to examine more closely the links between the impacts of hurricane-related damage on local population change based on empirical statistical analysis. A further study could assess the long-term effects of hurricanes on population displacement and return migration at multiple spatial scales. The most critical limitation lies in the fact that findings from the index-based approaches or demographic methodologies are data-driven and highly quantitative. Thus, further studies should adopt mixed method approaches to provide a complete picture of vulnerability intersecting multiple axes of race, gender, and class. (Anderson et al., 2019; Rickless, Yao, Orland, & Welch-Devine, 2020). The present study provides a good starting point for future work that considers the potential long-term scenarios of sea-level rise and global climate change in estimating future hurricane-related damage and the associated population vulnerability. In addition, a greater number of inter-categorical demographic variables (e.g., income level stratified by race/ethnicity and age groups) could produce interesting findings that could account

for an interlocked social system in shaping demographic differential vulnerability. Although this study utilizes the place-based approach using spatially aggregated census data, future research could incorporate microdata to further address the vulnerability of individuals. An individual-based approach will enable us to gain a better understanding of the vulnerability and resilience that are operating at both individual and aggregate levels (Kwan, 2009). To date, researchers in almost every discipline have been seeking to reduce population vulnerability by adopting individual approaches either following a geographical or demographic tradition (Marandola & Hogan, 2006). This dissertation calls for special attention from the natural hazard research community, local actors, and decision-makers to integrate geographic and demographic perspectives in developing targeted interventions. By focusing on integrated research, vulnerability and resiliency studies can be enhanced and lead to greater scientific contributions in the future (Taubenböck & Geiß, 2014).

References

Abbott, A. (1991). The order of professionalization: An empirical analysis. *Work and occupations, 18*(4), 355-384.

Abbott, A., & DeViney, S. (1992). The welfare state as transnational event: evidence from sequences of policy adoption. *Social Science History, 16*(2), 245-274.

Abbott, A., & Tsay, A. (2000). Sequence analysis and optimal matching methods in sociology: Review and prospect. *Sociological methods & research, 29*(1), 3-33.

Ache, B. W., Crossett, K. M., Pacheco, P. A., Adkins, J. E., & Wiley, P. C. (2015). "The coast" is complicated: a model to consistently describe the nation's coastal population. *Estuaries and Coasts, 38*(1), 151-155.

Adger, W. N. (2006). Vulnerability. *Global environmental change, 16*(3), 268-281.

Aggarwal, C. C. (2014). *Data classification: algorithms and applications*: CRC press.

Alvarez, C. H., & Evans, C. R. (2021). Intersectional environmental justice and population health inequalities: A novel approach. *Social Science & Medicine, 269*, 113559.

Anderson, C. C., Hagenlocher, M., Renaud, F. G., Sebesvari, Z., Cutter, S. L., & Emrich, C. T. (2019). Comparing index-based vulnerability assessments in the Mississippi Delta: Implications of contrasting theories, indicators, and aggregation methodologies. *International Journal of Disaster Risk Reduction, 39*, 101128.

Arkema, K. K., Guannel, G., Verutes, G., Wood, S. A., Guerry, A., Ruckelshaus, M., . . . Silver, J. M. J. N. c. c. (2013). Coastal habitats shield people and property from sea-level rise and storms. *3*(10), 913-918.

Bakkensen, L. A., Fox-Lent, C., Read, L. K., & Linkov, I. (2017). Validating resilience and vulnerability indices in the context of natural disasters. *Risk analysis, 37*(5), 982-1004.

Balderrama, E., Jankowski, P., Martinez, R. G., Pherigo, J., Valliani, N., & Verhoef, M. (2019). *Houston Facts 2019*. Retrieved from Houston, TX: https://www.houston.org/

Barnett, J., & Adger, W. N. (2018). Mobile worlds: choice at the intersection of demographic and environmental change. *Annual Review of Environment Resources, 43*, 245-265.

Barnett, J., Lambert, S., & Fry, I. (2008). The hazards of indicators: insights from the environmental vulnerability index. *Annals of the Association of American Geographers, 98*(1), 102-119.

Bauer, G. R., & Scheim, A. I. (2019). Methods for analytic intercategorical intersectionality in quantitative research: discrimination as a mediator of health inequalities. *Social Science & Medicine, 226*, 236-245.

Beccari, B. (2016). A comparative analysis of disaster risk, vulnerability and resilience composite indicators. *PLoS currents, 8*.

Berkes, F. (2007). Understanding uncertainty and reducing vulnerability: lessons from resilience thinking. *Natural hazards, 41*(2), 283-295.

Bin, O., Kruse, J. B., & Landry, C. E. (2008). Flood hazards, insurance rates, and amenities: Evidence from the coastal housing market. *Journal of Risk and Insurance, 75*(1), 63-82.

Birkmann, J. (2006). *Measuring vulnerability to promote disaster-resilient societies: Conceptual frameworks and definitions* (Vol. 1). Tokyo, Japan: United Nations University Press.

Bolin, B., & Kurtz, L. C. (2018). Race, class, ethnicity, and disaster vulnerability. In *Handbook of disaster research* (pp. 181-203): Springer.

Boon, J. D. (2012). Evidence of sea level acceleration at US and Canadian tide stations, Atlantic Coast, North America. *Journal of Coastal Research, 28*(6), 1437-1445.

Boose, E. R., Chamberlin, K. E., & Foster, D. R. (2001). Landscape and regional impacts of hurricanes in New England. *Ecological Monographs, 71*(1), 27-48.

Boose, E. R., Serrano, M. I., & Foster, D. R. (2004). Landscape and regional impacts of hurricanes in Puerto Rico. *Ecological Monographs, 74*(2), 335-352.

Brock, G., Pihur, V., Datta, S., & Datta, S. (2008). clValid: An R Package for Cluster Validation. *Journal of Statistical Software, 25*(4), 22 doi:10.18637/jss.v025.i04

Brzinsky-Fay, C., & Kohler, U. (2010). New Developments in Sequence Analysis. *Sociological Methods & Research, 38*(3), 359-364. doi:10.1177/0049124110363371

Burton, C., & Cutter, S. L. (2008). Levee failures and social vulnerability in the Sacramento-San Joaquin Delta area, California. *Natural Hazards Review, 9*(3), 136-149.

Burton, C. G. (2010). Social vulnerability and hurricane impact modeling. *Natural Hazards Review, 11*(2), 58-68.

Burton, C. G., Rufat, S., & Tate, E. (2018). Social vulnerability: conceptual foundations and geospatial modeling. In *Vulnerability and resilience to natural hazards* (pp. 53-81): Cambridge University Press.

Cannon, T. (1994). Vulnerability analysis and the explanation of 'natural'disasters. *Disasters, development and environment, 1*, 13-30.

Chakraborty, J., Grineski, S. E., & Collins, T. W. (2019). Hurricane Harvey and people with disabilities: disproportionate exposure to flooding in Houston, Texas. *Social Science & Medicine, 226*, 176-181.

Chakraborty, J., Tobin, G. A., & Montz, B. E. (2005). Population evacuation: assessing spatial variability in geophysical risk and social vulnerability to natural hazards. *Natural Hazards Review, 6*(1), 23-33.

Chang, H.-S., & Chen, T.-L. (2016). Spatial heterogeneity of local flood vulnerability indicators within flood-prone areas in Taiwan. *Environmental Earth Sciences, 75*(23), 1484.

Changnon, S. A., Pielke Jr, R. A., Changnon, D., Sylves, R. T., & Pulwarty, R. (2000). Human factors explain the increased losses from weather and climate extremes. *Bulletin of the American Meteorological Society, 81*(3), 437-442.

Chmutina, K., & Von Meding, J. (2019). A Dilemma of language:"Natural disasters" in academic literature. *International Journal of Disaster Risk Science, 10*(3), 283-292.

City of Houston. (2018). About Houston: Facts and Figures. Retrieved from https://www.houstontx.gov/abouthouston/houstonfacts.html

Clark, G. E., Moser, S. C., Ratick, S. J., Dow, K., Meyer, W. B., Emani, S., . . . Schwarz, H. E. (1998). Assessing the vulnerability of coastal communities to extreme storms: the case of

Revere, MA., USA. *Mitigation and Adaptation Strategies for Global Change, 3*(1), 59-82.

Cohen, D. (2019, August 18, 2020). About 60.2M Live in Areas Most Vulnerable to Hurricanes. Retrieved from https://www.census.gov/library/stories/2019/07/millions-of-americans-live-coastline-regions.html

Cohen, D. T. (2018, August 18, 2020). 60 Million Live in the Path of Hurricanes. Retrieved from https://www.census.gov/library/stories/2018/08/coastal-county-population-rises.html

Comber, A. J., Harris, P., & Tsutsumida, N. (2016). Improving land cover classification using input variables derived from a geographically weighted principal components analysis. *Journal of Photogrammetry Remote Sensing, 119*, 347-360.

Conver, A., Sepanik, J., Louangsaysongkham, B., & Miller, S. (2008). *Sea, lake, and overland surges from hurricanes (SLOSH) basin development handbook v2. 0*. Silver Springs, MD: NOAA/NWS/Meteorological Development Laboratory.

Crossett, K., Ache, B., Pacheco, P., & Haber, K. (2013). *National coastal population report, population trends from 1970 to 2020*. Retrieved from Washington: http://oceanservice.noaa.gov/facts/coastal-population-report.pdf

Crowell, M., Coulton, K., Johnson, C., Westcott, J., Bellomo, D., Edelman, S., & Hirsch, E. (2010). An estimate of the US population living in 100-year coastal flood hazard areas. *Journal of Coastal Research, 26*(2 (262)), 201-211.

Culliton, T. J., Warren, M. A., Goodspeed, T. R., Remer, D. G., Balackwell, C. M., & McDonough, J. J. (1990). *50 Years of Population Change Along the Nation's Coasts, 1960-2010* (Vol. 55). Rockville, Maryland: National Oceanic and Atmospheric Administration.

Cutter, S. L. (1996). Vulnerability to environmental hazards. *Progress in human geography, 20*(4), 529-539.

Cutter, S. L. (2001). *American hazardscapes: The regionalization of hazards and disasters*. Washington, D.C: Joseph Henry Press.

Cutter, S. L. (2003). The vulnerability of science and the science of vulnerability. *Annals of the Association of American Geographers, 93*(1), 1-12.

Cutter, S. L. (2009). Social science perspectives on hazards and vulnerability science. In *Geophysical hazards* (pp. 17-30): Springer.

Cutter, S. L., Boruff, B. J., & Shirley, W. L. (2003). Social vulnerability to environmental hazards. *Social science quarterly, 84*(2), 242-261.

Cutter, S. L., Burton, C. G., & Emrich, C. T. (2010). Disaster resilience indicators for benchmarking baseline conditions. *Journal of homeland security emergency management, 7*(1).

Cutter, S. L., & Emrich, C. T. (2006). Moral hazard, social catastrophe: The changing face of vulnerability along the hurricane coasts. *The Annals of the American Academy of Political Social Science, 604*(1), 102-112.

Cutter, S. L., & Finch, C. (2008). Temporal and spatial changes in social vulnerability to natural hazards. *Proceedings of the National Academy of Sciences, 105*(7), 2301-2306.

Cutter, S. L., Johnson, L. A., Finch, C., & Berry, M. (2007). The US hurricane coasts: increasingly vulnerable? *Environment: Science Policy for Sustainable Development, 49*(7), 8-21.

Cutter, S. L., Mitchell, J. T., & Scott, M. S. (2000). Revealing the vulnerability of people and places: A case study of Georgetown County, South Carolina. *Annals of the Association of American Geographers, 90*(4), 713-737.

Delmelle, E. C. (2016). Mapping the DNA of urban neighborhoods: Clustering longitudinal sequences of neighborhood socioeconomic change. *Annals of the American Association of Geographers, 106*(1), 36-56.

Demšar, U., Harris, P., Brunsdon, C., Fotheringham, A. S., & McLoone, S. (2013). Principal component analysis on spatial data: an overview. *Annals of the Association of American Geographers, 103*(1), 106-128.

Diaz, H. F., & Pulwarty, R. S. (2012). *Hurricanes: climate and socioeconomic impacts* (H. F. Diaz & R. S. Pulwarty Eds. 1 ed.): Springer-Verlag Berlin Heidelberg.

Do Yun, S., & Waldorf, B. S. (2016). The day after the disaster: forced migration and income loss after hurricanes Katrina and Rita. *Journal of Regional Science, 56*(3), 420-441.

Dolan, R., & Davis, R. E. (1994). Coastal storm hazards. *Journal of Coastal Research*, 103-114.

Dong, P., Sadeghinaeenifard, F., Xia, J., & Tan, S. (2019). Zonal lacunarity analysis: a new spatial analysis tool for geographic information systems. *Landscape Ecology, 34*(10), 2245-2249.

Donner, W., & Rodríguez, H. (2008). Population composition, migration and inequality: The influence of demographic changes on disaster risk and vulnerability. *Social forces, 87*(2), 1089-1114.

Emanuel, K. (2011). Global warming effects on US hurricane damage. *Weather, Climate, and Society, 3*(4), 261-268.

Emrich, C. T., & Cutter, S. L. (2011). Social vulnerability to climate-sensitive hazards in the southern United States. *Weather, Climate, and Society, 3*(3), 193-208.

Enarson, E., & Meyreles, L. (2004). International perspectives on gender and disaster: differences and possibilities. *International Journal of Sociology Social Policy*.

Evans, C. R. (2019). Modeling the intersectionality of processes in the social production of health inequalities. *Social Science & Medicine, 226*, 249-253.

Fekete, A. (2009). Validation of a social vulnerability index in context to river-floods in Germany. *Natural Hazards Earth System Sciences, 9*(2), 393-403.

Fekete, A. (2012). Spatial disaster vulnerability and risk assessments: challenges in their quality and acceptance. *Natural hazards, 61*(3), 1161-1178.

Fekete, A. (2019). Social vulnerability (re-) assessment in context to natural hazards: Review of the usefulness of the spatial indicator approach and investigations of validation demands. *International Journal of Disaster Risk Science, 10*(2), 220-232.

Fernández, S., Cotos-Yáñez, T., Roca-Pardiñas, J., & Ordóñez, C. (2018). Geographically weighted principal components analysis to assess diffuse pollution sources of soil heavy metal: application to rough mountain areas in Northwest Spain. *Geoderma, 311*, 120-129.

Finch, C., Emrich, C. T., & Cutter, S. L. (2010). Disaster disparities and differential recovery in New Orleans. *Population Environment, 31*(4), 179-202.

Findlay, A. M. (2005). Vulnerable spatialities. *Population, Space, and Place, 11*(6), 429-439.

Fisher, R. (1989). Urban Policy in Houston, Texas. *Urban Studies, 26*(1), 144-154.

Flanagan, B. E., Gregory, E. W., Hallisey, E. J., Heitgerd, J. L., & Lewis, B. (2011). A social vulnerability index for disaster management. *Journal of homeland security emergency management, 8*(1).

Flanagan, B. E., Hallisey, E. J., Adams, E., & Lavery, A. (2018). Measuring community vulnerability to natural and anthropogenic hazards: the Centers for Disease Control and Prevention's Social Vulnerability Index. *Journal of Environmental Health, 80*(10), 34.

Forbes, C., Rhome, J., Mattocks, C., & Taylor, A. (2014). Predicting the storm surge threat of Hurricane Sandy with the National Weather Service SLOSH model. *Journal of Marine Science Engineering, 2*(2), 437-476.

Fotheringham, A. S., & Brunsdon, C. (1999). Local forms of spatial analysis. *Geographical Analysis, 31*(4), 340-358.

Fotheringham, A. S., Charlton, M. E., & Brunsdon, C. (1998). Geographically weighted regression: a natural evolution of the expansion method for spatial data analysis. *Environment planning A, 30*(11), 1905-1927.

Frazier, T. G., Thompson, C. M., & Dezzani, R. J. (2014). A framework for the development of the SERV model: A Spatially Explicit Resilience-Vulnerability model. *Applied Geography, 51*, 158-172.

Frazier, T. G., Wood, N., Yarnal, B., & Bauer, D. H. (2010). Influence of potential sea level rise on societal vulnerability to hurricane storm-surge hazards, Sarasota County, Florida. *Applied Geography, 30*(4), 490-505.

Frey, W. H. (2018). *Diversity explosion: How new racial demographics are remaking America*. Washington, D.C: MA: Brookings Institution Press.

Frey, W. H. (2021). What the 2020 census will reveal about America: Stagnating growth, an aging population, and youthful diversity. Retrieved from https://www.brookings.edu/research/what-the-2020-census-will-reveal-about-america-stagnating-growth-an-aging-population-and-youthful-diversity/

Frey, W. H., & Singer, A. (2006). *Katrina and Rita impacts on gulf coast populations: First census findings*: Brookings Institution, Metropolitan Policy Program Washington.

Fujita, T. T. (1971). *Proposed characterization of tornadoes and hurricanes by area and intensity*. Chicago, IL: University of Chicago.

Füssel, H.-M. (2007). Vulnerability: A generally applicable conceptual framework for climate change research. *Global environmental change, 17*(2), 155-167.

Fussell, E., Curran, S. R., Dunbar, M. D., Babb, M. A., Thompson, L., & Meijer-Irons, J. (2017). Weather-related hazards and population change: a study of hurricanes and tropical storms in the United States, 1980–2012. *The Annals of the American Academy of Political Social Science, 669*(1), 146-167.

Gabadinho, A., Ritschard, G., Mueller, N. S., & Studer, M. (2011). Analyzing and visualizing state sequences in R with TraMineR. *Journal of Statistical Software, 40*(4), 1-37.

Gabadinho, A., Ritschard, G., Studer, M., & Müller, N. S. (2009). Mining sequence data in R with the TraMineR package: A users guide for version 1.2. *Geneva: University of Geneva*.

Gabadinho, A., Studer, M., Mueller, N. S., Bergin, R., & Ritschard, G. (2016). TraMineR: Trajectory Miner: a Toolbox for Exploring and Rendering Sequences. Retrieved from https://cran.r-project.org/web/packages/TraMineR/

Gall, M. (2007). *Indices of social vulnerability to natural hazards: a comparative evaluation.* University of South Carolina,

Glahn, B., Taylor, A., Kurkowski, N., & Shaffer, W. A. (2009). The role of the SLOSH model in National Weather Service storm surge forecasting. *National Weather Digest, 33*(1), 3-14.

Gollini, I., Lu, B., Charlton, M., Brunsdon, C., & Harris, P. (2015). GWmodel: an R package for exploring spatial heterogeneity using geographically weighted models. *Journal of Statistical Software, 63*(17), 85-101.

Gower, J. C. (1971). A general coefficient of similarity and some of its properties. *Biometrics*, 857-871.

Green, M. A., Evans, C. R., & Subramanian, S. V. (2017). Can intersectionality theory enrich population health research? *Social Science & Medicine*.

Grubesic, T. H., Wei, R., & Murray, A. T. (2014). Spatial clustering overview and comparison: Accuracy, sensitivity, and computational expense. *Annals of the Association of American Geographers, 104*(6), 1134-1156.

Harper, J. (2004). Breathless in Houston: a political ecology of health approach to understanding environmental health concerns. *Medical Anthropology, 23*(4), 295-326.

Harris, P., Brunsdon, C., & Charlton, M. (2011). Geographically weighted principal components analysis. *International Journal of Geographical Information Science, 25*(10), 1717-1736.

Harris, P., Clarke, A., Juggins, S., Brunsdon, C., & Charlton, M. (2015). Enhancements to a geographically weighted principal component analysis in the context of an application to an environmental data set. *Geographical Analysis, 47*(2), 146-172.

Harris, P., Howden, N., Peukert, S., Noacco, V., Ramezani, K., Tuominen, E., . . . Griffith, B. (2016). Contextualized geographically weighted principal components analysis for investigating baseline soils data on the North Wyke Farm Platform. In *Geostatistical and Geospatial Approaches for the Characterization of Natural Resources in the Environment* (pp. 651-655): Springer.

Heisler, E., & Shrestha, L. (2011). *The changing demographic profile of the United States*.

Hernández, R., & Moreno-Fernández, F. (2018). *Hispanic Map of the United States 2018*. Retrieved from http://cervantesobservatorio.fas.harvard.edu/en/reports/hispanic-map-united-states-2018

Hetzel, L., & Smith, A. (2001). *The 65 Years and over Population, 2000* (Vol. 8): US Department of Commerce, Economics and Statistics Administration, US ….

Hewitt, K. (1995). Excluded perspectives in the social construction of disaster. *International Journal of Mass Emergencies and Disasters, 13*(3), 317-339.

Hinkel, J. (2011). Indicators of vulnerability and adaptive capacity: towards a clarification of the science–policy interface. *Global environmental change, 21*(1), 198-208.

Hogan, D. J., & Marandola Jr, E. (2005). Towards an interdisciplinary conceptualisation of vulnerability. *Population, Space and Place, 11*(6), 455-471.

Hollister, M. (2009). Is optimal matching suboptimal? *Sociological Methods & Research, 38*(2), 235-264.

Holman, D., & Walker, A. (2020). Understanding unequal ageing: towards a synthesis of intersectionality and life course analyses. *European Journal of Ageing*, 1-17.

Homer, C., Dewitz, J., Jin, S., Xian, G., Costello, C., Danielson, P., . . . Stehman, S. (2020). Conterminous United States land cover change patterns 2001–2016 from the 2016 national land cover database. *ISPRS Journal of Photogrammetry Remote Sensing, 162*, 184-199.

Hopkins, P. (2019). Social geography I: intersectionality. *Progress in human geography, 43*(5), 937-947.

Houston, S. H., Shaffer, W. A., Powell, M. D., & Chen, J. (1999). Comparisons of HRD and SLOSH surface wind fields in hurricanes: Implications for storm surge modeling. *Weather Forecasting, 14*(5), 671-686.

Hunter, L. M. (2005). Migration and environmental hazards. *Population and Environment, 26*(4), 273-302.

Jelesnianski, C. P., Chen, J., Shaffer, W., & Gilad, A. (1984). *SLOSH-A hurricane storm surge forecast model.* Paper presented at the OCEANS 1984.

Jelesnianski, C. P., Chen, J., & Shaffer, W. A. (1992). SLOSH: Sea, lake, and overland surges from hurricanes.

Joh, C.-H., Arentze, T., Hofman, F., & Timmermans, H. (2002). Activity pattern similarity: a multidimensional sequence alignment method. *Transportation Research Part B: Methodological, 36*(5), 385-403.

Jones, B., & Andrey, J. (2007). Vulnerability index construction: methodological choices and their influence on identifying vulnerable neighbourhoods. *International journal of emergency management, 4*(2), 269-295.

Kadetz, P., & Mock, N. B. (2018). Problematizing vulnerability: unpacking gender, intersectionality, and the normative disaster paradigm. In *Creating Katrina, Rebuilding Resilience* (pp. 215-230): Elsevier.

Kates, R. W. (1971). Natural hazard in human ecological perspective: hypotheses and models. *Economic Geography, 47*(3), 438-451.

Kates, R. W., & White, G. F. (1986). *Geography, Resources and Environment, Volume 1: Selected Writings of Gilbert F. White* (Vol. 1): University of Chicago Press.

Kaufman, L., & Rousseeuw, P. J. (2009). *Finding groups in data: an introduction to cluster analysis*. Hoboken: New Jersey: John Wiley & Sons.

King, D. (2001). Uses and limitations of socioeconomic indicators of community vulnerability to natural hazards: data and disasters in Northern Australia. *Natural hazards, 24*(2), 147-156.

King, D., & MacGregor, C. (2000). Using social indicators to measure community vulnerability to natural hazards. *Australian Journal of Emergency Management,, 15*(3), 52.

King, T. (2013). A framework for analysing social sequences. *Quality & Quantity, 47*(1), 167-191. doi:10.1007/s11135-011-9510-5

Kruk, M. C., Gibney, E. J., Levinson, D. H., & Squires, M. (2010). A climatology of inland winds from tropical cyclones for the eastern united states. *Journal of Applied Meteorology Climatology, 49*(7), 1538-1547.

Kruskal, J. B. (1983). An overview of sequence comparison: Time warps, string edits, and macromolecules. *SIAM review, 25*(2), 201-237.

Kumar, S., Lal, R., & Lloyd, C. D. (2012). Assessing spatial variability in soil characteristics with geographically weighted principal components analysis. *Computational Geosciences, 16*(3), 827-835.

Kuran, C. H. A., Morsut, C., Kruke, B. I., Krüger, M., Segnestam, L., Orru, K., . . . Gabel, F. (2020). Vulnerability and vulnerable groups from an intersectionality perspective. *International Journal of Disaster Risk Reduction, 50*, 101826.

Kwan, M. P. (2009). From place-based to people-based exposure measures. *Social science medicine, 69*(9), 1311-1313.

Kwan, M. P., Xiao, N., & Ding, G. (2014). Assessing activity pattern similarity with multidimensional sequence alignment based on a multiobjective optimization evolutionary algorithm. *Geographical Analysis, 46*(3), 297-320.

Lam, N.-N., Arenas, H., Li, Z., & Liu, K.-B. (2009). An estimate of population impacted by climate change along the US coast. *Journal of Coastal Research*, 1522-1526.

Landsea, C. W., & Franklin, J. L. (2013). Atlantic hurricane database uncertainty and presentation of a new database format. *Monthly Weather Review, 141*(10), 3576-3592.

Landsea, C. W., Franklin, J. L., & Beven, J. (2015). The revised Atlantic hurricane database (HURDAT2).

Lee, J. H., Davis, A., Yoon, S. Y., & Goulias, K. G. (2017). Exploring Daily Rhythms of Interpersonal Contacts: Time-of-Day Dynamics of Human Interactions with Latent Class Cluster Analysis. *Transportation Research Record: Journal of the Transportation Research Board*(2666), 58-68.

Lee, K. O., Smith, R., & Galster, G. (2017). Neighborhood trajectories of low-income US households: An application of sequence analysis. *Journal of Urban Affairs, 39*(3), 335-357.

Lember, J., Matzinger, H., & Vollmer, A. (2014). Optimal alignments of longest common subsequences and their path properties. *Bernoulli, 20*(3), 1292-1343.

Lesnard, L. (2006). Optimal matching and social sciences.

Levenshtein, V. I. (1966). *Binary codes capable of correcting deletions, insertions, and reversals.* Paper presented at the Soviet physics doklady.

Lin, N., Emanuel, K. A., Smith, J., & Vanmarcke, E. (2010). Risk assessment of hurricane storm surge for New York City. *Journal of Geophysical Research: Atmospheres, 115*(D18).

Llorente-Marrón, M., Díaz-Fernández, M., Méndez-Rodríguez, P., & Gonzalez Arias, R. (2020). Social vulnerability, gender and disasters. The case of Haiti in 2010. *Sustainability, 12*(9), 3574.

Lloyd, C. D. (2010). Analysing population characteristics using geographically weighted principal components analysis: a case study of Northern Ireland in 2001. *Computers, Environment and Urban Systems, 34*(5), 389-399.

Logan, J. R. (2009). Unnatural disaster: social impacts and policy choices after Katrina. In R. D. Bullard & B. Wright (Eds.), *Race, place, and environmental justice after Hurricane Katrina: Struggles to reclaim, rebuild, and revitalize New Orleans and the Gulf Coast*. Boulder, CO: Routledge;.

Logan, J. R., Issar, S., & Xu, Z. (2016). Trapped in place? Segmented resilience to hurricanes in the Gulf Coast, 1970–2005. *Demography, 53*(5), 1511-1534.

Logan, J. R., & Xu, Z. (2015). Vulnerability to hurricane damage on the US Gulf Coast since 1950. *Geographical review, 105*(2), 133-155.

Losada, N., Alen, E., Cotos-Yanez, T. R., & Dominguez, T. (2019). Spatial heterogeneity in Spain for senior travel behavior. *Tourism Management, 70*, 444-452.

Lutz, H. (2015). Intersectionality as method. *Journal of Diversity Gender Studies, 2*(1-2), 39-44.

Magnus, G. (2008). *The age of aging: How demographics are changing the global economy and our world*. Hoboken, NJ: John Wiley & Sons.

Maloney, M. C., & Preston, B. L. (2014). A geospatial dataset for US hurricane storm surge and sea-level rise vulnerability: Development and case study applications. *Climate Risk Management, 2*, 26-41.

Marandola, E., & Hogan, D. J. (2006). Vulnerabilities and risks in population and environment studies. *Population and Environment, 28*(2), 83-112.

Martine, G., & Guzman, J. M. (2002). Population, poverty, and vulnerability: Mitigating the effects of natural disasters. *Environmental Change and Security Project Report, 8*, 45-68.

Maul, G. A., & Duedall, I. W. (2019). Demography of Coastal Populations. In C. W. Finkl & C. Makowski (Eds.), *Encyclopedia of Coastal Science* (pp. 692-700). Cham: Springer International Publishing.

Mercado, A. (1994). On the use of NOAA's storm surge model, SLOSH, in managing coastal hazards—the experience in Puerto Rico. *Natural hazards, 10*(3), 235-246.

Mileti, D. S., Darlington, J., Passerini, E., Forrest, B. C., & Myers, M. F. (1995). Toward an integration of natural hazards and sustainability. *Environmental Professional, 17*(2), 117-126.

Mishra, S. V. (2018). Urban deprivation in a global south city-a neighborhood scale study of Kolkata, India. *Habitat International, 80*, 1-10.

Morrow, B. H. (1999). Identifying and mapping community vulnerability. *Disasters, 23*(1), 1-18.

Morse, S. (2004). *Indices and indicators in development: An unhealthy obsession with numbers*. Sterling, VA: Routledge.

Moser, S. C. (2010). Now more than ever: the need for more societally relevant research on vulnerability and adaptation to climate change. *Applied Geography, 30*(4), 464-474.

Murillo, F. H. S., Olmo, J. C., & Builes, N. M. S. (2019). Spatial Variability Analysis of Quality of Life and Its Determinants: A Case Study of Medellín, Colombia. *Social Indicators Research*, 1-24.

Murray, A. T., & Estivill-Castro, V. (1998). Cluster discovery techniques for exploratory spatial data analysis. *International Journal of Geographical Information Science, 12*(5), 431-443.

Muttarak, R., Lutz, W., & Jiang, L. (2015). What can demographers contribute to the study of vulnerability? *Vienna Yearbook of Population Research, 13*, 1-13.

Myers, C. A., Slack, T., & Singelmann, J. (2008). Social vulnerability and migration in the wake of disaster: the case of Hurricanes Katrina and Rita. *Population and Environment, 29*(6), 271-291.

National Academies of Sciences, E., Medicine. (2016). *Attribution of extreme weather events in the context of climate change*: National Academies Press.

Needleman, S. B., & Wunsch, C. D. (1970). A general method applicable to the search for similarities in the amino acid sequence of two proteins. *Journal of molecular biology, 48*(3), 443-453.

Neumayer, E., & Plümper, T. (2007). The gendered nature of natural disasters: The impact of catastrophic events on the gender gap in life expectancy, 1981–2002. *Annals of the Association of American Geographers, 97*(3), 551-566.

NOAA Office for Coastal Management. (March 29, 2021). Fast facts - Economics and Demographics. Retrieved from https://coast.noaa.gov/states/fast-facts/economics-and-demographics.html

NOAA Office for Coastal Management. (March 29, 2021). Fast facts - Hurricane Coasts. Retrieved from https://coast.noaa.gov/states/fast-facts/hurricane-costs.html

NOAA Office for Coastal Management. (2021, March 11, 2021). Defining Coastal Counties. Retrieved from https://coast.noaa.gov/digitalcoast/training/defining-coastal-counties.html

O'Connell, H. (2016). *The Shifting City: Houston's Unequal History of Racial Change*. Retrieved from https://kinder.rice.edu/research/shifting-city-houstons-unequal-history-racial-change

O'Connell, H., & Howell, J. (2016). Disparate City: Understanding Rising Levels of Concentrated Poverty and Affluence in Greater Houston.

O'Keefe, P., Westgate, K., & Wisner, B. (1976). Taking the naturalness out of natural disasters. *Nature, 260*, 566-567.

Openshaw, S., Charlton, M., Wymer, C., & Craft, A. (1987). A mark 1 geographical analysis machine for the automated analysis of point data sets. *International Journal of Geographical Information System, 1*(4), 335-358.

Parida, P. K. (2015). The social construction of gendered vulnerability to tsunami disaster: The case of coastal Sri Lanka. *Journal of Social Economic Development, 17*(2), 200-222.

Park, G., & Xu, Z. (2020). Spatial and Temporal Dynamics of Social Vulnerability in the United States from 1970 to 2010: A County Trajectory Analysis. *International Journal of Applied Geospatial Research, 11*(1), 36-54.

Paxson, C., & Rouse, C. E. J. A. E. R. (2008). Returning to new orleans after hurricane katrina. *98*(2), 38-42.

Pelling, M. (2003). *The vulnerability of cities: natural disasters and social resilience*. Sterling, VA: Earthscan.

Penner, A. M., & Saperstein, A. (2013). Engendering racial perceptions: An intersectional analysis of how social status shapes race. *Gender & Society, 27*(3), 319-344.

Pielke, R. A. (1997). Vulnerability to hurricanes along the US Atlantic and Gulf coasts: Considerations of the use of long-term forecasts. In *Hurricanes* (pp. 147-184): Springer.

Podani, J. (1999). Extending Gower's general coefficient of similarity to ordinal characters. *Taxon, 48*(2), 331-340.

Pompe, J., & Haluska, J. (2011). Estimating the Vulnerability of US Coastal Areas to Hurricane Damage. In *Recent Hurricane Research-Climate, Dynamics, and Societal Impacts*: IntechOpen.

Pozzi, F., & Small, C. (2005). Analysis of urban land cover and population density in the United States. *Photogrammetric Engineering Remote Sensing, 71*(6), 719-726.

Pulwarty, R. S., & Riebsame, W. E. (1997). The political ecology of vulnerability to hurricane-related hazards. In *Hurricanes* (pp. 185-214): Springer.

Qian, Z. (2010). Without zoning: Urban development and land use controls in Houston. *Cities, 27*(1), 31-41.

Rahmstorf, S. (2017). Rising hazard of storm-surge flooding. *Proceedings of the National Academy of Sciences, 114*(45), 11806-11808.

Rencher, A. C., & Christensen, W. F. (2012). *Methods of multivariate analysis* (3rd ed.). Hoboken, NJ: John Wiley & Sons.

Rickless, D. S., Yao, X. A., Orland, B., & Welch-Devine, M. (2020). Assessing social vulnerability through a local lens: an integrated geovisual approach. *Annals of the American Association of Geographers, 110*(1), 36-55.

Robinson, C., Lindley, S., & Bouzarovski, S. (2019). The Spatially Varying Components of Vulnerability to Energy Poverty. *Annals of the American Association of Geographers*, 1-20.

Rogerson, P. A. (2014). *Statistical methods for geography: a student's guide*. Thousand Oaks, CA: Sage.

Rufat, S. (2013). Spectroscopy of urban vulnerability. *Annals of the Association of American Geographers, 103*(3), 505-525.

Rufat, S., Eric, T., Emrich, C. T., & Antolini, F. (2019). How Valid Are Social Vulnerability Models? *Annals of the American Association of Geographers*, 1-23.

Rufat, S., Tate, E., Burton, C. G., & Maroof, A. S. (2015). Social vulnerability to floods: Review of case studies and implications for measurement. *International Journal of Disaster Risk Reduction, 14*, 470-486.

Ryder, S. S. (2017). A bridge to challenging environmental inequality: Intersectionality, environmental justice, and disaster vulnerability. *Social Thoughts and Research*, 85-115.

Rygel, L., O'Sullivan, D., & Yarnal, B. (2006). A method for constructing a social vulnerability index: an application to hurricane storm surges in a developed country. *Mitigation and Adaptation Strategies for Global Change, 11*(3), 741-764.

Sabokbar, H. F., Roodposhti, M. S., & Tazik, E. (2014). Landslide susceptibility mapping using geographically-weighted principal component analysis. *Geomorphology, 226*, 15-24.

Saib, M.-S., Caudeville, J., Beauchamp, M., Carré, F., Ganry, O., Trugeon, A., & Cicolella, A. (2015). Building spatial composite indicators to analyze environmental health inequalities on a regional scale. *Environmental Health, 14*(1), 68.

Sallenger, A. H., Doran, K. S., & Howd, P. A. (2012). Hotspot of accelerated sea-level rise on the Atlantic coast of North America. *Nature Climate Change, 2*(12), 884-888.

Schmidtlein, M. C., Deutsch, R. C., Piegorsch, W. W., & Cutter, S. L. (2008). A sensitivity analysis of the social vulnerability index. *Risk Analysis: An International Journal, 28*(4), 1099-1114.

Schultz, J., & Elliott, J. R. (2013). Natural disasters and local demographic change in the United States. *Population and Environment, 34*(3), 293-312.

Shepherd, J. M., & Knutson, T. (2007). The current debate on the linkage between global warming and hurricanes. *Geography Compass, 1*(1), 1-24.

Shoval, N., & Isaacson, M. (2007). Sequence alignment as a method for human activity analysis in space and time. *Annals of the Association of American geographers, 97*(2), 282-297.

Smith, K. (2013). *Environmental hazards: assessing risk and reducing disaster* (6th ed.). Milton Park, Abingdon: Routledge.

Smith, K., & Petley, D. N. (2009). Severe storm hazards. In *Environmental hazards: Assessing risk and reducing disaster* (5th ed., pp. 181-206). Milton Park, Abingdon: Routledge.

Smith, N. (2006). There's no such thing as a natural disaster. Retrieved from https://items.ssrc.org/understanding-katrina/theres-no-such-thing-as-a-natural-disaster/

Spielman, S. E., Tuccillo, J., Folch, D. C., Schweikert, A., Davies, R., Wood, N., & Tate, E. (2020). Evaluating social vulnerability indicators: criteria and their application to the Social Vulnerability Index. *Natural hazards, 100*(1), 417-436.

Stehle, S., & Peuquet, D. J. (2015). Analyzing spatio-temporal patterns and their evolution via sequence alignment. *Spatial Cognition & Computation, 15*(2), 68-85.

Stork, S. V., & Sneed, M. (2002). *Houston-Galveston Bay area, Texas, from Space—a new tool for mapping land subsidence*. Retrieved from Reston, VA: https://pubs.usgs.gov/fs/fs-110-02/pdf/FS_110-02.pdf

Streutker, D. R. (2003). Satellite-measured growth of the urban heat island of Houston, Texas. *Remote Sensing of Environment, 85*(3), 282-289.

Strobl, E. (2011). The economic growth impact of hurricanes: Evidence from US coastal counties. *Review of Economics Statistics, 93*(2), 575-589.

Strode, G., Mesev, V., Bleisch, S., Ziewitz, K., Reed, F., & Morgan, J. D. (2020). Exploratory Bivariate and Multivariate Geovisualizations of a Social Vulnerability Index. *Cartographic Perspectives*(95), 5-23.

Studer, M., & Ritschard, G. (2016). What matters in differences between life trajectories: A comparative review of sequence dissimilarity measures. *Journal of the Royal Statistical Society: Series A (Statistics in Society), 179*(2), 481-511.

Tarling, H. A. (2017). *Comparative analysis of social vulnerability indices: CDC's SVI and SoVI*®. Retrieved from

Tate, E. (2012). Social vulnerability indices: a comparative assessment using uncertainty and sensitivity analysis. *Natural Hazards, 63*(2), 325-347.

Tate, E. (2013). Uncertainty analysis for a social vulnerability index. *Annals of the Association of American Geographers, 103*(3), 526-543.

Taubenböck, H., & Geiß, C. (2014). Vulnerability and resilience research: a critical perspective. *International Journal of Disaster Risk Science, 5*(1), 86-87.

Tellman, B., Schank, C., Schwarz, B., Howe, P. D., & de Sherbinin, A. (2020). Using Disaster Outcomes to Validate Components of Social Vulnerability to Floods: Flood Deaths and Property Damage across the USA. *Sustainability, 12*(15), 6006.

Thomas, D. S., Phillips, B. D., Lovekamp, W. E., & Fothergill, A. (2013). *Social vulnerability to disasters* (2nd ed.). Boca Raton, FL: CRC Press.

Tobin, G. A., & Montz, B. E. (1997). *Natural hazards: explanation and integration*. New York, NY: Guilford Publications.

Turner, B. L., Kasperson, R. E., Matson, P. A., McCarthy, J. J., Corell, R. W., Christensen, L., . . . Martello, M. L. (2003). A framework for vulnerability analysis in sustainability science. *Proceedings of the National Academy of Sciences, 100*(14), 8074-8079.

U.S. Census Bureau. (2018). American Community Survey 1-year estimates. Retrieved from https://censusreporter.org/profiles/33000US288-houston-the-woodlands-tx-csa/

Van Aalst, M. K. (2006). The impacts of climate change on the risk of natural disasters. *Disasters, 30*(1), 5-18.

Viruell-Fuentes, E. A., Miranda, P. Y., & Abdulrahim, S. (2012). More than culture: structural racism, intersectionality theory, and immigrant health. *Social Science & Medicine, 75*(12), 2099-2106.

Wang, C., & Yarnal, B. (2012). The vulnerability of the elderly to hurricane hazards in Sarasota, Florida. *Natural hazards, 63*(2), 349-373.

Wang, H., Cheng, Q., & Zuo, R. (2015). Quantifying the spatial characteristics of geochemical patterns via GIS-based geographically weighted statistics. *Journal of Geochemical Exploration, 157*, 110-119.

Ward Jr, J. H. (1963). Hierarchical grouping to optimize an objective function. *Journal of the American statistical association, 58*(301), 236-244.

Williams, B., Onsman, A., & Brown, T. (2010). Exploratory factor analysis: A five-step guide for novices. *Australasian Journal of Paramedicine, 8*(3).

Wisner, B., Blaikie, P. M., Blaikie, P., Cannon, T., & Davis, I. (2004). *At risk: natural hazards, people's vulnerability and disasters* (2nd ed.). London: Routledge.

Wood, N. J., Burton, C. G., & Cutter, S. L. (2010). Community variations in social vulnerability to Cascadia-related tsunamis in the US Pacific Northwest. *Natural hazards, 52*(2), 369-389.

Wu, Yarnal, B., & Fisher, A. (2002). Vulnerability of coastal communities to sea-level rise: a case study of Cape May County, New Jersey, USA. *Climate Research, 22*(3), 255-270.

Wu, C., Hu, W., Zhou, M., Li, S., & Jia, Y. (2019). Data-driven regionalization for analyzing the spatiotemporal characteristics of air quality in China. *Atmospheric Environment, 203*, 172-182.

Wu, C., Ye, X., Ren, F., & Du, Q. (2018). Modified Data-Driven Framework for Housing Market Segmentation. *Journal of Urban Planning Development, 144*(4), 04018036.

Yang, L., Jin, S., Danielson, P., Homer, C., Gass, L., Bender, S. M., . . . Fry, J. (2018). A new generation of the United States National Land Cover Database: Requirements, research priorities, design, and implementation strategies. *ISPRS Journal of Photogrammetry Remote Sensing, 146*, 108-123.

Yoon, D. K. (2012). Assessment of social vulnerability to natural disasters: a comparative study. *Natural hazards, 63*(2), 823-843.

Zachry, B. C., Booth, W. J., Rhome, J. R., & Sharon, T. M. (2015). A national view of storm surge risk and inundation. *Weather, Climate, and Society, 7*(2), 109-117.

Zhang, W., Villarini, G., Vecchi, G. A., & Smith, J. A. (2018). Urbanization exacerbated the rainfall and flooding caused by hurricane Harvey in Houston. *Nature, 563*(7731), 384.

Curriculum Vitae

Gainbi Park

Department of Geography
University of Wisconsin-Milwaukee

EDUCATION

2014-2021 **Ph.D., Geography**
University of Wisconsin-Milwaukee, USA.
Dissertation: "Vulnerability and Resilience of People and Places to Hurricane Damage in U.S. Gulf and Atlantic Coasts from 1950 to 2018"
Committee: Dr. Zengwang Xu (chair), Dr. Woonsup Choi, Dr. Alison Donnelly, Dr. Ryan Holifield, Dr. Margo Anderson (UWM, History), Dr. John Logan (Brown University, Sociology)

2011-2013 **M.A., Geography** (Specialization: GIScience and Cartography)
Sungshin Women's University, Seoul, South Korea.

2007-2011 **B.A., Geography**
Sungshin Women's University, Seoul, South Korea.

RESEARCH & TEACHING INTERESTS

- Geographic Information Science (GIS)
- Geospatial Data Science
- Human-Environment Interactions
- Environmental Justice
- Vulnerability Science
- Social Vulnerability to Natural Hazards
- Environment-induced Population Change
- Environmental Health Disparities

PUBLICATIONS

Park, G., & Xu, Z. (2021). The constituent components and local indicator variables of social vulnerability index. *Natural Hazards* (https://doi.org/10.1007/s11069-021-04938-9)

Park, G., & Xu, Z. (2020). Spatial and temporal dynamics of social vulnerability in the United States from 1970 to 2010: A county trajectory analysis. *International Journal of Applied Geospatial Research*. *11*(1), 36-54.

Jeong, J., **Park, G.**, & Choi, Y. (2013). GIS-based climate map making, *Journal of the Korean Cartographic Association*, *13*(2), 55-66. (in Korean with English abstract)

Park, G., & Jeong, J. (2013). Generating countable symbol maps and semi-circle symbol maps using attribute data manipulation, *Journal of the Korean Cartographic Association*, *13*(1), 59-72. (in Korean with English abstract)

Choi, Y., Jeong, J., Lee, J., Kim, H., Roh, K., Kim, E., **Park, G.**, Kim, Y., & Park, C. (2011). Defining class intervals and color scheme of choropleth maps for the production of 1981-2010 Korea climate atlas, *Journal of the Korean Cartographic Association*, *11*(3), 105-112. (in Korean with English abstract)

JOURNAL ARTICLES IN PREPARATION

Simanek, A.M., **Park, G**., Schluectermann, S., Hagy, A., & Xu, Z. (2021). Area-level correlates of vaccines for children program eligibility, spatial access to vaccine services and childhood vaccine series completion rates in Milwaukee, WI from 2015-2017.

TECHNICAL REPORTS TO SPONSORS

Korea Meteorological Administration: Meteorological Industry and Information Technology. (2012). *1981-2010 The climate atlas of Korea*. DOI: 10.978.89951739/61

- All the climate maps in this atlas were created by Jeong, J., & **Park. G**. using GIS. Atlas has been published in both English and Korean.

Jeong, J., & **Park. G**. (2012). 2010 Climate report of the Republic of Korea. Research Agency for Climate Science (RACS) Task #2010-4013 (in Korean).

AWARDS & FELLOWSHIPS

2021 **KSEA-KUSCO Graduate Scholarship,** Korean-American Scientists and Engineers Association (KSEA) ($1,500)

2021 **First Place**, The Best Graduate Student GIS Project Competition, University of Wisconsin-Milwaukee, GIS Council ($300)

2021 **Mary Jo Read Travel Award**, Department of Geography, University of Wisconsin-Milwaukee ($250)

2020 **Second Place,** Doctoral Oral Paper Competition, West Lake Division of the American Association of Geographers 2020 Annual Meeting ($75)

2020 **First Place,** Applied Geography Conference (AGC) Student Paper Competition ($500)

2020–2021 **Mary Jo Read Graduate Scholarship,** Department of Geography, University of Wisconsin-Milwaukee ($1,500)

2019–2020 **Northwestern Mutual Data Science Scholarship,** Northwestern Mutual Data Science Institution (NMDSI) ($5,000)

2019–2020 **Distinguished Dissertation Fellowship (DDF),** Graduate School, University of Wisconsin-Milwaukee (18 were selected campus-wide, $16,500 stipend with $1,000 travel support)

2019–2020 **Mary Jo Read Graduate Scholarship,** Department of Geography, University of Wisconsin-Milwaukee ($3,000)

2019 **Korean Geographic Society** (**KGS) Best Student Paper Award,** KGS ($250)

2019 **Travel Award**, Graduate School, University of Wisconsin-Milwaukee ($304)

2019 **Mary Jo Read Travel Award**, Department of Geography, University of Wisconsin-Milwaukee ($1,100)

2018–2019 **Mary Jo Read Graduate Scholarship,** Department of Geography, University of Wisconsin-Milwaukee ($1,000)

2018 **Travel Award**, National Center for Atmospheric Research (NCAR) GIS Program – BRIGHTE Workshop Series ($1,444)

2018 **The Outstanding Graduate Student Service Award**, Department of Geography, University of Wisconsin-Milwaukee

2018 **Travel Award**, Graduate School, University of Wisconsin-Milwaukee ($405)

2018 **Mary Jo Read Travel Award**, Department of Geography, University of Wisconsin-Milwaukee ($1,000)

2018 **Sim Student Travel Award**, Korean American Association of Geospatial and Environmental Science ($500)

2017–2018 **Mary Jo Read Graduate Scholarship,** Department of Geography, University of Wisconsin-Milwaukee ($2,500)

2017 **Mary Jo Read Travel Award**, Department of Geography, University of Wisconsin-Milwaukee ($1,350)

2016 **Second Place**, The Best Graduate Student GIS Project Competition, University of Wisconsin-Milwaukee, GIS Council ($200)

2016–2017 **Mary Jo Read Graduate Scholarship,** Department of Geography, University of Wisconsin-Milwaukee ($2,500)

2016 **Mary Jo Read Travel Award**, for the Inter-University Consortium for Political and Social Research (ICPSR) Summer Program, Department of Geography, University of Wisconsin-Milwaukee ($3,275)

2016 **Mary Jo Read Travel Award**, Department of Geography, University of Wisconsin-Milwaukee ($1,100)

2015–2016 **Chancellor's Graduate Student Award**, Department of Geography, University of Wisconsin-Milwaukee ($2,500)

2015 **Mary Jo Read Travel Award**, Department of Geography, University of Wisconsin-Milwaukee ($800)

2014–2015 **Mary Jo Read Graduate Scholarship,** Department of Geography, University of Wisconsin-Milwaukee ($2,500)

2014–2015 **Chancellor's Graduate Student Award**, Department of Geography, University of Wisconsin-Milwaukee ($6,500)

2012 **Graduate Scholarship**, Department of Geography, Sungshin Women's University ($1,000)

2011 **Graduate Scholarship** (awarded to the most outstanding student), Department of Geography, Sungshin Women's University ($8,650)

2011 **Honors Award (most outstanding honors graduate),** Sungshin Women's University

2007–2010 **Academic Excellence Scholarship,** Department of Geography, Sungshin Women's University ($13,950)

CONFERENCE PRESENTATIONS

Park, G. Examining spatial accessibility to hospitals and COVID-19 vaccine providers: a case study of Milwaukee County. UWM GIS Day Student Competition (Virtual), University of Wisconsin-Milwaukee, WI, April 12, 2021.

Park, G. Vulnerability of People and Places to Hurricane Impacts in the U. S. Gulf and Atlantic

Coasts Since 1950, The Annual Meeting of the Association of American Geographers, (Virtual), April 7, 2021.

Park, G. Dissertation presentation – Vulnerability of People and Places to Hurricane Impacts in the U. S. Gulf and Atlantic Coasts Since 1950, Geography Colloquium, University of Wisconsin-Milwaukee, WI, April 2, 2021.

Park, G. Exploring local heterogeneity in social vulnerability using Geographically Weighted Principal Components Analysis (GWPCA) and Sequential Alignment Analysis, West Lake Division of the American Association of Geographers 2020 Annual Meeting (Virtual), November 13, 2020.

Park, G. Exploring local heterogeneity in social vulnerability using Geographically Weighted Principal Components Analysis (GWPCA), The 2020 Applied Geography Conference (Virtual), October 20, 2020.

Kang, J. Y., Kim, M., & **Park, G.** The current situation and challenges on online Geography classes during COVID-19 pandemic: A case Study on U.S. Universities, The Annual Fall Meeting of the Korean Geomorphological Association (Virtual), September 19, 2020.

Simanek, A.M., **Park, G**., Schluechtermann, S., Hagy, A., Sill, D. and Xu, Z. Area-Level socioeconomic disadvantage, vaccines for children eligibility, spatial access to vaccine services and vaccine series completion rates among children two years of age in the City of Milwaukee from 2015-2017. The Annual Meeting of the American Public Health Association, Philadelphia, PA, November 2, 2019. (Poster presentation)

Park, G. & Xu, Z. Vulnerability assessment of the Houston-Galveston area for Hurricane Harvey, The Annual Meeting of the Association of American Geographers, Washington, D.C., April 7, 2019.

Park, G. **(Panelist),** Vulnerability and resilience of people and places to hurricane damage in U.S. Gulf and East Coast since 1950, The Annual Meeting of the Association of American Geographers, New Orleans, LA, April 12, 2018.

Park, G. & Xu, Z. Flooding vulnerability to Hurricane Harvey in Houston area, The Annual Meeting of the Association of American Geographers, New Orleans, LA, April 12, 2018.

Park, G. "Vulnerability and resilience of people and places to hurricane damage in U.S. Gulf and East Coast since 1950." Geography Colloquium, University of Wisconsin-Milwaukee, WI, September 22, 2017.

Park, G. & Xu, Z. Temporal dynamics of social vulnerability in the United States from 1970-2010: A sequence alignment analysis, The Annual Meeting of the Association of American Geographers, Boston, MA, April 8, 2017.

Park, G. & Xu, Z. Exploring the social vulnerability of the United States at multiple spatial scales from 1990-2010, The Annual Meeting of the Association of American Geographers, San Francisco, CA, March 31, 2016.

Park, G. & Xu, Z. Spatial and social vulnerability to hurricane damage: A study on hurricane Sandy (2012) and Irene (2011) in New York City", The Annual Meeting of the Association of American Geographers, Chicago, IL, April 25, 2015.

Park, G. & Jeong, J. A study on a proportional symbol mapping using a GIS software, The Annual Fall Meeting of the Korean Cartographic Association, Seoul, South Korea, December 22, 2012.

INTERNAL INVITED TALKS & OCCASIONAL LECTURES

Park, G. "Spatial and temporal dynamics of social vulnerability in the United States from 1970-2010: A county trajectory analysis", GEOG547: Spatial Analysis, Department of Geography, University of Wisconsin-Milwaukee, Milwaukee, WI, November 13, 2018.

Park, G. "Point pattern analysis", GEOG625: Intermediate Geographic Information Science, Department of Geography, University of Wisconsin-Milwaukee, Milwaukee, WI, September 25, 2018.

- Delivered 75-min lectures on GIS to undergraduate/graduate students

Park, G. "Vector data analysis", GEOG525: Geographic Information Science, Department of Geography, University of Wisconsin-Milwaukee, Milwaukee, WI, April 27, 2017.

- Delivered 75-min lectures on GIS to undergraduate/graduate students

Park, G. "Application of statistical methods in social vulnerability research", GEOG247: Quantitative Analysis in Geography, Department of Geography, University of Wisconsin-Milwaukee, Milwaukee, WI, November 17, 2015.

RESEARCH EXPERIENCE

2018 – 2020 **Research Assistant,** Project on *Area-level correlates of vaccines for children program eligibility, spatial access to vaccine services and childhood vaccine series completion rates in Milwaukee, WI from 2015-2017.* Joseph J. Zilber School of Public Health – Department of Epidemiology, University of Wisconsin-Milwaukee.

- Conducted statistical and spatial analyses to examine the association between socioeconomic disadvantage status and vaccine series completion rates.

2016 (Oct) **Research Assistant,** for Keith Busby's book project "*French in Medieval Ireland*", Department of French and Italian, University of Wisconsin-Milwaukee.

Created a historical map of Ireland in the middle ages using GIS.

2014 (Sep – Dec) **Research Assistant,** Project on *Spatial and social vulnerability to hurricane damage: a study on Hurricane Sandy and Irene in New York City.* Department of Geography, University of Wisconsin-Milwaukee.

- Modeled the spatial extent of the storm surge and wind damage of Hurricane Irene (2011) and Hurricane Sandy (2012).
- Analyzed the degree of social vulnerability in terms of different social-demographic and economic characteristics in space over time using GIS.

2010– 2012 **Research Assistant,** Project on *Development of Climate Application Mapping Technique to Augment the Use of Climate Information.* Department of Geography, Sungshin Women's University, South Korea. (funded by the Korea Meteorological Administration, in collaboration with Konkuk University).

Constructed base map/database that can be directly used in the maintenance plan of weather stations and climate application maps.

- Created climate maps/extreme climate risk maps using GIS for the publication of 2010 climate report and the climate atlas of Korea.

TEACHING EXPERIENCE

SP 21 **Online Lab Instructor**, *Geographic Information System (GEOG525/726)*, Department of Geography, University of Wisconsin-Milwaukee.

FA 20 **Online Lab Instructor**, *ArcGIS Programming with Python (GEOG 647/748)*, Department of Geography, University of Wisconsin-Milwaukee.

FA 19 **Lab Instructor**, *ArcGIS Programming with Python (GEOG 647/748)*, Department of Geography, University of Wisconsin-Milwaukee.

SP 19 **Lab Instructor**, *Introduction to Data Science with R, Python, and ArcGIS (GEOG 325)*, Department of Geography, University of Wisconsin-Milwaukee.

SP 19 **Discussion Instructor**, *Introduction to Environmental Geography (GEOG 125)*, Department of Geography, University of Wisconsin-Milwaukee.

FA 18 **Lab Instructor**, *Spatial Analysis (GEOG547/747)*, Department of Geography, University of Wisconsin-Milwaukee.

SP 18 **Lab Instructor**, *Geographic Information System (GEOG525/726)*, Department of Geography, University of Wisconsin-Milwaukee.

FA 17 **Lab Instructor**, *Spatial Analysis (GEOG547/747)* & *Quantitative Analysis in Geography (GEOG 247)*, Department of Geography, University of Wisconsin-Milwaukee.

SP 17 **Discussion Instructor**, *Introduction to Environmental Geography (GEOG 125)*, Department of Geography, University of Wisconsin-Milwaukee.

FA 15 – 16 **Lab Instructor**, *Geographic Information System (GEOG525/726)*, Department of Geography, University of Wisconsin-Milwaukee.

FA 13 (Oct) **Instructor,** *Practical Remote Sensing (BD 042), Geography and Basic GIS (BD 033), Advanced GIS (BD 024)*, Department of Geography, Sungshin Women's University, South Korea.

SP 13 (Apr) **Instructor,** *Quantitative Geography (BD 311)*, Department of Geography, Sungshin Women's University, South Korea.

SP 11 **Lab Instructor,** *GIS (BD 036)*, Department of Geography, Sungshin Women's University, South Korea.

PROFESSIONAL SERVICE

2021 **Project Assistant** for Lectures Committee, Department of Geography, University of Wisconsin-Milwaukee.

2020 **Project Assistant** for Public Relations Committee & Lectures Committee, Department of Geography, University of Wisconsin-Milwaukee.

2019 **Project Assistant** for Online GIS Master's degree and Certificate Program Course Development, Department of Geography, University of Wisconsin-Milwaukee.

2019 **Project Assistant** for Lectures Committee, Department of Geography, University of Wisconsin-Milwaukee.

2018 **Event Supervisor/Volunteer,** Wisconsin Science Olympiad – Remote Sensing Division.

2016 – 2017 **Graduate Student Representative**, Department of Geography, University of Wisconsin-Milwaukee.

2015 – 2016 **Project Assistant** for Cartography & GIS Center, Department of Geography, University of Wisconsin-Milwaukee.

2013 – 2014 **Assistant Administrator,** The Korean Cartographic Association (KCA)

PROFESSIONAL DEVELOPMENT

2019 (Jul. 23-24) NOAA Office for Coastal Management, *Coastal Inundation Mapping Training*, Florida Gulf Coast University, Fort Myers, FL.

2019 UWM Center for Excellence in Teaching and Learning, *Online and Blended Teaching Program*, University of Wisconsin-Milwaukee, WI.

2018 (Jul.31-Aug.3) The National Center for Atmospheric Research (NCAR) BRIGHTE Workshop Series, *Envisioning Risk of Hurricane Storm Surge and Sea Level Rise*, Boulder, CO.

2017 (Jul.31-Aug.11) Korea Social Science Data Archive (KOSSDA) Advanced Statistics Workshop, *Hierarchical Linear Models (HLM)*, Seoul National University, Seoul, South Korea.

2017 (Jan.5-7) The Consortium for the Advancement of Research Methods and Analysis (CARMA) Short Courses, *Introduction to multilevel analysis*, University of South Carolina, Columbia, SC.

2016 (Jun.20-Jul.15) The Inter-University Consortium for Political and Social Research (ICPSR) Summer Program: Quantitative Methods of Social Research, *1) Bayesian Modeling for the Social Sciences I: Introduction and Application, 2) Time Series Analysis I: Introduction, 3) Introduction, Multivariate Statistical Methods: Advanced Topics, 4) Introduction to the R Statistical Computing Environment, 5) Introduction to the LaTeX Text Processing System*, University of Michigan, Ann Arbor, MI.

TECHNICAL SKILLS

- Programming and Statistical Analysis: R, Python, SPSS, STATA
- Spatial Analysis: ArcGIS Desktop/Pro, GeoDa, Erdas Imagine, TerrSet, Google Earth
- Hurricane Models: SLOSH (Sea, Lake, and Overland Surges from Hurricanes; storm surge modeling), HURRECON (Hurricane Wind Speed, Direction and Damage modeling)